– An international journal for New Concepts in Global Tectonics –

NCGT JOURNAL

Volume 9, Number 1, March 2021: ISSN 2202-0039.
Editor-in-Chief: Louis HISSINK M.Sc. (louis.hissink@bigpond.com)

CONTENTS

Please feel free to contact the CEO of the GeoPlasma Research Institute, Mr. Bruce Leybourne, (GeoPlasmaResearchInstitute.org) at admin@geoplasmaresearchinstitute.org or by contact, correspondence, or inclusion of material in the NCGT Journal please use the following methods: *NEWCONCEPTSINGLOBAL TECTONICS.* 1. E-mail: louis.hissink@bigpond.com.com; 2. Mail, air express, etc., 33 Fields Road, Tanja, NSW 2550, Australia (files in MS Word or ODT format, and figures in gif, bmp or tif format) as separate files; 3. Telephone, +61 419 283 775. *DISCLAIMER*: The opinions, observations and ideas published in this journal are the responsibility of the contributors and do not necessarily reflect those of the Editor and the Editorial Board. *NCGT Journal* is a refereed quarterly international online journal and appears in March, June, September and December. *ISSN number*: ISSN 2202-0039.

From the Editor

This edition of the NCGT Journal continues from the previous issue with additional reports (3) on some of the 2021 earthquakes inferred to have been caused by space weather by our Italian researchers G and D Caltaldi and V. Straser. V and L Gordienko propose a new hypothetical mechanism triggering crustal earthquakes while Cliff Ollier has written a thought provoking paper about the significance of vertical dykes in earth history, M.Shiva has written a comprehensive analysis of earthquake distribution in the Japanese archipelago, concluding that the plate tectonics cannot have caused these earthquakes, and finally there is an overview of hydrocarbon potential of a region in Pakistan.

Unannounced cancelling of personal web-blogs seems to be increasing with no advice or guidance given to the blog owner(s); one web-blog particularly known to the editor was abruptly cancelled with no explanation from the hosting platform. To this end I have made sure that all of the NCGT news and journal issues have been safely archived in case the NCGT Journal's website is cancelled for perceived scientific error.

Additionally I recently learnt of the discovery of a massive deeply buried biosphere that is interpreted to dwarf the Earth's surface biosphere but strangely work on this topic seems to have stopped during 2018. Perhaps it was realized that the existence of such a large deeply buried (5km +) biosphere would have supported the late Tommy Gold's hypothesis described in his controversial book *The Deep Hot Biosphere* in which he proposed the abiotic theory of petroleum among other innovative explanations for coal deposits. And as this deep biosphere is also a major emitter of CH4, one wonders whether this recent discovery had political implications.

Louis Hissink M.Sc. MAIG(retired) MIEEE.

Letter to the Editor

Dear Mr. Hissink, Editor-in-Chief of the NCGT Journal and readers,

> We, the Japanese readers, read the NCGT-J 8.3 "From the Editor" column published at the end of last year (NCGTJ V8 N3) with great pleasure and gratitude to you.
>
> We would like to thank you again for your generosity in publishing our comments on the proposal to change the name of the NCGT Journal. We will continue to work for the further development of the NCGT Journal with great confidence in you, Mr. Editor.
>
> Sincerely yours,

NCGT Journal Japan Readers' Volunteers

Space weather and geomagnetic activity related to Chilean M6.7 earthquake recorded on February 3, 2021

Gabriele Cataldi[1], Daniele Cataldi[1-2], Valentino Straser[3]

(1) Radio Emissions Project (I). ltpaobserverproject@gmail.com
(2) Fondazione Permanente G. Giuliani - Onlus (I). daniele77c@hotmail.it
(3) Department of Science and Environment UPKL Brussel (B). valentino.straser@gmail.com

Abstract

On February 3, 2021, at 05:23:44 UTC, an M6.7 earthquake was recorded off the west coast of Chile. The monitoring of solar activity and terrestrial geomagnetic activity allowed the authors to highlight that the Chilean seismic event was preceded by a solar wind proton density increase (Interplanetary Seismic Precuror) and by an increase in terrestrial geomagnetic activity (Seismic Geomagnetic Precursor), confirming also this time that all potentially destructive earthquakes that are recorded on a global scale are always preceded by an increase in solar activity.

Keywords: proton density increase, seismic precursors, solar activity, geomagnetic activity, seismic prevision.

Introduction

Electromagnetic monitoring, intended as a scientific method capable of monitoring electromagnetic phenomena of solar origin and those produced through the coupling function between the solar ion flux and the terrestrial magnetosphere, has allowed the authors to establish that the M6+ seismic activity that is recorded on our planet is always preceded by an increase in the solar ion flux [1] [4] [5] [6] [7] [8] [9] [10] [11] [12] [13] [14] [15] [16] [17] [18] [19] [20] [21] [22] [23]. This type of correlation has been scientifically ascertained over a long period (from 1 January 2012 to date) thanks to the studies conducted by the authors in this research area. This work will present the results of solar activity monitoring and terrestrial geomagnetic activity monitoring related to the Chilean M6.7 earthquake recorded on February 3, 2021 at 05:23:44 UTC (**Fig. 1**).

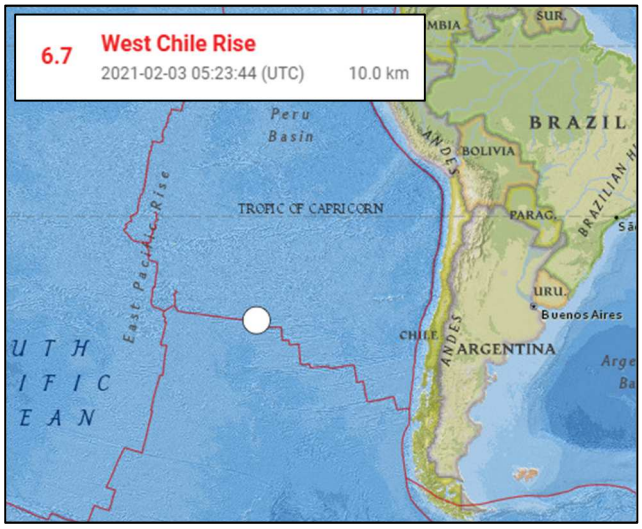

Fig. 1 – Seismic epicenter of the Chilean earthquake recorded on February 3, 2021. The map above shows the seismic epicenter of the Chilean earthquake recorded on February 3, 2021 off the west coast of Chile.
Credits: USGS, Radio Emissions Project.

Data analysis

Between January 30, 2021 at 00:00 UTC and February 6, 2021 at 04:30 UTC the DSCOVR Satellite (located in Lagrangian orbit L1) detected a solar wind proton density increase whose maximum peak was recorded on February 1 at 23:31 UTC (**Fig. 2**). 77 hours after the start of the proton increase (and 66 hours after the maximum peak) the Chilean M6.7 earthquake was recorded. (**Fig. 2**).

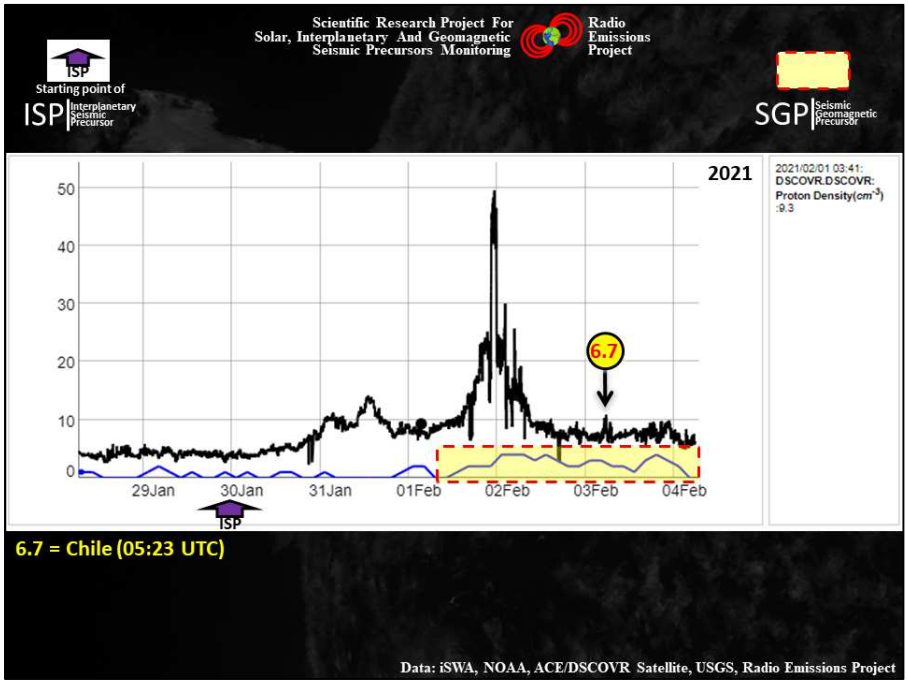

Fig. 2 – Variation in solar ion flux and Earth's geomagnetic activity related to the M6.7 Chilean earthquake recorded on February 3, 2021. The graph above shows the time marker of the Chilean M6.7 earthquake recorded on February 3, 2021 at 05:23 UTC (black vertical arrow). Analyzing the data in the graph it is evident that the Chilean earthquake was preceded by a solar wind proton density increase (Interplanetary Seismic Precursor; black curve) and by an increase of Kp Index (Seismic Geomagnetic Precursor; blue curve highlighted by the yellow area). The purple arrow indicates the start of solar wind proton density increase. Credits: iSWA, USGS, Radio Emissions Project.

The authors have not yet been able to identify the related seismogenic mechanism at solar wind proton density increase but it is known that when the solar ion flux is dense and/or fast has a significant impact on the terrestrial magnetosphere causing one or more perturbations of the terrestrial geomagnetic field, also related to seismic activity [2] [3] [5] [10] [12] [14] [17] [19] [23]. It is therefore conceivable that the seismogenic mechanism could be represented by a form of electromagnetic interaction [19] [22] [23]. An example of the impact that solar activity has on the Earth's geomagnetic field can be observed through **Fig. 3**; that is through what is defined as "Solar Wind Driven Magnetosphere-Ionosphere System" (WINDMI). Analyzing the WINDMI graph it is possible to observe the presence of an intense and vast geomagnetic perturbation (AL Index) which reached 400nT in intensity: this perturbation was highlighted on February 2, 2021 at 00:00 UTC and ended at 20:00 UTC. During this disturbance the DST Index reached -40nT indicating that a low degree geomagnetic storm was in progress. But that is not all. On February 3, 2021 at 00:00 UTC the AL Index suddenly began to increase again and during this second increase the Chilean M6.7 earthquake was recorded. The increases in the solar ion flux and, subsequently, the perturbations of the geomagnetic field are in effect electromagnetic seismic precursors closely linked to each other due to the coupling function between the solar ion flux and the terrestrial magnetosphere: however, being closely related to seismic activity, the authors defined the first as "Interplanetary seismic Precursors" or ISPs, the second as "Seismic Geomagnetic Precursors" or SGPs as they precede the seismic activity [1-23].

Further confirmation of the correlation existing between solar activity and potentially destructive seismic activity that is recorded on a global scale is highlighted through the graph relating to the modulation of the Interplanetary Magnetic Field (IMF) (**Fig. 4**) and that relating to the speed of the solar wind (**Fig. 5**). The first "electromagnetic anomaly" of Interplanetary Seismic Precursors (IMF) that the authors correlated to the M6+ global seismic activity was observed in 2011: the authors defined it as "Italic S" as the variation curve related to the anomaly resembled a Italic "S". It was thanks to the studies conducted in 2011 on Interplanetary Magnetic Field (IMF) that it was later possible to identify what the authors themselves define today as "the most important known electromagnetic precursor": that is, the solar wind proton density increase.

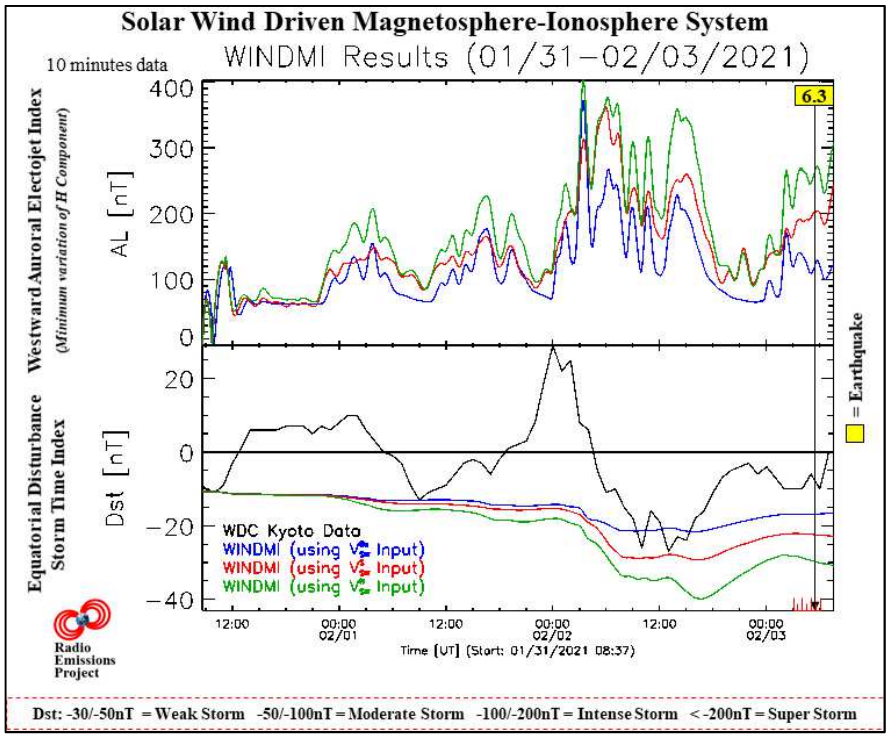

Fig. 3 – Low-dimensional model of the energy transfer from the solar wind through the magnetosphere and into the ionosphere (WINDMI). The picture shows the variation of the AL-Index (at top) and the DST-Index (at bottom) in the hours that preceded the Chilean M6.7 earthquake recorded on February 3, 2021 (the time marker of the earthquake is indicated by a vertical black line). The DST-Index is a direct measure of the Earth's geomagnetic horizontal (H) component variation due to the equatorial ring current, while the AL-Index (Auroral Lower) is at all times, the minimum value of the variation of the geomagnetic H component of the geomagnetic field recorded by observers of reference and provides a quantitative measure of global Westward Auroral Electroject (WEJ) produced by increased of ionospheric currents therein present. Model developed by the Institute for Fusion Studies, Department of Physics, University of Texas at Austin. Credits: iSWA, USGS, Radio Emissions Project.

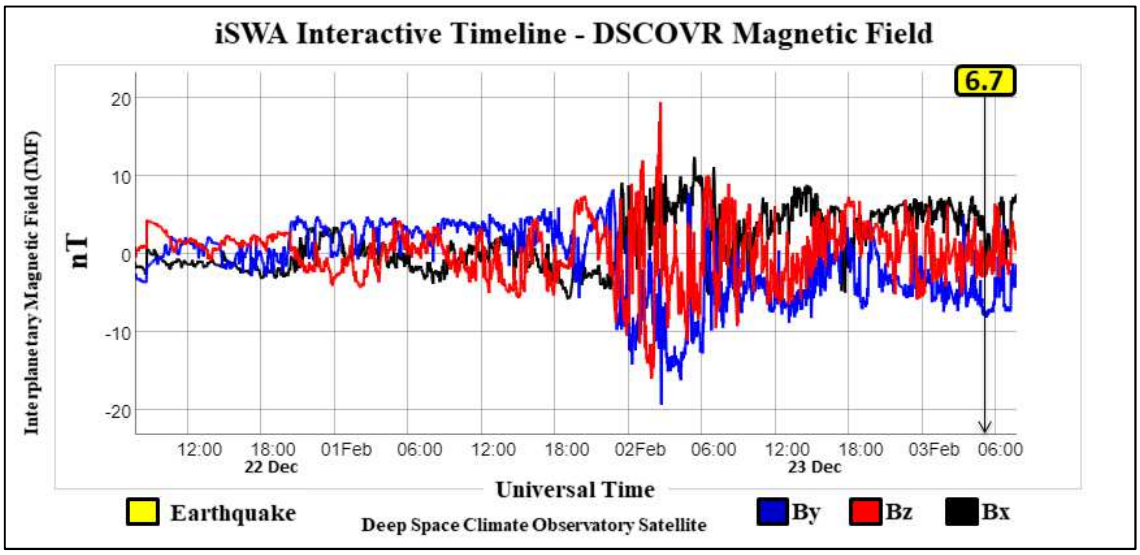

Fig. 4 – Interplanetary Magnetic Field (IMF) related to Chilean M6.7 earthquake recorded on February 3, 2021. The graph above shows a disturbance of Interplanetary Magnetic Field (IMF) which preceded the Chilean M6.7 earthquake recorded on February 3, 2021 (black vertical arrow) by almost 36 hours. Credits: iSWA, USGS, Radio Emissions Project.

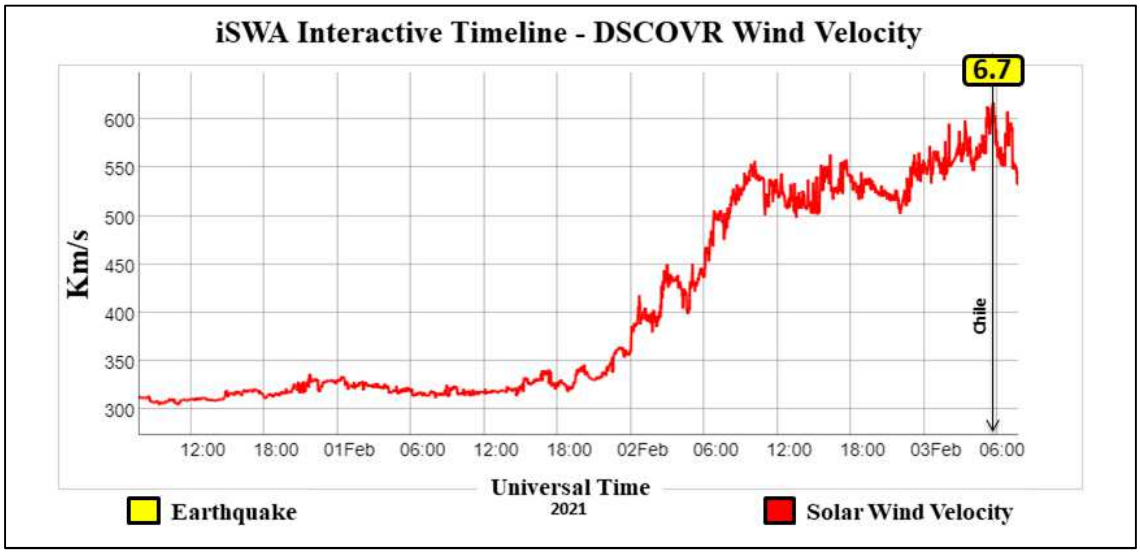

Fig. 5 – Solar wind velocity related to Chilean M6.7 earthquake recorded on February 2, 2021. The graph above shows an increase in solar wind speed that preceded the Chilean M6.7 earthquale recorded on February 3, 2021 (black vertical arrow) by almost 42 hours. Credits: iSWA, USGS, Radio Emissions Project.

Conclusions

This work has once again highlighted the existence of a close and evident correlation between electromagnetic phenomena of solar origin, terrestrial geomagnetic perturbations and M6+ global seismic activity. This type of correlation was first observed by the authors in 2011 by analyzing the modulation of Interplanetary Magnetic Field (IMF). The authors have already presented this important result to the international scientific community but this has not been followed by a constructive debate capable of creating a new unanimously shared point of view in the seismological field and above all in scientific research dedicated to the prediction of potentially destructive earthquakes that are recorded on a global scale. The authors are convinced that this is a serious mistake. The future of seismic prediction research is set to reconsider the old beliefs that many scientists and researchers hold about electromagnetic seismic precursors.

Credits

[1] G. Cataldi, D. Cataldi, V. Straser. (2013). Variations Of Terrestrial Geomagnetic Activity Correlated To M6+ Global Seismic Activity. EGU (European Geosciences Union) 2013, General Assembly, Seismology Section (SM3.1), Earthquake precursors, bio-anomalies prior to earthquakes and prediction, Geophysical Research Abstracts, Vol. 15. EGU2013-2617, Vienna, Austria. Harvard-Smithsonian Center for Astrophysics, High Energy Astrophysics Division, SAO/NASA Astrophysics Data System.

[2] G. Cataldi, D. Cataldi and V. Straser. (2014). Earth's magnetic field anomalies that precede the M6+ global seismic activity. European Geosciences Union (EGU) General Assembly 2014, Geophysical Research Abstract, Vol. 16, EGU2014-1068, Vienna, Austria. Natural Hazard Section (NH4.3), Electro-magnetic phenomena and connections with seismo-tectonic activity, Harvard-Smithsonian Center for Astrophysics, High Energy Astrophysics Division, SAO/NASA Astrophysics Data System.

[3] D. Cataldi, G. Cataldi and V. Straser. (2014). Variations of the Electromagnetic field that preceded the Peruvian M7.0 earthquake occurred on September 25, 2013. European Geosciences Union (EGU) General Assembly 2014, Geophysical Research Abstract, Vol. 16, EGU2014-1075, Natural Hazard Section (NH4.3), Electro-magnetic phenomena and connections with seismo-tectonic activity, Vienna, Austria. Harvard-Smithsonian Center for Astrophysics, High Energy Astrophysics Division, SAO/NASA Astrophysics Data System.

[4] T. Rabeh, G. Cataldi, V. Straser. (2014). Possibility of coupling the magnetosphere–ionosphere during the time of earthquakes. European Geosciences Union (EGU) General Assembly 2014, Geophysical Research Abstract, Vol. 16, EGU2014-1067, Vienna, Austria. Natural Hazard Section (NH4.3), Electro-magnetic phenomena and connections with seismo-tectonic activity. Harvard-Smithsonian Center for Astrophysics, High Energy Astrophysics Division, SAO/NASA Astrophysics Data System.

[5] V. Straser, G. Cataldi. (2014). Solar wind proton density increase and geomagnetic background anomalies before strong M6+ earthquakes. Space Research Institute of Moscow, Russian Academy of Sciences, MSS-14. 2014. Moscow, Russia. pp280-286.

[6] V. Straser, G. Cataldi. (2015). Solar wind ionic variation associated with earthquakes greater than magnitude M6.0. New Concepts in Global Tectonics Journal, V. 3, No. 2, June 2015, Australia. P.140-154.

[7] G. Cataldi, D. Cataldi, V. Straser. (2015). Solar wind proton density variations that preceded the M6+ earthquakes occurring on a global scale between 17 and 20 April 2014. European Geosciences Union (EGU) General Assembly 2015, Vienna, Austria. Natural Hazard Section (NH5.1), Sea & Ocean Hazard - Tsunami, Geophysical Research Abstract, Vol. 17, EGU2015-4157-2, Harvard-Smithsonian Center for Astrophysics, High Energy Astrophysics Division, SAO/NASA Astrophysics Data System.

[8] G. Cataldi, D. Cataldi, V. Straser. (2015). Solar wind ion density variations that preceded the M6+ earthquakes occurring on a global scale between 3 and 15 September 2013. European Geosciences Union (EGU) General Assembly 2015, Geophysical Research Abstract, Vol. 17, EGU2015-4581, Vienna, Austria. Natural Hazard Section (NH5.1), Sea & Ocean Hazard - Tsunami, Harvard-Smithsonian Center for Astrophysics, High Energy Astrophysics Division, SAO/NASA Astrophysics Data System.

[9] G. Cataldi, D. Cataldi, V. Straser. (2015). Solar wind proton density variations that preceded the M6,1 earthquake occurred in New Caledonia on November 10, 2014. European Geosciences Union (EGU) General Assembly 2015, Geophysical Research Abstract, Vol. 17, EGU2015-4167, Vienna, Austria. Natural Hazard Section (NH5.1), Sea & Ocean Hazard - Tsunami, Harvard-Smithsonian Center for Astrophysics, High Energy Astrophysics Division, SAO/NASA Astrophysics Data System.

[10] V. Straser, G. Cataldi, D. Cataldi. (2015). Solar wind ionic and geomagnetic variations preceding the Md8.3 Chile Earthquake. New Concepts in Global Tectonics Journal, V. 3, No. 3, September 2015, Australia. P.394-399.

[11] G. Cataldi, D. Cataldi, V. Straser. (2016). Solar activity correlated to the M7.0 Japan earthquake occurred on April 15, 2016. New Concepts in Global Tectonics Journal, V. 4, No. 2, pp202-208, June 2016.

[12] G. Cataldi, D. Cataldi, V. Straser. (2016). Tsunami related to solar and geomagnetic activity. European Geosciences Union (EGU) General Assembly 2016, Natural Hazard Section (NH5.6), Complex modeling of earthquake, landslide, and volcano tsunami sources. Geophysical Research Abstract, Vol. 18, EGU2016-9626, Vienna, Austria. Harvard-Smithsonian Center for Astrophysics, High Energy Astrophysics Division, SAO/NASA Astrophysics Data System.

[13] G. Cataldi, D. Cataldi, V. Straser. (2017). SELF-VLF electromagnetic signals and solar wind proton density variations that preceded the M6.2 Central Italy earthquake on August 24, 2016. International Journal of Modern Research in Electrical and Electronic Engineering, Vol. 1, No. 1, 1-15. DOI: 10.20448/journal.526/2017.1.1/526.1.1.15.Harvard-Smithsonian Center for Astrophysics, High Energy Astrophysics Division, SAO/NASA Astrophysics Data System.

[14] G. Cataldi, D. Cataldi, V. Straser. (2017). Solar and Geomagnetic Activity Variations Correlated to Italian M6+ Earthquakes Occurred in 2016. European Geosciences Union (EGU), General Assembly 2017. Geophysical Research Abstracts Vol. 19, EGU2017-3681, 2017. Seismology (SM1.2)/Natural Hazards (NH4.7)/Tectonics & Structural Geology (TS5.5) The 2016 Central Italy Seismic sequence: overview of data analyses and source models.Harvard-Smithsonian Center for Astrophysics, High Energy Astrophysics Division, SAO/NASA Astrophysics Data System.

[15] G. Cataldi, D. Cataldi, V. Straser. (2017). Solar wind proton density increase that preceded Central Italy earthquakes occurred between 26 and 30 October 2016. European Geosciences Union (EGU), General Assembly 2017. Geophysical Research Abstracts Vol. 19, EGU2017-3774, 2017. Seismology (SM1.2)/Natural Hazards (NH4.7)/Tectonics & Structural Geology (TS5.5) The 2016 Central Italy Seismic sequence: overview of data analyses and source models. Harvard-Smithsonian Center for Astrophysics, High Energy Astrophysics Division, SAO/NASA Astrophysics Data System.

[16] V. Straser, G. Cataldi, D. Cataldi. (2017). Solar and electromagnetic signal before Mexican Earthquake M8.1, September 2017. New Concepts in Global Tectonics Journal, V. 5, No. 4, December 2017. pp600-609.

[17] G. Cataldi, D. Cataldi, V. Straser. (2017). Solar and Geomagnetic Activity Variations Correlated to Italian M6+Earthquakes Occurred in 2016. EGU General Assembly 2017. EGU2017-3681, Vol. 19.

[18] G. Cataldi, D. Cataldi, V. Straser. (2019). Solar wind ionic density variations related to M6+ global seismic activity between 2012 and 2018. European Geosciences Union (EGU) General Assembly 2019, Short-term Earthquake Forecast (StEF) and multy-parametric time-Dependent Assessment of Seismic Hazard (t-DASH) (NH4.3/AS4.62/EMRP2.40/ESSI1.7/Gi2.13/SM3.9), General Contribution on Earthquakes, Earth Structure, Seismology (SM1.1), Geophysical Research Abstract, Vol. 21, EGU2019-3067, 2019, Vienna, Austria. Harvard-Smithsonian Center for Astrophysics, High Energy Astrophysics Division, SAO/NASA Astrophysics Data System.

[19] G. Cataldi. (2020). Precursori Sismici – Monitoraggio Elettromagnetico. Kindle-Amazon, ISNB: 9798664537970. ASIN Code: B08CPDBGX9.

[20] G. Cataldi, D. Cataldi, V. Straser. (2019). Wolf Number Related To M6+ Global Seismic Activity. New Concepts in Global Tectonics Journal, Volume 7, Number 3, December 2019, pp. 178-186.

[21] V. Straser, G. Cataldi, D. Cataldi. (2020). The Space Weather Related to the M7+ Seismic Activity Recorded on a Global Scale between 28 January and 25 March 2020. Acta Scientific Agriculture 4.12 (2020): 55-62.

[22] G. Cataldi, V. Straser, D. Cataldi. (2020). Space Weather related to potentially destructive seismic activity recorded on a global scale. New Concepts in Global Tectonics Journal. Vol.8, No.3, pp.233-253, December 2020. ISSN 2202-0039.

[23] G. Cataldi. (2021). Radio Emissions Project – A new approach to seismic prediction. Kindle-Amazon, ISNB: 9798709593411.

ON A HYPOTHETICAL MECHANISM TRIGGERING CRUSTAL EARTHQUAKES IN ALPINE GEOSYNCLINES

Vadim Gordienko and Lyudmila Gordienko
Institute of Geophysics, National Academy of Sciences, Kiev, Ukraine
tectonos@igph.kiev.ua

Abstract: In Alpine geosynclines, the sedimentary layer consists of two portions. During the period of recent activation, the upper portion underwent transformation at the level of dia- and catagenesis. The lower portion experienced a stage of metamorphism, including granitization. At the top, the increase in density was accompanied by an increase in the velocity of seismic waves. But this process was less intensive than in the case of crystalline rocks. This is the reason why, as the velocity approached 6 km/sec, the density of metapelites exceeded, by about 0.1 g/cm3, the density of the underlying rocks which make up the upper portion of the "granitic" layer. A likely upheaval of a four-km thick decompacted rock body did not exceed 10 to 12 km. The listed parameters of the substance motion suggest that relevant earthquakes are fairly widespread in the Alpides. For the sake of comparison, we also included the Laramides of Mexico and the Andes in our review. The forecast earthquakes have been registered within all Alpides. In regions other than those of Alpides, earthquakes at similar depths could be triggered by other mechanisms. One of them might well be vertical motions of crustal blocks during recent activation.

Keywords: earthquakes, Alpides, dia- and catagenic rocks.

INTRODUCTION

It was suggested in an earlier publication (Gordienko, 2017b) that earthquakes could be triggered within the upper crust of Alpine geosynclines at the stage of recent activation at interfaces between layers with dissimilar extents of primary sedimentary rock transformation. Considerations supporting the validity of the purported phenomenon are listed below.

In many Alpides, the young sedimentary layer with the age of folding ranging from 10 to 30 million years is underlain by Hercynian (250-300 million years), Caledonian (500-600 million years), Baikalian (900 million years), or Gothian (1,200 million years) layers. The total thickness of the upper series of layers reaches 10-15 km. The level of their transformation during recent activation (about 0-7 million years) is dia- and catagenic. The lower series experienced the stage of metamorphism, including granitization, and became part of the crystalline basement. There formed a zone of density (σ) inversion. It may have triggered the crustal material displacement and seismicity. Parameters of the zone were described, in particular, for the Carpathians, and the relevant bibliography is available in the publication (Gordienko et al., 2011). No velocity inversion of longitudinal seismic waves (V_p) could be recorded within the same depth range (approximately 6 to18 km). This can be accounted for by the fact that the types of relationship between σ and V_p are not the same for the sedimentary layer and basement rocks. Density inversion zones are not widespread. They may be totally absent beneath the entire region of folding or its larger areas in regions with intensive basification (typical of Pacific areas).

It might be of interest to analyze displacements of the crustal material in greater detail and correlate between predicted and observed events. However, some synchronous crustal seismicity of a different nature may distort results of such a correlation. In the case of Alpine geosynclines that experienced recent activation, there may also be, in addition to the aforementioned types of earthquakes, others, such as

1) Those associated with processes of folding during which the youngest series of rocks (at depths between zero and 6 km) had slipped down basement uplifts;

2) Magmatic earthquakes (with major crustal foci occurring at depths of 25-30 km and on the path of magma ascent to the site of eruption at 0-25 km);

3) Earthquakes triggered by movements of plunging eclogitized bodies in the lower crust and in the mantle (below 25 km) (Gordienko, 2017b). However, an analysis of large amounts of evidence may reveal concentrations of hypocenters at predicted depths. All the more so considering that we have at our disposal the data on major vertical displacements of geosynclinal crustal blocks. Such displacements were observed in the Carpathians (Gordienko et al., 2011; Danilovich, 1988) — down to 30 km, in the Alps (Alps…, 1978) — down to 20 km, as well as in areas of UHP rock blocks — within a much larger depth range (Gordienko, 2018).

BLOCK DISPLACEMENT HARAMETERS

As temperatures and pressures increase in the course of further sinking, this is accompanied by catagenetic transformations that, at about 400°C, reach a metagenetic level (**Fig.1**).

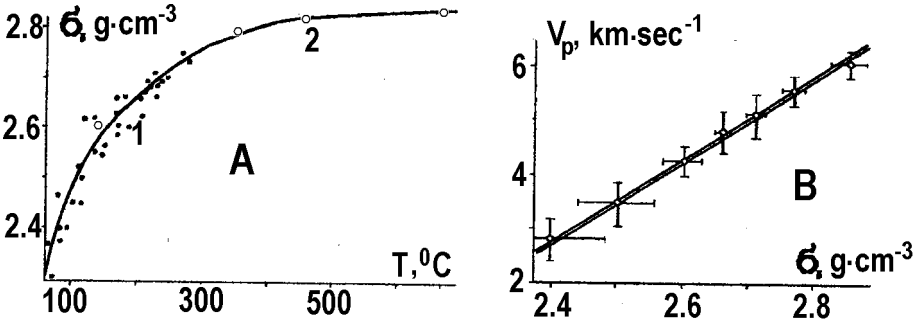

Fig. 1. Density variations in metapelites as a function of temperature and related changes in seismic wave velocities in rocks:1- the data based on isolated rock samples; 2 - averaged data for groups of samples

An increase in density is accompanied by higher seismic wave velocities, although this process is less intensive than in the case of crystalline rocks. This is the reason why, as the velocity approaches 6 km/sec, the density of metapelites exceeds, by about 0.1 g/cm^3, the density of the underlying rocks which make up the upper portion of the "granitic" layer (Gordienko, 1999). A likely upheaval of a four-km thick decompacted rock body is 10 - 12 km.

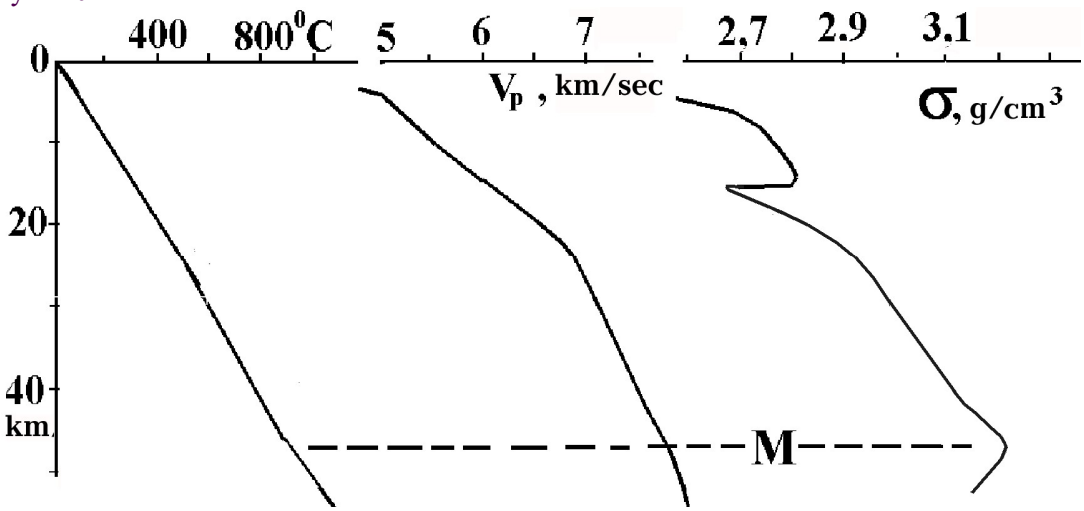

Fig. 2. Patterns of distribution of temperatures (T), seismic wave velocities, and densities in crustal rocks of the Carpathians.

Displacement is only possible when the strength of rock masses is overcome. The available estimates of this parameter appear to be quite similar for various experimental data, and some of them are listed in **Fig. 3**.

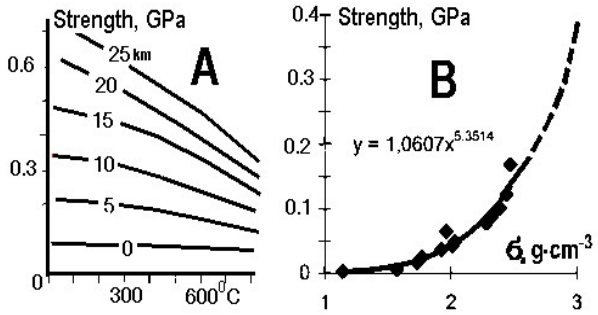

Fig. 3. A - The strength of crustal rocks as a function of depth and temperature (Gordienko, 2017c); B - The strength of andesite rocks versus density (Ladygin et al., 2004).

The pressure exerted by rock bodies with abnormal density is tens of times lower than the rock strength (about 0.01hPa). Yet, earthquakes at such depths in the Alpides are not uncommon. Evaluation of stresses associated with other potential sources does not produce higher figures. Fluidization of rocks sharply lowers their strength. The temperature distribution depicted in Fig. 2 refers to a margin of the foredeep, whereas temperatures in the folded Carpathians are higher. At depths somewhat larger than 20 km, there lies the top of the partially molten layer of rocks in the amphibolite facies. It is overlain by rocks containing fluids formed in the process of melting. Their presence is confirmed by zones with abnormally high electrical conductivity (Gordienko et al., 2011). Earthquakes are much less common in areas with the

highest values of the parameter because high plasticity prevents stress accumulation (Kovachikova et al., 2016) (Fig. 4).

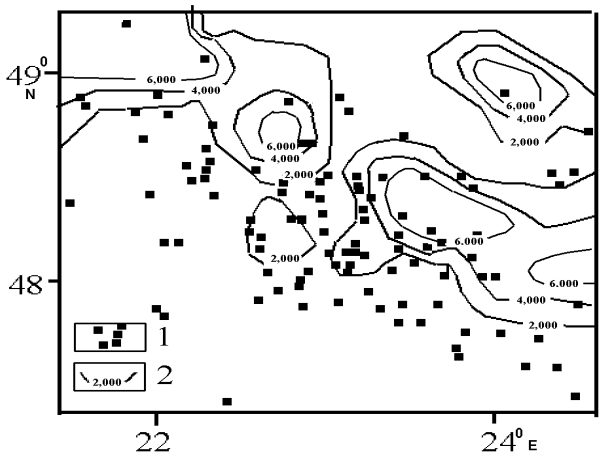

Fig. 4. (1) Earthquake epicenters and (2) zones of cumulative longitudinal electrical conductivity in S units in the Carpathians at depths from 7 to 13 km (Kovachikova et al., 2016).

This changes the very concept of strength as differential stress violating the integrity of a rock mass. Studies of paleodislocations in crustal xenolytes indicate that, within a geologically specific period of time, displacements involving intergranual gliding, occur at relatively small stresses (0.1 to 0.05 GPa) (Chen et al, 2006, 2007, Dimanov et al., 2005). Stresses released by earthquakes are even smaller: 0.001 to 0.01GPa (Yanovskaya, 2006).

According to the Stokes equation, the rock substance flow velocity $v = 1.5\Delta\sigma \cdot g \cdot r^2/\eta$, where $\Delta\sigma$ is density anomaly, g – acceleration of gravity, r – half-size of the moving body, and η – viscosity. Viscosity estimates for the situation in question, with the use of various approaches, amount to $10^{20\pm1}$Pa·sec (Gordienko, 2017a). For specific dimensions, the rate will amount to 0.1-1.0 cm per year. In other words, it may take about 2 million years for the density inversion process to smooth out. Such events are most likely to occur in discrete periods. At any rate, this is how vertical displacements of the surface manifest themselves (Study…, 2005) (Fig. 5).

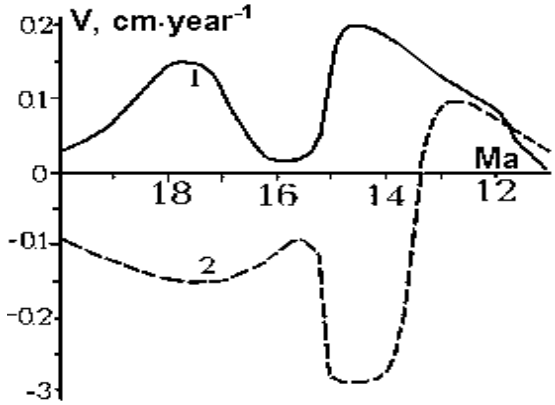

Fig. 5. Rates of vertical motions in the folded Carpathins (1) and in the Ciscarpathian trough (2)

The process will roll across the folded zone with the speed of the "Aubouin wave," which for Kamchatka, for example, can be estimated in terms of the age of magmatic manifestations during the period of recent activation (Koloskov et al., 2004) -- at about 10 cm per year.

EXPERIMENTAL DATA

The listed parameters of the substance motion suggest that relevant earthquakes are fairly widespread in the Alpides. For the sake of comparison, we also included the Laramides of Mexico and the Andes in our review (the age of folding is about 70 million years and the activation started 25 million years ago). We proceeded from the age of hypocenter depths down to 40 km (**International…,**) over the period between 2006 and 2018.

These data are by no means sufficient for a complete analysis of seismicity in each region. We generally used the data for relatively small areas thereof. In some cases, we quoted evidence from already available generalizations made by other authors for different periods of time (Gorshkov, 1987; Nazarevich, 2012; and others). In most cases, the selected interval for graphs showing distribution of hypocenters versus depth amounted to 5 km. This was due to a potential error of at least 3 km (Shevchenko et al., 2019; Seismological…, 2004, 2006, Tarakanov, 2006 and others). The number of earthquakes differs widely from region to region. Therefore, the distributions were constructed in the form of values referred to the maximum (Fig. 6).

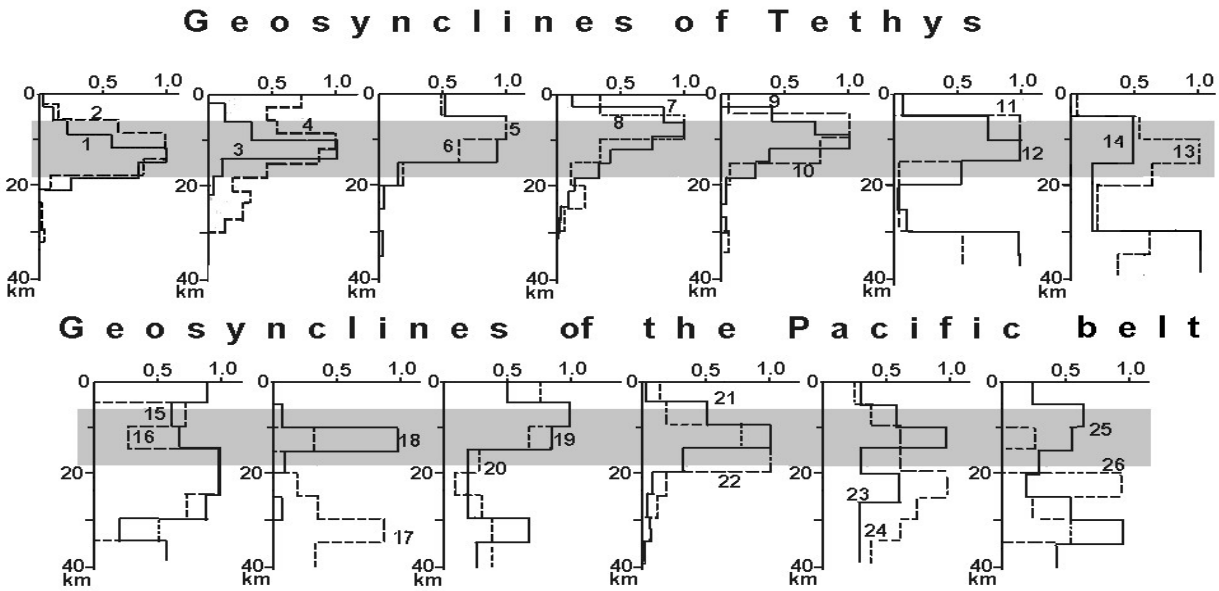

Fig. 6. Earthquake depth distribution patterns for the Tethys and Pacific belts (International… and others). The estimated depth range is shown in gray.
Region numbers: 1 – the Pyrenees, 2 – the Alps, 3 – the Apennines, 4 – the Carpathians, 5 – the Balkans, 6 – the Pontids, 7 - Dagestan, 8 - Elburs, 9 – Kopet-Dag, 10 - Zagros, 11 - Hindu Kush, 12 – the Himalayas, 13 - Burma, 14 - Sumatra, 15 - Kamchatka, 16 – the Kuriles, 17 - Hokkaido, 18 - Kyushu, 10 - New Zealand, 20 - Alaska, 21 – the Cordillera Cascade Range, 22 – the Cordillera Coastal Range, 23 – the western Sierra Madre, 24 - the Andes of Colombia, 25 – the Andes of central Chile, 26 – the Andes of southern Chile.

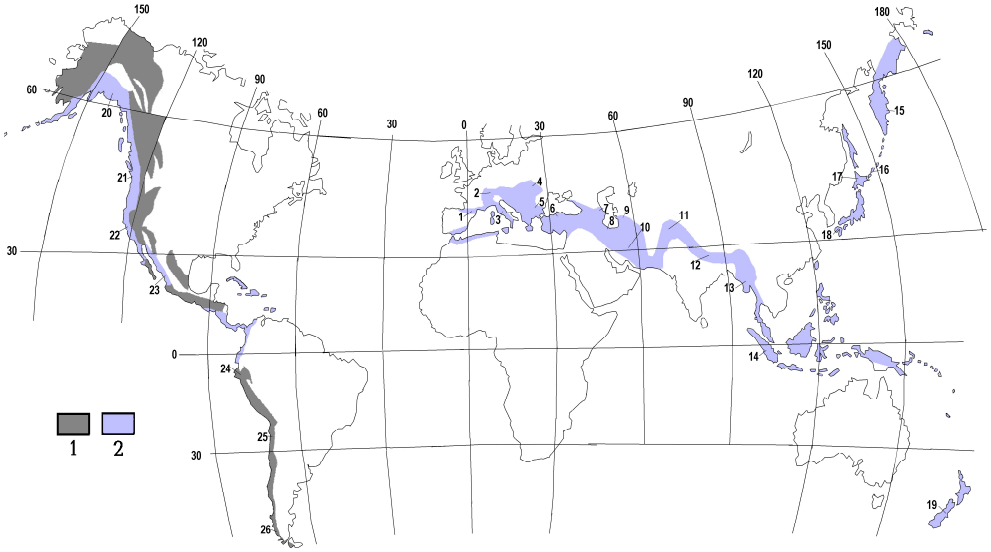

Fig. 7. The Tethys geosynclinal belt and the Pacific Rim.
Folded regions: 1) Alpides, 2) Laramides of the Pacific belt. The names of regions match the numbers in Fig. 6.

The forecast earthquakes have been registered within all Alpides. Seismic events at other depths have been reported less frequently in 100 percent for the Tethys and in 70 percent for the Pacific belt or else they were separated by depth intervals with smaller clusters of hypocenters. In the rest of cases, at other depths (different causes, perhaps?), they are more widespread. They also include portions of the Laramian Andes. This is not at variance with our forecast. The above hypothesis has been positively verified. Notwithstanding the fact that in regions other than those of Alpides, earthquakes at similar depths could be triggered by other mechanisms. One of them might well be vertical motions of crustal blocks with cracking during recent activation. Relevant examples are illustrated in Fig. 8.

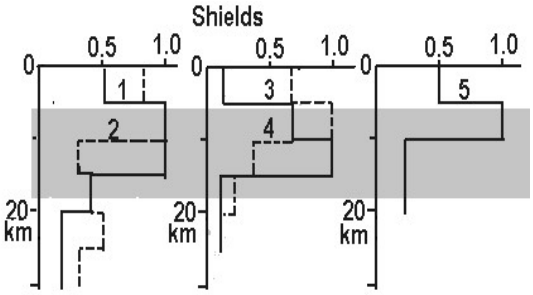

Fig. 8. Patterns of earthquake depth distribution on shields (International… and others).
1 - Baltic shield, 2 - Canadian shield, 3 - Western Australian shield, 4 - Slope of the Voronezh crystalline massif, 5 - Slope of the Ukrainian shield.

CONCLUSION

The derived result corroborates the forecast partially based on a geological theory advanced by the authors. Models of deep-seated processes within geosynclines and zones of recent activation have been constructed in terms of our theory. However, we largely focused in our prediction on the data regarding the effect of PT conditions on physical properties of rocks with dissimilar composition that formed as a result of such processes. The said information has also been corroborated. Yet, we cannot claim that our version is final and indisputable. Approaches based on other evaluations of possible parameters of the medium can be worked out and the number of regions covered can be expanded.

References

Alps, Apennines, Hellenides. Eds.: H. Closs, D. Roder, K. Schmidt. Stuttgart: Nägele und Obermiller. - 1978. 620p.

Chen S, Hiraga K, Kohlstedt D. Water weakening of clinopyroxene in the dislocation creep regime. J. Geophys. Res. 2006.B08203/

Chen, X., Lin, C., Shi, L. 2007. Rheology of the lower crust beneath the northern part of North China: Inferences from lower crustal xenoliths from Hannuoba basalts, Hebei Province, China. Science in China Series D: Earth Sciences. 2007. 8, pp. 1128-1141.

Danilovich Yu.Z. Rock-forming minerals and metamorphism of the crystalline basement of the Ukrainian Carpathians. Kiev: Naukova Dumka. 1988.167p. (in Russian).

Dimanov A, Dresen G. Rheology of synthetic anorthite-diopside aggregates: implications for ductile shear zones. J. Geophys. Res. 2005. v.110: B07203, doi:10.1029/2004JB003431.

Gordienko V.V. Density models of the tectonosphere of Ukraine. Kiev: Intellect. 1999. 101p. (in Russian).

Gordienko V.V. On the viscosity of the tectonospheric matter of continents and oceans. Geology and minerals of the World Ocean. 2017a. 1.pp.45-57. (in Russian).

Gordienko V.V. Thermal processes, geodynamics, deposits. 2017b. 283p. https://d4d10b6a-c83d-45d7-b6dc-b2c3ccafe1ce.filesusr.com/ugd/6d9890_c2445800a51b49adb03b8f949f3d6abb.pdf

Gordienko V. Deep-seated processes and seismicity. NCGT Journal. 2017c. 2. pp. 176-201.

Gordienko V. Deep-seated processes and diamond-bearing rocks. NCGT Journal, 1. 2018. p. 4-20.

Gordienko V.V., Gordienko I.V.,. Zavgorodnyaya O.V ,Kovachikova S., Logvinov I.M., Tarasov V.N., Usenko O.V. Ukrainian Carpathians (geophysics, deep processes). Kiev: Logos. 2011. 128p. (in Russian).

Gorshkov G.P. Seismotectonics of the Kopetdag. Moscow: Nauka. 1987. 50 p. (in Russian).

International Seismological Centre, On-line Bulletin, http://www.isc.ac.uk.

Koloskov A.V., Anosov G.I. Sketches of the vortex concept of the development of the West Pacific transition zone in the Cenozoic. Materials of the IV International Meeting on Processes in Subduction Zones. Petropavlovsk-Kamchatsky. 2004.pp. 95-96. (in Russian).

Kovachikova S., Logvinov I.M., Peck J., Tarasov V.N. Modeling the earth's crust of Ukraine based on the results of magnetotelluric studies using new inversion techniques. Geophys. J. 2016. 6. pp. 83-100. (in Russian).

Ladygin, V.M., Girina, O.A. & Frolova, Y.V. Petrophysical features of lava flows from Bezymyannyi Volcano, Kamchatka. J. Volcanolog. Seismol. 2012. 6, pp.341–351.

Nazarevich L, Nazarevich A. Seismicity and deeds in the particularity of seismotectonics of the Ukrainian Carpathians. Geodynamics. 2012.1.pp 145-151. (in Ukrainian).

Seismological Bulletin of Ukraine for 2004. Sevastopol: NPC Ekosi-Hydrophysics. 2004.166p. . (in Ukrainian).

Seismological Bulletin of Ukraine for 2006. Sevastopol: NPC Ekosi-Hydrophysics. 2006.295p. (in Ukrainian).

Shevchenko V. I., Lukk A. A., Guseva T. V. Autonomous and Plate-Tectonic Geodynamics of Some Mobile Belts and Mobile Edi ices. Moskov: GEOS, 2017. 612 p. (in Russian).

Study of the current geodynamics of the Ukrainian Carpathians. Ed. V.I. Starostenko. Kiev: Naukova Dumka. 2005. 256p. (in Ukrainian).

Tarakanov R.Z. Velocity models and hodographs of P-waves for the Far Eastern region. Bulletin of the Far Eastern Branch of the Russian Academy 2006. 1. pp.81-95. (in Russian).

Yanovskaya T. B., Fundamentals of Seismology. Saint-Petersburg: VVM. 2006. 288p. (in Russian).

Space weather and geomagnetic activity related to the Japanese M7.1 earthquake recorded on February 13, 2021

Gabriele Cataldi[1], Daniele Cataldi[1-2], Valentino Straser[3]

(1) Radio Emissions Project (I). ltpaobserverproject@gmail.com
(2) Fondazione Permanente G. Giuliani - Onlus (I). daniele77c@hotmail.it
(3) Department of Science and Environment UPKL Brussel (B). valentino.straser@gmail.com

Abstract

On February 13, 2021 at 14:07:50 UTC, an M7.1 earthquake was recorded in Japan at a depth of 49.9 km. The analysis of solar activity and terrestrial geomagnetic activity allowed the authors to verify that the M7.1 Japanese earthquake was preceded by an increase in solar activity which subsequently produced an increase in terrestrial geomagnetic activity: phenomena of electromagnetic nature that the authors have related to the M6+ global seismic activity since 2011.

Keywords: proton density increase, seismic precursors, solar activity, geomagnetic activity.

Introduction

Japan is located in a geographic area influenced, from a tectonic point of view, by North America plate, Pacific plate, Philippine Sea plate, and Eurasia plate. This feature makes Japan one of the most seismically active areas and the highest seismic risk on the planet. Between 2012 and 2020, the authors highlighted that the seismic events recorded in Japan are closely related to solar activity and terrestrial geomagnetic activity [1] [2] [5] [6] [7] [12] [13] [19] [20] [21] [23] confirming the results obtained between 2012 and 2021: potentially destructive seismic events that are recorded on a global scale are always preceded by an increase in the density of the solar ion flux (especially the proton density) and by a consequent increase in the Earth's geomagnetic activity [1-24]. On February 13, 2021 at 14:07:50 UTC, an M7.1 earthquake was recorded in Japan (**Fig. 1**) just during the terminal phase of an increase in the density of the solar ion flux which also generated an increase in geomagnetic terrestrial activity.

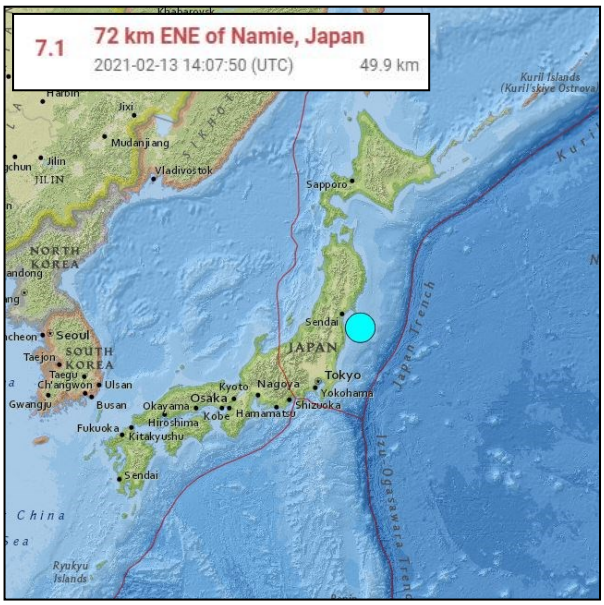

Fig. 1 – Epicenter of the M7.1 Japanese earthquake. The image above shows the map of Japan and the epicenter of the M7.1 earthquake recorded on 13 February 2021 at 14:07:50 UTC, at a depth of 49.9 km.
Credits: USGS, Radio Emissions Project.

Data analysis

Thanks to the data provided by the DSCOVR Satellite located in the Lagrangian orbit L1, on February 10, 2021 at 20:30 UTC the authors started following the evolution of a solar wind proton density increase which ended on February 14, 2021 at 02:00 UTC and whose maximum peak was reached on February 13, 2021 at 01:23 UTC. Four potentially destructive seismic events were recorded during this proton density increase (**Fig. 2**):

1. M6.2 Loyalty Islands earthquake, recorded on February 10, 2021 at 21:24 UTC.
2. M6.0 Loyalty Islands earthquake, recorded on February 11, 2021 at 06:52 UTC.
3. M7.1 Japan earthquake, recorded on February 13, 2021 at 14:07 UTC.
4. M6.0 Papua New Guinea earthquake, recorded on February 13, 2021 at 15:33 UTC.

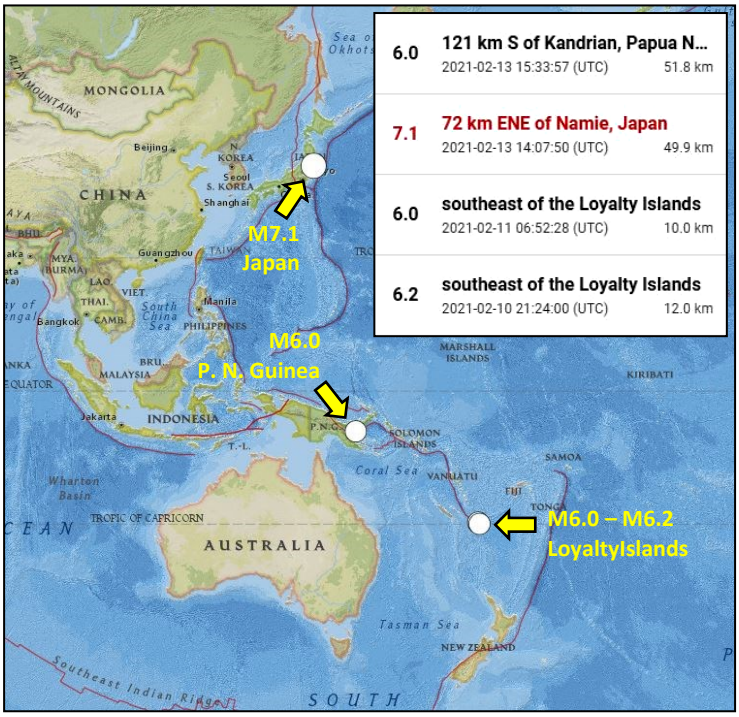

Fig. 2 – Potentially destructive seismic events related to the proton increase of 10-14 February 2021. The image shows the epicenters of potentially destructive earthquakes related to the proton increase recorded between 10 and 14 February 2021. Credits: USGS, Radio Emissions Project.

Analyzing the temporal data of the four seismic events with the space weather data provided by DSCOVR Satellite between 10 and 14 February 2021, the authors were able to calculate the time intervals recorded between the start of the proton increment (Interplanetary Seismic Precursor) and the four M6+ seismic events:

1. M6.2 Loyalty Islands earthquake, recorded on February 10, 2021 at 21:24 UTC ≈ **1** hour.
2. M6.0 Loyalty Islands earthquake, recorded on February 11, 2021 at 06:52 UTC ≈ **10** hours.
3. M7.1 Japan earthquake, recorded on February 13, 2021 at 14:07 UTC ≈ **66** hours.
4. M6.0 Papua New Guinea earthquake, recorded on February 13, 2021 at 15:33 UTC ≈ **67** hours.

The average time interval calculated by analyzing the seismic activity and the solar activity that occurred between 1 January 2012 and 18 February 2021 is equal to 108.8 hours: the average was calculated by analyzing 1192 M6+ seismic events that occurred in the same period. Among the four potentially destructive seismic events related to the proton increase that occurred between 10 and 14 February 2021, the authors focused their attention on the M7.1 Japanese earthquake as it is of greater magnitude than the others and occurred immediately after an important geomagnetic increase (Seismic Geomagnetic Precursor) recorded

between 12:00 UTC on February 12, 2021 and 20:00 UTC on February 13, 2021, an increase that was associated with a weak geomagnetic storm (Seismic Geomagnetic Precursor) (**Fig. 4**).

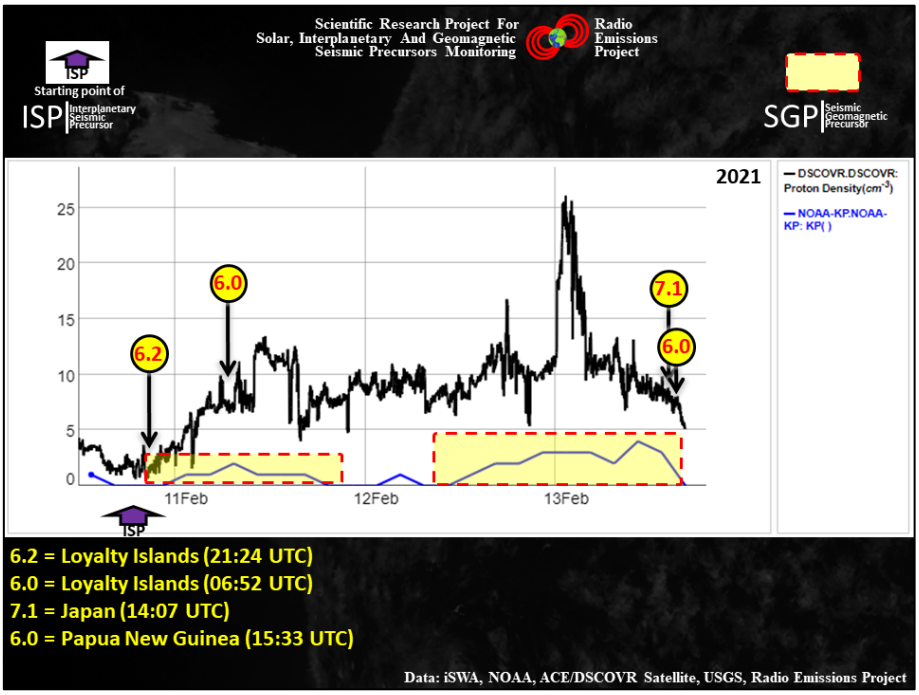

Fig. 3 – Interplanetary and Geomagnetic Seismic Precursors. The graph above shows the temporal markers (black arrows) of the four related seismic events at solar wind proton density increase (Interplanetary Seismic Precursor) recorded between 10 and 24 February 2021. The proton increase produced two geomagnetic increases (Seismic Geomagnetic Precursors) which have been highlighted within the yellow areas. Credits: USGS, Radio Emissions Project.

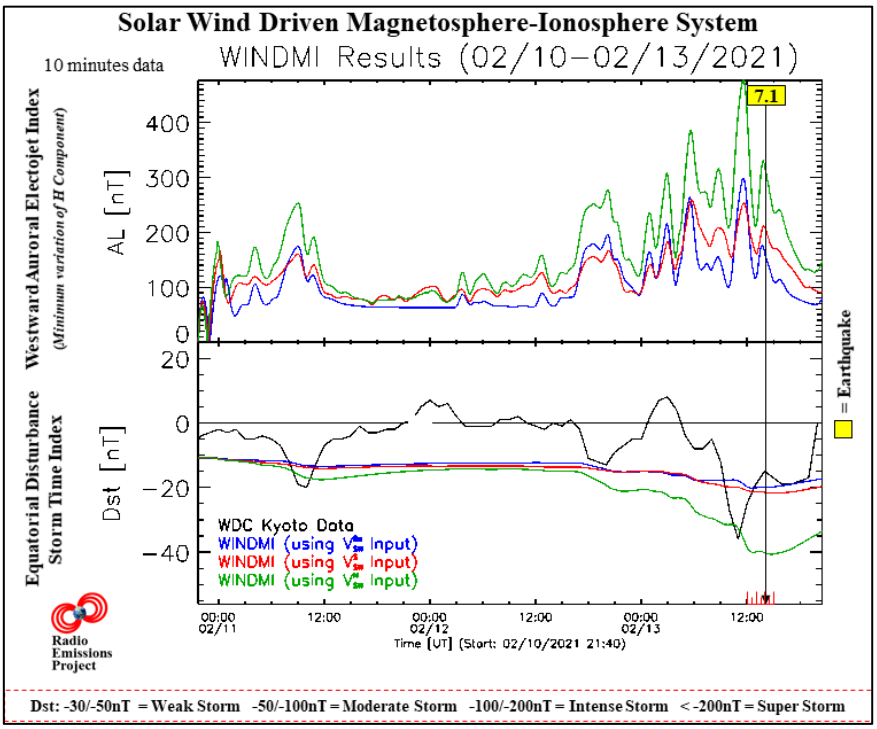

Fig. 4 – Low-dimensional model of the energy transfer from the solar wind through the magnetosphere and into the ionosphere (WINDMI). The picture shows the variation of the AL-Index (at top) and the DST-Index (at bottom) in the hours that preceded the Japanese M7.1 earthquake occurred on February 13, 2021 (the time marker of the earthquake is indicated by a vertical black line). The DST-Index is a direct measure of the Earth's geomagnetic horizontal (H) component variation due to the equatorial ring current, while the AL-Index (Auroral Lower) is at all times, the minimum value of the variation of the geomagnetic H component of the geomagnetic field recorded by observers of reference and provides a quantitative measure of global Westward Auroral Electroject (WEJ) produced by increased of ionospheric currents therein present. Model developed by the Institute for Fusion Studies, Department of Physics, University of Texas at Austin. Credits: iSWA, USGS, Radio Emissions Project.

To confirm the correlation found between solar activity and the M7.1 Japanese earthquake, the authors identified a disturbance of the Interplanetary Magnetic Field (IMF) (**Fig. 4**) that preceded the seismic event by about 18 hours. Furthermore, analyzing the data on the speed of the solar wind, the authors identified a rapid increase in the speed of the solar ion flux that preceded the M7.1 Japanese earthquake by about 24 hours (**Fig. 5**). Both of these phenomena are manifestations of solar electromagnetic activity that have been defined by the authors as "Interplanetary Seismic Precursors" or ISP, since they precede seismic events of high magnitude that are recorded on a global scale.

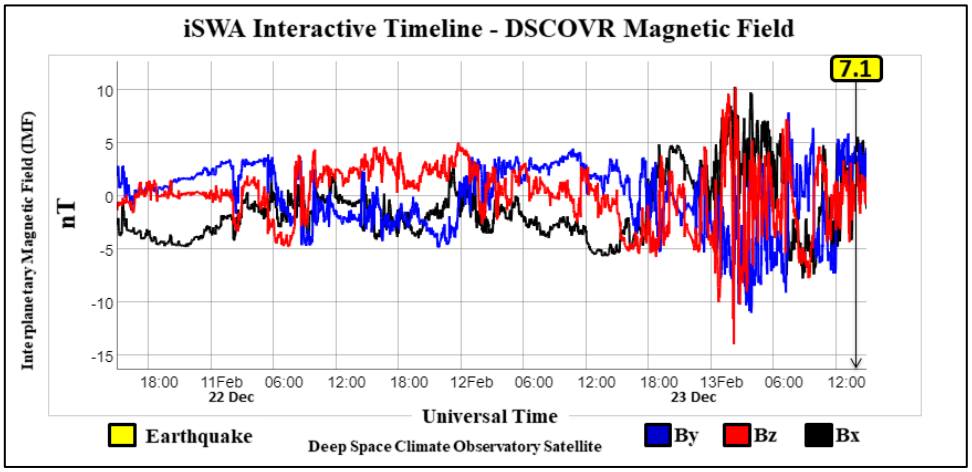

Fig. 4 – Interplanetary Magnetic Field (IMF) related to M7.1 Japan earthquake. The graph above shows a disturbance of Interplanetary Magnetic Field (IMF) which preceded the Japanese M7.1 earthquake recorded on February 13, 2021 by almost 18 hours (black vertical arrow).
Credits: iSWA, USGS, Radio Emissions Project.

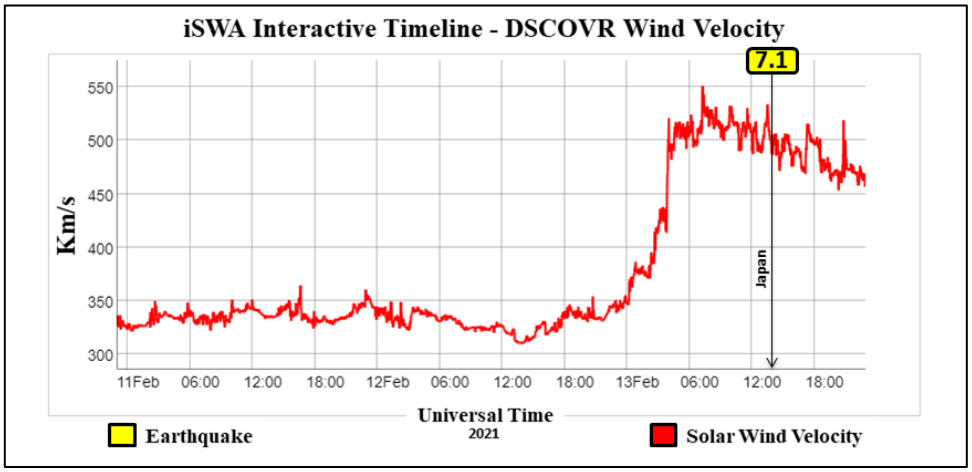

Fig. 5 – Solar wind velocity related to M7.1 Japan earthquake. The graph above shows a rapid increase in the speed of the solar wind that preceded the Japanese M7.1 earthquake recorded on February 13, 2021 (black vertical arrow).
Credits: iSWA, USGS, Radio Emissions Project.

Perturbations of Interplanetary Magnetic Field (IMF) and increases in the speed of the solar ion flow explain, through the coupling function between solar activity and the terrestrial magnetosphere, why an increase in AL Index and DST Index was recorded (**Fig. 4**). From a temporal point of view, solar activity and terrestrial geomagnetic activity show a series of electromagnetic phenomena connected to each other up to the seismic event related to them. By following this chain of electromagnetic events backwards, it was possible to identify a first seismic precursor of the electromagnetic type responsible for the variations in the density of the solar ion flux present in interplanetary space; the authors called this seismic precursor the "Solar Seismic Precursor" or SSP. This term refers to electromagnetic phenomena visible on the photosphere, in the chromosphere and in the solar corona that can also be monitored from the Earth:

a) coronal hole and high speed solar wind (HSSW);
b) sunspots and magnetic loops;
c) solar flare and coronal mass ejections (CMEs);

Conclusions

The monitoring of solar activity combined with the monitoring of the Earth's geomagnetic activity continues to provide important and evident indications about the close correlation that exists between electromagnetic phenomena of solar origin and potentially destructive seismic events that are recorded on our planet [23] [24]. The solar and geomagnetic data that the authors correlated to the Japanese M7.1 earthquake recorded on February 13, 2021 provide a further indication of the potential (in terms of seismic prediction) that monitoring of solar activity and terrestrial geomagnetic activity have. Although the first important studies on this type of correlation were carried out between 1960 and 1970 [25] [26] [27] [28], we can certainly affirm that the basis of a new and innovative seismic forecasting method based on the monitoring and analysis of solar activity and terrestrial geomagnetic activity were built by the authors thanks to the studies conducted in this research area from 2012 to today [24] and thanks to the development of technology dedicated to crustal diagnosis [24].

Credits

[1] G. Cataldi, D. Cataldi, V. Straser. (2013). Variations Of Terrestrial Geomagnetic Activity Correlated To M6+ Global Seismic Activity. EGU (European Geosciences Union) 2013, General Assembly, Seismology Section (SM3.1), Earthquake precursors, bio-anomalies prior to earthquakes and prediction, Geophysical Research Abstracts, Vol. 15. EGU2013-2617, Vienna, Austria. Harvard-Smithsonian Center for Astrophysics, High Energy Astrophysics Division, SAO/NASA Astrophysics Data System.

[2] G. Cataldi, D. Cataldi and V. Straser. (2014). Earth’s magnetic field anomalies that precede the M6+ global seismic activity. European Geosciences Union (EGU) General Assembly 2014, Geophysical Research Abstract, Vol. 16, EGU2014-1068, Vienna, Austria. Natural Hazard Section (NH4.3), Electro-magnetic phenomena and connections with seismo-tectonic activity, Harvard-Smithsonian Center for Astrophysics, High Energy Astrophysics Division, SAO/NASA Astrophysics Data System.

[3] D. Cataldi, G. Cataldi and V. Straser. (2014). Variations of the Electromagnetic field that preceded the Peruvian M7.0 earthquake occurred on September 25, 2013. European Geosciences Union (EGU) General Assembly 2014, Geophysical Research Abstract, Vol. 16, EGU2014-1075, Natural Hazard Section (NH4.3), Electro-magnetic phenomena and connections with seismo-tectonic activity, Vienna, Austria. Harvard-Smithsonian Center for Astrophysics, High Energy Astrophysics Division, SAO/NASA Astrophysics Data System.

[4] T. Rabeh, G. Cataldi, V. Straser. (2014). Possibility of coupling the magnetosphere–ionosphere during the time of earthquakes. European Geosciences Union (EGU) General Assembly 2014, Geophysical Research Abstract, Vol. 16, EGU2014-1067, Vienna, Austria. Natural Hazard Section (NH4.3), Electro-magnetic phenomena and connections with seismo-tectonic activity. Harvard-Smithsonian Center for Astrophysics, High Energy Astrophysics Division, SAO/NASA Astrophysics Data System.

[5] V. Straser, G. Cataldi. (2014). Solar wind proton density increase and geomagnetic background anomalies before strong M6+ earthquakes. Space Research Institute of Moscow, Russian Academy of Sciences, MSS-14. 2014. Moscow, Russia. pp280-286.

[6] V. Straser, G. Cataldi, D. Cataldi. (2015). Radio-anomalies: tool for earthquakes and tsunami forecasts. European Geosciences Union (EGU) General Assembly 2015, Natural Hazard Section (NH5.1), Sea & Ocean Hazard - Tsunami, Geophysical Research Abstract, Vol. 17, Vienna, Austria. Harvard-Smithsonian Center for Astrophysics, High Energy Astrophysics Division, SAO/NASA Astrophysics Data System.

[7] V. Straser, G. Cataldi. (2015). Solar wind ionic variation associated with earthquakes greater than magnitude M6.0. New Concepts in Global Tectonics Journal, V. 3, No. 2, June 2015, Australia. P.140-154.

[8] G. Cataldi, D. Cataldi, V. Straser. (2015). Solar wind proton density variations that preceded the M6+ earthquakes occurring on a global scale between 17 and 20 April 2014. European Geosciences Union (EGU) General Assembly 2015, Vienna, Austria. Natural Hazard Section (NH5.1), Sea & Ocean Hazard - Tsunami, Geophysical Research Abstract, Vol. 17, EGU2015-4157-2, Harvard-Smithsonian Center for Astrophysics, High Energy Astrophysics Division, SAO/NASA Astrophysics Data System.

[9] G. Cataldi, D. Cataldi, V. Straser. (2015). Solar wind ion density variations that preceded the M6+ earthquakes occurring on a global scale between 3 and 15 September 2013. European Geosciences Union (EGU) General Assembly 2015, Geophysical Research Abstract, Vol. 17, EGU2015-4581, Vienna, Austria. Natural Hazard Section (NH5.1), Sea & Ocean Hazard - Tsunami, Harvard-Smithsonian Center for Astrophysics, High Energy Astrophysics Division, SAO/NASA Astrophysics Data System.

[10] G. Cataldi, D. Cataldi, V. Straser. (2015). Solar wind proton density variations that preceded the M6,1 earthquake occurred in New Caledonia on November 10, 2014. European Geosciences Union (EGU) General Assembly 2015, Geophysical Research Abstract, Vol. 17, EGU2015-4167, Vienna, Austria. Natural Hazard Section (NH5.1), Sea & Ocean Hazard - Tsunami, Harvard-Smithsonian Center for Astrophysics, High Energy Astrophysics Division, SAO/NASA Astrophysics Data System.

[11] V. Straser, G. Cataldi, D. Cataldi. (2015). Solar wind ionic and geomagnetic variations preceding the Md8.3 Chile Earthquake. New Concepts in Global Tectonics Journal, V. 3, No. 3, September 2015, Australia. P.394-399.

[12] G. Cataldi, D. Cataldi, V. Straser. (2016). Solar activity correlated to the M7.0 Japan earthquake occurred on April 15, 2016. New Concepts in Global Tectonics Journal, V. 4, No. 2, pp202-208, June 2016.

[13] G. Cataldi, D. Cataldi, V. Straser. (2016). Tsunami related to solar and geomagnetic activity. European Geosciences Union (EGU) General Assembly 2016, Natural Hazard Section (NH5.6), Complex modeling of earthquake, landslide, and volcano tsunami sources. Geophysical Research Abstract, Vol. 18, EGU2016-9626, Vienna, Austria. Harvard-Smithsonian Center for Astrophysics, High Energy Astrophysics Division, SAO/NASA Astrophysics Data System.

[14] G. Cataldi, D. Cataldi, V. Straser. (2017). SELF-VLF electromagnetic signals and solar wind proton density variations that preceded the M6.2 Central Italy earthquake on August 24, 2016. International Journal of Modern Research in Electrical and Electronic Engineering, Vol. 1, No. 1, 1-15. DOI: 10.20448/journal.526/2017.1.1/526.1.1.15.Harvard-Smithsonian Center for Astrophysics, High Energy Astrophysics Division, SAO/NASA Astrophysics Data System.

[15] G. Cataldi, D. Cataldi, V. Straser. (2017). Solar and Geomagnetic Activity Variations Correlated to Italian M6+ Earthquakes Occurred in 2016. European Geosciences Union (EGU), General Assembly 2017. Geophysical Research Abstracts Vol. 19, EGU2017-3681, 2017. Seismology (SM1.2)/Natural Hazards (NH4.7)/Tectonics & Structural Geology (TS5.5) The 2016 Central Italy Seismic sequence: overview of data analyses and source models. Harvard-Smithsonian Center for Astrophysics, High Energy Astrophysics Division, SAO/NASA Astrophysics Data System.

[16] G. Cataldi, D. Cataldi, V. Straser. (2017). Solar wind proton density increase that preceded Central Italy earthquakes occurred between 26 and 30 October 2016. European Geosciences Union (EGU), General Assembly 2017. Geophysical Research Abstracts Vol. 19, EGU2017-3774, 2017. Seismology (SM1.2)/Natural Hazards (NH4.7)/Tectonics & Structural Geology (TS5.5) The 2016 Central Italy Seismic sequence: overview of data analyses and source models. Harvard-Smithsonian Center for Astrophysics, High Energy Astrophysics Division, SAO/NASA Astrophysics Data System.

[17] V. Straser, G. Cataldi, D. Cataldi. (2017). Solar and electromagnetic signal before Mexican Earthquake M8.1, September 2017. New Concepts in Global Tectonics Journal, V. 5, No. 4, December 2017, pp. 600-609.

[18] G. Cataldi, D. Cataldi, V. Straser. (2017). Solar and Geomagnetic Activity Variations Correlated to Italian M6+Earthquakes Occurred in 2016. EGU General Assembly 2017. EGU2017-3681, Vol. 19.

[19] G. Cataldi, D. Cataldi, V. Straser. (2019). Solar wind ionic density variations related to M6+ global seismic activity between 2012 and 2018. European Geosciences Union (EGU) General Assembly 2019, Short-term Earthquake Forecast (StEF) and multy-parametric time-Dependent Assessment of Seismic Hazard (t-DASH) (NH4.3/AS4.62/EMRP2.40/ESSI1.7/Gi2.13/SM3.9), General Contribution on Earthquakes, Earth Structure, Seismology (SM1.1), Geophysical Research Abstract, Vol. 21, EGU2019-3067, 2019, Vienna, Austria. Harvard-Smithsonian Center for Astrophysics, High Energy Astrophysics Division, SAO/NASA Astrophysics Data System.

[20] G. Cataldi. (2020). Precursori Sismici – Monitoraggio Elettromagnetico. Kindle-Amazon, ISNB: 9798664537970. ASIN Code: B08CPDBGX9.

[21] G. Cataldi, D. Cataldi, V. Straser. (2019). Wolf Number Related To M6+ Global Seismic Activity. New Concepts in Global Tectonics Journal, Volume 7, Number 3, December 2019, pp. 178-186.

[22] V. Straser, G. Cataldi, D. Cataldi. (2020). The Space Weather Related to the M7+ Seismic Activity Recorded on a Global Scale between 28 January and 25 March 2020. Acta Scientific Agriculture 4.12 (2020): 55-62.

[23] G. Cataldi, V. Straser, D. Cataldi. (2020). Space Weather related to potentially destructive seismic activity recorded on a global scale. New Concepts in Global Tectonics Journal. Vol.8, No.3, pp. 233-253, December 2020. ISSN 2202-0039.

[24] G. Cataldi. (2021). Radio Emissions Project – A new approach to seismic prediction. Kindle-Amazon, ISNB: 9798709593411.

[25] P. Velinov. (1975). The effect of solar activity on geophysical processes. Bu/g Geofiz. Spis., vol. 1, pp. 51-77.

[26] I. F. Simpson. (1968). Solar activity as a triggering mechanism for earthquakes. Earth and Planet, Sci. Letter, 1968, v.3, No.5, pp. 417-425.

[27] Y. D. Kalinin. (1974). Solar conditionality of days duration change and seismic activity. Krasnoyarsk, Institute of Physics of Siberian Department of USSR Academy of Science, 1974, p.23.

[28] I. K. Gribbin. (1974). The next California earthquake. New York. Walker, 1974, p. 136.

Space weather and geomagnetic activity related to M6+ global seismic activity recorded on February 7, 2021

Gabriele Cataldi[1], Daniele Cataldi[1-2], Valentino Straser[3]

(1) Radio Emissions Project (I). ltpaobserverproject@gmail.com
(2) Fondazione Permanente G. Giuliani - Onlus (I). daniele77c@hotmail.it
(3) Department of Science and Environment UPKL Brussel (B). valentino.straser@gmail.com

Abstract

On February 7, 2021 two M6+ seismic events were recorded on our planet (M6.0 Philippines earthquake, recorded at 04:22:56 UTC; M6.3 Papua New Guinea earthquake, recorded at 05:45:52 UTC). The authors, analyzing the characteristics of solar ion flux and terrestrial geomagnetic activity, verified that the two potentially destructive seismic events were preceded by a solar wind proton density increase and by an increase in terrestrial geomagnetic activity. This type of correlation is already known to the international scientific community thanks to the studies conducted by the authors in this field of research since 2011.

Keywords: proton density increase, seismic precursors, solar activity, geomagnetic activity, solar ion flux.

Introduction

Every year on our planet are recorded on average 129 potentially destructive earthquakes (average calculated on the period 2012-2020) which does not follow a random modulation distribution: the studies conducted by the authors from 2011 to date [1] [4] [5] [6] [7] [8] [9] [10] [11] [12] [13] [14] [15] [16] [17] [18] [19] [20] [21] [22] [23] made it possible to highlight that potentially destructive seismic events are always preceded by an increase in solar activity, and precisely by an increase in the density of the solar ion flux (especially of the proton type) which also influences the terrestrial geomagnetic activity [2] [3] [5] [10] [12] [14] [17] [19] [23]. This work will present some of the results obtained by the authors in this research area: attention will be focused on potentially destructive seismic events recorded on February 7, 2021 (**Fig. 1**):

1. M6.0 Philippines earthquake, recorded on February 7, 2021 at 04:22 UTC;
2. M6.3 Papua New Guinea earthquake, recorded on February 7, 2021 at 05:45 UTC.

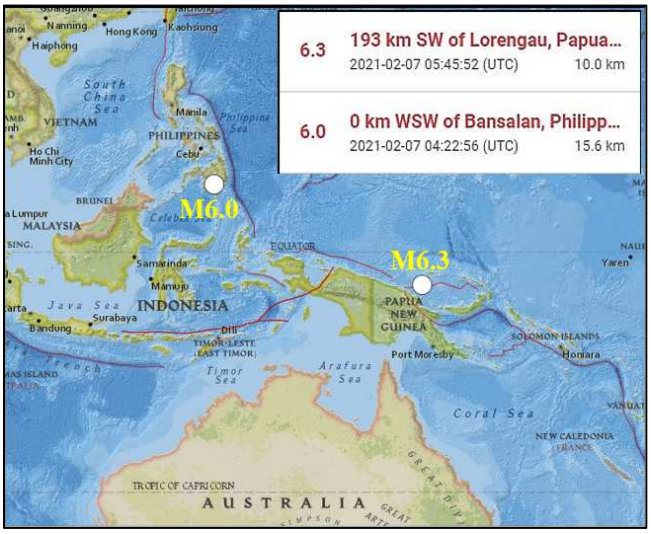

Fig. 1 – Seismic epicenters of potentially destructive earthquakes recorded on February 7, 2021. The map above shows the seismic epicenters of the two potentially destructive earthquakes recorded on February 7, 2021.
Credits: USGS, Radio Emissions Project.

Data analysis

On February 6, 2021 at 04:40 UTC the DSCOVR Satellite, located in Lagrangian orbit L1, provided the first data of a solar wind proton density increase which ended on February 8, 2021 at 12:00 UTC. The peak of this increase was recorded on February 6, 2021 at 16:30 UTC after which two potentially destructive earthquakes were recorded. (**Fig. 1** and **2**):

1. M6.0 Philippines earthquake, recorded on February 7, 2021 at 04:22 UTC;
2. M6.3 Papua New Guinea earthquake, recorded on February 7, 2021 at 05:45 UTC.

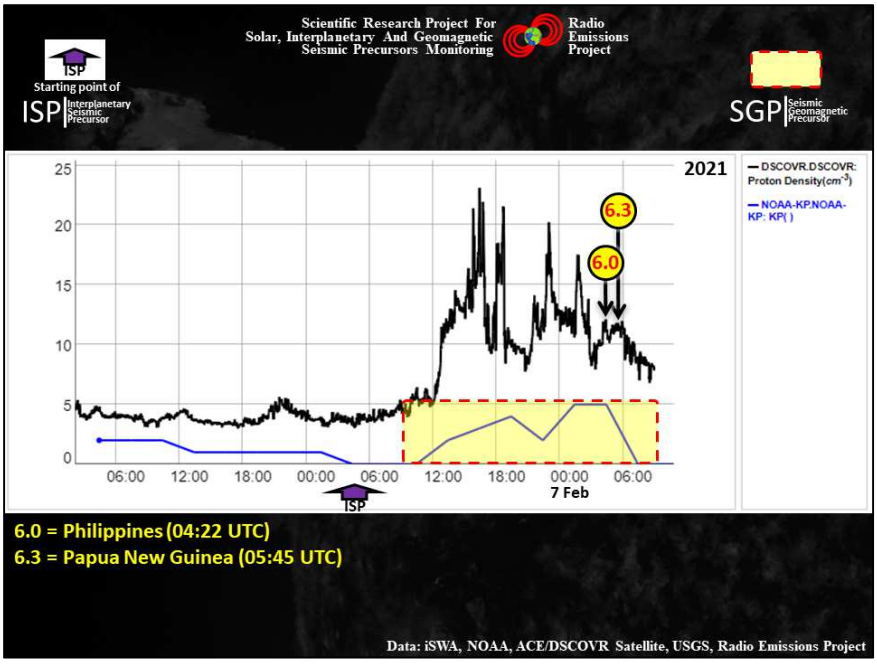

Fig. 2 – Variation in solar ion flux and Earth's geomagnetic activity related to potentially destructive seismic events recorded on February 7, 2021. The graph above shows the time markers of the two M6+ earthquakes recorded on February 7, 2021 and which are correlated to the variation of solar wind proton density (black curve) and a subsequent increase in the Earth's geomagnetic activity (blue curve highlighted by the yellow area). The purple arrow indicates the beginning of the solar wind proton density increase. Credits: iSWA, USGS, Radio Emissions Project.

Analyzing the temporal data of the two seismic events with the space weather data provided by DSCOVR Satellite between 6 and 8 February 2021, the authors were able to calculate the time intervals recorded between the start of the proton increment (Interplanetary Seismic Precursor) and the two M6+ seismic events:

1. M6.0 Philippines earthquake, recorded on February 7, 2021 at 04:22 UTC ≈ **25** hours
2. M6.3 Papua New Guinea earthquake, recorded on February 7, 2021 at 05:45 UTC ≈ **26** hours

The average time interval calculated by analyzing the seismic activity and the solar activity that occurred between January 1, 2012 and February 18, 2021 is equal to 108.8 hours: the average was calculated by analyzing 1192 M6+ seismic events that occurred in the same period (the 100% of M6+ seismic events recorded on a global scale).
Since the increases in solar ion flux also have a significant impact on the Earth's magnetosphere following the coupling function between solar activity and terrestrial geomagnetic activity, the two seismic events analyzed in this work were preceded by an evident increase in the Kp Index which has reached the value of 5 (a level very close to the first degree of geomagnetic storm: G1, Kp=6) (**Fig. 2**).
What has just been stated is evident by analyzing the data on solar wind driven Magnetosphere-Ionosphere system (WINDMI) (**Fig. 3**): the two M6+ seismic events recorded on February 7, 2021 occurred right behind a strong increase in the H component of the Earth's geomagnetic field which has reached 440nT (AL Index). Furthermore, at the same time the DST Index showed that a weak geomagnetic storm was in progress. These perturbations of the Earth's geomagnetic field have been defined by the authors as "Seismic Geomagnetic Precursors" or SGPs.

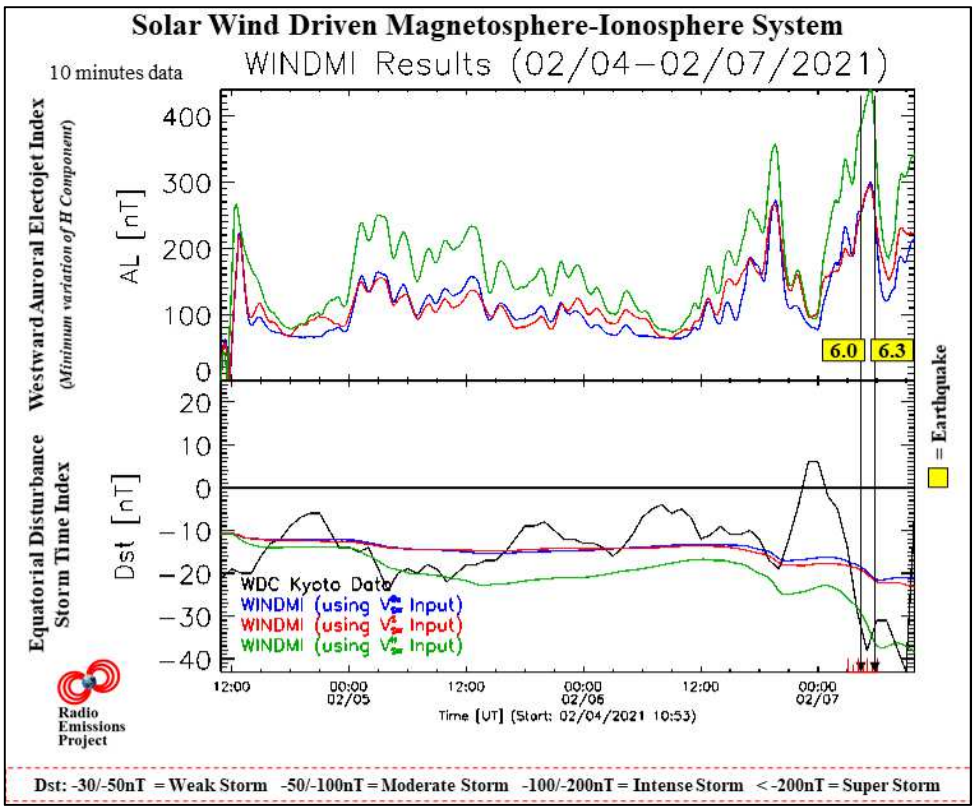

Fig. 3 – Low-dimensional model of the energy transfer from the solar wind through the magnetosphere and into the ionosphere (WINDMI). The picture shows the variation of the AL-Index (at top) and the DST-Index (at bottom) in the hours that preceded the M6+ earthquakes recorded on February 7, 2021 (the time marker of the earthquakes is indicated by a vertical black line). The DST-Index is a direct measure of the Earth's geomagnetic horizontal (H) component variation due to the equatorial ring current, while the AL-Index (Auroral Lower) is at all times, the minimum value of the variation of the geomagnetic H component of the geomagnetic field recorded by observers of reference and provides a quantitative measure of global Westward Auroral Electroject (WEJ) produced by increased of ionospheric currents therein present. Model developed by the Institute for Fusion Studies, Department of Physics, University of Texas at Austin. Credits: iSWA, USGS, Radio Emissions Project.

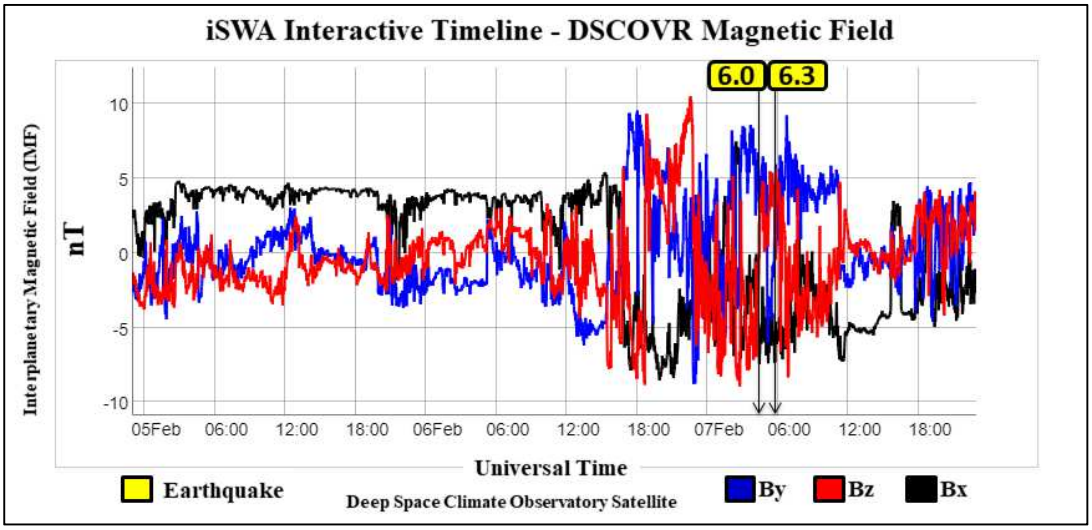

Fig. 4 – Interplanetary Magnetic Field (IMF) related to M6+ seismic events recorded on February 7, 2021. The graph above shows a perturbation of Interplanetary Magnetic Field (IMF) which preceded the two M6+ seismic events recorded on February 7, 2021 (black vertical arrows) by 18 hours. Credits: iSWA, USGS, Radio Emissions Project.

This type of correlation confirms the clear and close relationship that solar activity and terrestrial geomagnetic activity have with respect to the M6+ seismic activity that is recorded on our planet. From a predictive point of view, it is possible to use this type of analysis to predict in advance when to expect a resumption of M6+ global seismic activity and to issue a state of general alert useful to all those countries that are located in

seismically active areas with a high seismic risk to prepare for a possible high intensity earthquake. This is possible thanks to the results that the authors have obtained from 2012 to today [19] [22] [23], that is, since they ascertained that every potentially destructive seismic event that is recorded on our planet is always preceded by an increase in solar ion flux density (Interplanetary Seismic Precursor or ISP). Over the last eight years, the authors have had the opportunity to present these results several times to the international scientific community but the discovery has not had the right media echo and the right scientific recognition which, it is right to reiterate, is unprecedented in the history of scientific research dedicated to seismic prediction.

To confirm the correlation that the authors found between solar activity and the two potentially destructive seismic events recorded on February 7, 2021, you can see the next two graphs (**Fig. 4** and **5**).

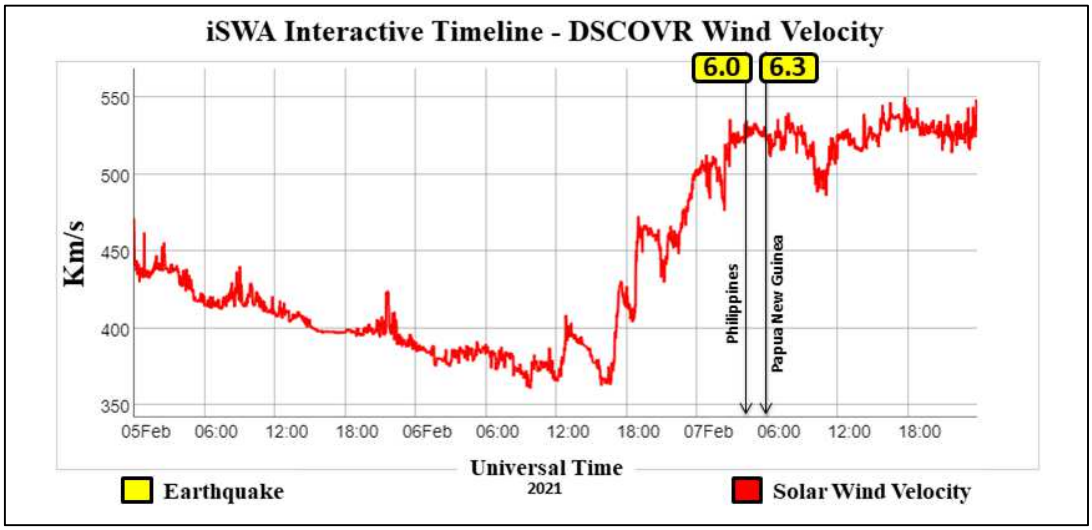

Fig. 5 – Solar wind velocity related to M6+ seismic events recorded on February 7, 2021. The graph above shows a rapid increase in the solar wind speed that preceded the two potentially destructive seismic events recorded on February 7, 2021 (vertical black arrows).
Credits: iSWA, USGS, Radio Emissions Project.

The perturbation of the Interplanetary Magnetic Field (IMF) visible in **Fig. 4** confirms that the Earth has been reached by a dense solar ion flux; while **Fig. 5** confirms that this flow had a high speed. In both cases, both the perturbation of the Interplanetary Magnetic Field and the increase in the speed of the solar wind have been defined by the authors as "Interplanetary Seismic Precursors" or ISPs. The "Interplanetary Seismic Precursors" always precede the "Seismic Geomagnetic Precursors" (**Fig. 3**) [19] [22] [23]: in both cases it is always a direct or indirect expression of solar activity, and is therefore we must turn our attention to the Sun if we want to create an innovative seismic forecasting method.

Conclusions

The term "Seismic Prediction" has evolved so much over the decades that it has undergone a conceptual split through the word "Forecast" and the word "Forecast". When we talk about "Seismic Forecast" we refer to a series of scientific methods through which it is possible to make seismic predictions by analyzing statistical data (for example, historical seismometric data); otherwise, when we talk about "Seismic Prevision" we refer to a scientific method through which it is possible to make seismic prediction using one or more physical phenomena that precede the expected seismic event. Today, research on earthquake prediction is focused on the term "Prevision" rather than the word "Forecast" and we can say it seems beyond doubt that the authors have shown many times that have identified a physical phenomenon that allows us to understand (on average well in advance) when a resumption of M6+ seismic activity can occur on Earth [19] [22] [23].

Credits

[1] G. Cataldi, D. Cataldi, V. Straser. (2013). Variations Of Terrestrial Geomagnetic Activity Correlated To M6+ Global Seismic Activity. EGU (European Geosciences Union) 2013, General

Assembly, Seismology Section (SM3.1), Earthquake precursors, bio-anomalies prior to earthquakes and prediction, Geophysical Research Abstracts, Vol. 15. EGU2013-2617, Vienna, Austria. Harvard-Smithsonian Center for Astrophysics, High Energy Astrophysics Division, SAO/NASA Astrophysics Data System.

[2] G. Cataldi, D. Cataldi and V. Straser. (2014). Earth's magnetic field anomalies that precede the M6+ global seismic activity. European Geosciences Union (EGU) General Assembly 2014, Geophysical Research Abstract, Vol. 16, EGU2014-1068, Vienna, Austria. Natural Hazard Section (NH4.3), Electro-magnetic phenomena and connections with seismo-tectonic activity, Harvard-Smithsonian Center for Astrophysics, High Energy Astrophysics Division, SAO/NASA Astrophysics Data System.

[3] D. Cataldi, G. Cataldi and V. Straser. (2014). Variations of the Electromagnetic field that preceded the Peruvian M7.0 earthquake occurred on September 25, 2013. European Geosciences Union (EGU) General Assembly 2014, Geophysical Research Abstract, Vol. 16, EGU2014-1075, Natural Hazard Section (NH4.3), Electro-magnetic phenomena and connections with seismo-tectonic activity, Vienna, Austria. Harvard-Smithsonian Center for Astrophysics, High Energy Astrophysics Division, SAO/NASA Astrophysics Data System.

[4] T. Rabeh, G. Cataldi, V. Straser. (2014). Possibility of coupling the magnetosphere–ionosphere during the time of earthquakes. European Geosciences Union (EGU) General Assembly 2014, Geophysical Research Abstract, Vol. 16, EGU2014-1067, Vienna, Austria. Natural Hazard Section (NH4.3), Electro-magnetic phenomena and connections with seismo-tectonic activity. Harvard-Smithsonian Center for Astrophysics, High Energy Astrophysics Division, SAO/NASA Astrophysics Data System.

[5] V. Straser, G. Cataldi. (2014). Solar wind proton density increase and geomagnetic background anomalies before strong M6+ earthquakes. Space Research Institute of Moscow, Russian Academy of Sciences, MSS-14. 2014. Moscow, Russia. pp280-286.

[6] V. Straser, G. Cataldi. (2015). Solar wind ionic variation associated with earthquakes greater than magnitude M6.0. New Concepts in Global Tectonics Journal, V. 3, No. 2, June 2015, Australia. P.140-154.

[7] G. Cataldi, D. Cataldi, V. Straser. (2015). Solar wind proton density variations that preceded the M6+ earthquakes occurring on a global scale between 17 and 20 April 2014. European Geosciences Union (EGU) General Assembly 2015, Vienna, Austria. Natural Hazard Section (NH5.1), Sea & Ocean Hazard - Tsunami, Geophysical Research Abstract, Vol. 17, EGU2015-4157-2, Harvard-Smithsonian Center for Astrophysics, High Energy Astrophysics Division, SAO/NASA Astrophysics Data System.

[8] G. Cataldi, D. Cataldi, V. Straser. (2015). Solar wind ion density variations that preceded the M6+ earthquakes occurring on a global scale between 3 and 15 September 2013. European Geosciences Union (EGU) General Assembly 2015, Geophysical Research Abstract, Vol. 17, EGU2015-4581, Vienna, Austria. Natural Hazard Section (NH5.1), Sea & Ocean Hazard - Tsunami, Harvard-Smithsonian Center for Astrophysics, High Energy Astrophysics Division, SAO/NASA Astrophysics Data System.

[9] G. Cataldi, D. Cataldi, V. Straser. (2015). Solar wind proton density variations that preceded the M6,1 earthquake occurred in New Caledonia on November 10, 2014. European Geosciences

Union (EGU) General Assembly 2015, Geophysical Research Abstract, Vol. 17, EGU2015-4167, Vienna, Austria. Natural Hazard Section (NH5.1), Sea & Ocean Hazard - Tsunami, Harvard-Smithsonian Center for Astrophysics, High Energy Astrophysics Division, SAO/NASA Astrophysics Data System.

[10] V. Straser, G. Cataldi, D. Cataldi. (2015). Solar wind ionic and geomagnetic variations preceding the Md8.3 Chile Earthquake. New Concepts in Global Tectonics Journal, V. 3, No. 3, September 2015, Australia. P.394-399.

[11] G. Cataldi, D. Cataldi, V. Straser. (2016). Solar activity correlated to the M7.0 Japan earthquake occurred on April 15, 2016. New Concepts in Global Tectonics Journal, V. 4, No. 2, pp202-208, June 2016.

[12] G. Cataldi, D. Cataldi, V. Straser. (2016). Tsunami related to solar and geomagnetic activity. European Geosciences Union (EGU) General Assembly 2016, Natural Hazard Section (NH5.6), Complex modeling of earthquake, landslide, and volcano tsunami sources. Geophysical Research Abstract, Vol. 18, EGU2016-9626, Vienna, Austria. Harvard-Smithsonian Center for Astrophysics, High Energy Astrophysics Division, SAO/NASA Astrophysics Data System.

[13] G. Cataldi, D. Cataldi, V. Straser. (2017). SELF-VLF electromagnetic signals and solar wind proton density variations that preceded the M6.2 Central Italy earthquake on August 24, 2016. International Journal of Modern Research in Electrical and Electronic Engineering, Vol. 1, No. 1, 1-15. DOI: 10.20448/journal.526/2017.1.1/526.1.1.15.Harvard-Smithsonian Center for Astrophysics, High Energy Astrophysics Division, SAO/NASA Astrophysics Data System.

[14] G. Cataldi, D. Cataldi, V. Straser. (2017). Solar and Geomagnetic Activity Variations Correlated to Italian M6+ Earthquakes Occurred in 2016. European Geosciences Union (EGU), General Assembly 2017. Geophysical Research Abstracts Vol. 19, EGU2017-3681, 2017. Seismology (SM1.2)/Natural Hazards (NH4.7)/Tectonics & Structural Geology (TS5.5) The 2016 Central Italy Seismic sequence: overview of data analyses and source models.Harvard-Smithsonian Center for Astrophysics, High Energy Astrophysics Division, SAO/NASA Astrophysics Data System.

[15] G. Cataldi, D. Cataldi, V. Straser. (2017). Solar wind proton density increase that preceded Central Italy earthquakes occurred between 26 and 30 October 2016. European Geosciences Union (EGU), General Assembly 2017. Geophysical Research Abstracts Vol. 19, EGU2017-3774, 2017. Seismology (SM1.2)/Natural Hazards (NH4.7)/Tectonics & Structural Geology (TS5.5) The 2016 Central Italy Seismic sequence: overview of data analyses and source models. Harvard-Smithsonian Center for Astrophysics, High Energy Astrophysics Division, SAO/NASA Astrophysics Data System.

[16] V. Straser, G. Cataldi, D. Cataldi. (2017). Solar and electromagnetic signal before Mexican Earthquake M8.1, September 2017. New Concepts in Global Tectonics Journal, V. 5, No. 4, December 2017. pp600-609.

[17] G. Cataldi, D. Cataldi, V. Straser. (2017). Solar and Geomagnetic Activity Variations Correlated to Italian M6+Earthquakes Occurred in 2016. EGU General Assembly 2017. EGU2017-3681, Vol. 19.

[18] G. Cataldi, D. Cataldi, V. Straser. (2019). Solar wind ionic density variations related to M6+ global seismic activity between 2012 and 2018. European Geosciences Union (EGU) General

Assembly 2019, Short-term Earthquake Forecast (StEF) and multy-parametric time-Dependent Assessment of Seismic Hazard (t-DASH) (NH4.3/AS4.62/EMRP2.40/ESSI1.7/Gi2.13/SM3.9), General Contribution on Earthquakes, Earth Structure, Seismology (SM1.1), Geophysical Research Abstract, Vol. 21, EGU2019-3067, 2019, Vienna, Austria. Harvard-Smithsonian Center for Astrophysics, High Energy Astrophysics Division, SAO/NASA Astrophysics Data System.

[19] G. Cataldi. (2020). Precursori Sismici – Monitoraggio Elettromagnetico. Kindle-Amazon, ISNB: 9798664537970. ASIN Code: B08CPDBGX9.

[20] G. Cataldi, D. Cataldi, V. Straser. (2019). Wolf Number Related To M6+ Global Seismic Activity. New Concepts in Global Tectonics Journal, Volume 7, Number 3, December 2019, pp. 178-186.

[21] V. Straser, G. Cataldi, D. Cataldi. (2020). The Space Weather Related to the M7+ Seismic Activity Recorded on a Global Scale between 28 January and 25 March 2020. Acta Scientific Agriculture 4.12 (2020): 55-62.

[22] G. Cataldi, V. Straser, D. Cataldi. (2020). Space Weather related to potentially destructive seismic activity recorded on a global scale. New Concepts in Global Tectonics Journal. Vol.8, No.3, pp.233-253, December 2020. ISSN 2202-0039.

[23] G. Cataldi. (2021). Radio Emissions Project – A new approach to seismic prediction. Kindle-Amazon, ISNB: 9798709593411.

THE SIGNIFICANCE OF VERTICAL DYKES IN EARTH HISTORY

Cliff OLLIER

School of Earth and Environment, The University of Western Australia,
Crawley, W.A. 6009, Australia

cliff.ollier@uwa.edu.au

Abstract:

All over the world dykes in the crust of the Earth are vertical. This shows that the crust was never folded after dyke intrusion. Yet dykes go back to the Proterozoic. Only piles of sedimentary strata are folded, and the best explanation for that is gravity tectonics. Folded strata are never refolded after dyke intrusion. These observations suggest that models of global tectonics need much revision.

Keywords: dykes, vertical, folding, gravity tectonics

Introduction

NCGT published my first paper on dykes (Ollier 2011) and a more extensive treatment was published a year later (Ollier, 2012a). These papers were about the space-filling properties of dykes, which cause extension such as the 6.8% extension in Arran, Scotland, and the extension of an 80 km wide strip in Iceland by 5 km between 1975 and 1985. The story was elaborated in a book chapter (Ollier, 2020) but this time a new topic was introduced:

> ***Significance of Vertical Dykes:*** *Most dykes and dyke swarms are nearly vertical, indicating that the intruded rocks have not been folded since the dykes were intruded. The crust has remained essentially stable, which rules out significant compression and folding the in area. And this is most of the Earth's surface. Dykes not only signify crustal extension but also the lack of compression. Their very existence undermines many ideas of compression, folding and mountain building.*

Dyke swarms occur all over the world and throughout Earth history. The remarkable fact, which has drawn very little attention before, is that virtually all dyke swarms consist of dykes that are vertical or very near vertical. This shows that wherever there is a dyke swarm the crust has not been folded after the dyke intrusion.

The present article expands on this topic.

The evidence

There are thousands of reports of vertical dykes, and several volumes of collected papers (e.g. Hanski et al. 2006; Srivastava et al. 2020) with abundant regional details, but virtually no comment on the significance of the verticality. Here are few illustrative examples to show the range.

The largest dyke swarm on Earth is probably the Mackenzie dyke swarm in the Canadian Shield, which is about 3,000 km long 500 km wide, and about 1270 Ma old. Ernst and Baragar (1992) report that the dykes are vertical. **"**Our results indicate that magma was injected vertically" The Canadian Shield has not been folded since Archaean times.

Many Proterozoic and Palaeozoic dykes show the same (e.g., Macouin et al. 2003; Polyansky et al. 2017).

When we get to the Mesozoic, we find many more examples. For instance, Lopez de Luchia and Rapalinib (2002) describe the role of Middle Jurassic volcanism in the evolution of Patagonia, Argentina. "Regional, structural, and, to a certain extent, petrological evidence for the Middle Jurassic dyke swarms of the Sierra de Mamil Choique point to an extensional intracontinental tectonic setting in which older structures controlled the development of the volcanism".

Amato et al. (2003) describe Late Cretaceous dyke swarms on Seward Peninsula in northwestern Alaska, which represent the youngest local manifestation of a 115–75 Ma magmatic event in the Bering Strait region. The orientation of dykes and normal faults suggest that between 110 and 90 Ma extension was generally oriented NS to NNW-SSE.

Velazquez et al. (2011) describe a Cretaceous dyke swarm in Paraguay associated with the Asuncion Rift. The morphological features, the regional en-echelon distribution, and the NW-SE orientation pattern suggest that the dykes were injected along fractures under a tensional tectonic regime. The pattern of orientation of dykes is consistent, temporally and spatially, with the phases of regional deformation that occurred during the process of the Atlantic Ocean opening.

Wingate and Giddings (2000) studied dykes intruding Archean and Proterozoic sedimentary rocks in the Pilbara Craton, Western Australia, and note that all dykes observed during their study dip within 5° of vertical and appear to be undeformed.

Dyke injection continues to the present time. Steinthorsson and Thoraninsson (1997) report dyke intrusion between 1975 and 1985 in part of northern Iceland.

The extensive Harrat lava province of Arabia formed during the past 30 million years in response to Red Sea rifting. Between April and June 2009 a swarm of more than 30,000 earthquakes struck in northwest Saudi Arabia. Pallister et al. (2010) used geologic, geodetic and seismic data to show that the earthquakes resulted from intrusion of a dyke about 10 km long.

The only exceptions seem to be when the rocks are so deeply buried that they undergo metamorphism and deformation. For example some dykes are deformed in Dronning Maud Land, Antarctica, where dykes were emplaced at ~900–1000 Ma and 'folded' at ~460–530 Ma (Grantham et al. 2006). This action took place in the plastic depths of the Earth, not in the crust.

The significance of verticality

Archaean dykes are vertical but are generally intruded into metamorphic rocks or granites so cannot be related to any earlier folding. In Phanerozoic rocks dykes often intrude folded sedimentary rocks. So in the latter we have a history of deposition > folding > dyke intrusion > no more folding. In plain words, in a place with folds and dykes, the folds came first, and the dykes second, and there is never any further folding after dyke intrusion.

If the crust was folded after insertion of dykes, then some of the dykes must be inclined (Fig. 1), Suppose dykes are intruded into horizontal strata. After folding, the limbs of the folds would have a dip. If a limb dipped at 45° than the dykes would be tilted at 45°. If the limb had a dip of 30°, the dyke would dip at 60°. This has never been observed anywhere in the world.

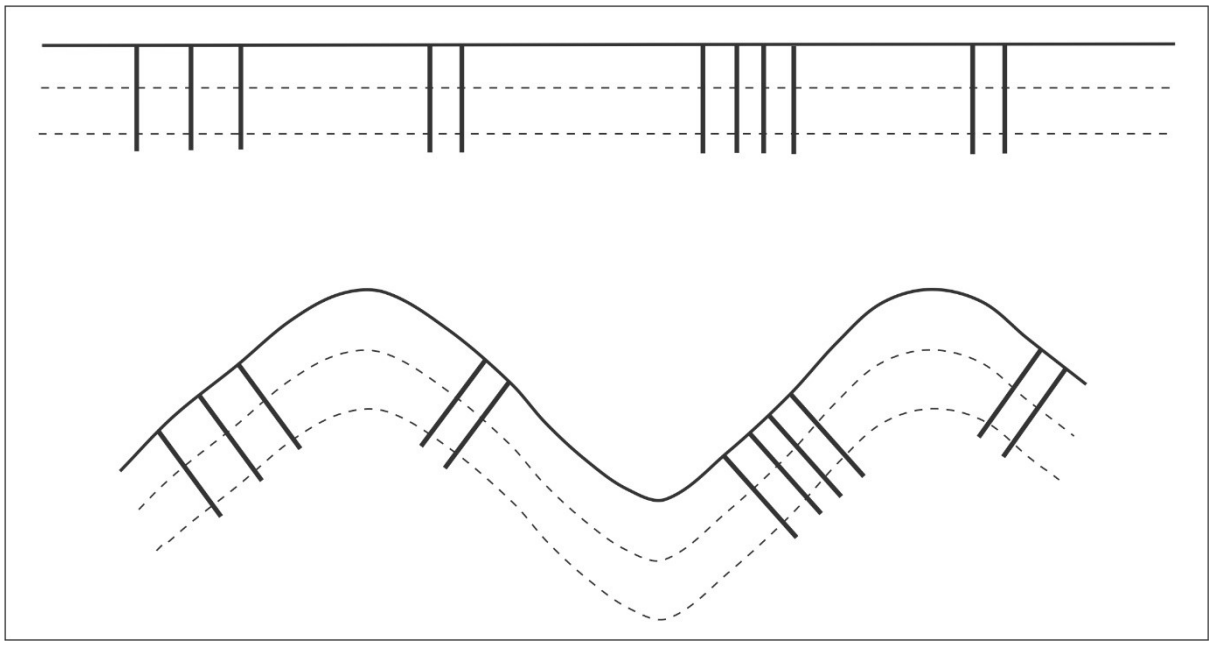

Figure 1. Top. Vertical dykes. For simplicity they are intruded into horizontal strata. Bottom. After folding the dykes would be inclined, as explained in the text.

Somehow the dykes seem to freeze or fix that part of the Earth's crust so it is no longer capable of folding. Perhaps more surprisingly, folding occurs only in rocks that have not previously been intruded by dykes. It seems that we are not able to fold the crust of the Earth, but nevertheless some stratified rocks have been folded. How?

The folding of stratified rocks

The common idea that folding occurs by compression of the Earth's crust. If this were so it should apply to both crust with dykes and crust without dykes. Yet thousands of examples show that folding has not occurred since the crust was intruded by dykes. But how can this be?

The universal verticality of dykes invalidates arguments for folding rocks by compression, by plate tectonics (described later) or any other mechanism (many are described in structural geology textbooks of pre-plate tectonic times). So what mechanism remains that can fold stratified rocks?

The best possibility as I see it is gravity tectonics, which has been suggested repeatedly by many authors (Van Bemmelen, 1955; De Jong and Scholten, 1973; De Sitter, 1952; Korn and Martin, 1959; Rubey and Hubbert, 1959). It is not possible to describe all the evidence here, but I can mention a few salient points.

Folded rocks are found to be underlain by an unfolded unconformity or glide plane, so the upper folded rocks were folded independently. A classic example is the Jura Mountains. The Jura folds are often likened to the folds that can be generated in a tablecloth when pushed across a table. The table doesn't fold, but the tablecloth does. This homely analogy is very misleading, for there is no geological equivalent of the moving hand that does the pushing and it folds where the hand is, not at the other end of the table. It is simply not possible to push a sheet of rocks sideways like a tablecloth. If the table were tilted and the cloth slid down into folds the analogy is better, and works under gravity, and the folds are at the lower end of the table. Many examples are known where vast sheets of sedimentary rock have been apparently pushed over a hundred kilometres over a basement. In plate tectonics this is called thin-skinned tectonics.

Perhaps the finest example of gravity-slide tectonics is provided by the Naukluft Mountains in southwest Africa, described in masterly fashion by Korn and Martin (1959). The basement bedrock of Precambrian rocks is unfolded, but is overlain by a series of intensely folded rocks which evidently moved from northwest to southeast. The intensity of deformation increases to the southeast, where imbricate structure are found. This is the effect of breakers-at-the-nappe-front found in many Alpine fold regions.

But there is an even more remarkable feature in the Naukluft. After the faulted and folded rocks were emplaced, they were eroded to a plain, and then a new series of sedimentary rocks were deposited unconformably on the lower, folded and faulted series. The upper series would have been nearly horizontal originally, but this upper series later underwent another phase of folding and thrusting. It slid down the unconformity and was intensely deformed without any effect on the underlying rocks.

The unconformity between the two sets of folded rocks is marked by a distinctive yellow dolomite only five to ten metres thick which evidently provided the lubricated layer allowing decollement of the overlying mass. Even so the lower part of the dolomite is virtually undisturbed, and the upper part becomes gradually deformed towards the upper adjacent rocks. A slab of rocks several kilometres thick slid on a lubricated plane over a dolomite layer only ten metres thick, and without disturbing any of the underlying rocks at all. There can be no question of crustal shortening or subduction here. Everything points to gravity sliding on a huge scale.

Perhaps the best example of large-scale gravity sliding in action is seen in the Niger delta, which consists of Tertiary marine and fluvial deposits. Structurally it has fold and thrust belts, sometimes separated from one another by several kilometres of undeformed strata. The deformation of the Niger Delta is driven by gravitational collapse of shelf sediments (Bilotti and Shaw, 2005). This style of gravitationally driven systems is common in passive-margin deltas (Rowan et al., 2004), including the Gulf of Mexico basin (e.g., Peel et al., 1995).

The Niger Delta is on the same scale as many 'fold mountain' belts and has many of the features of an Alpine Fold Belt, but it has never been mountainous – indeed not above sea level. In many ancient settings the thrusting at the front would be interpreted in plate tectonic terms as the results of subduction, but the Niger Delta is on a passive margin and subduction is impossible. The major features are shown in Fig. 2.

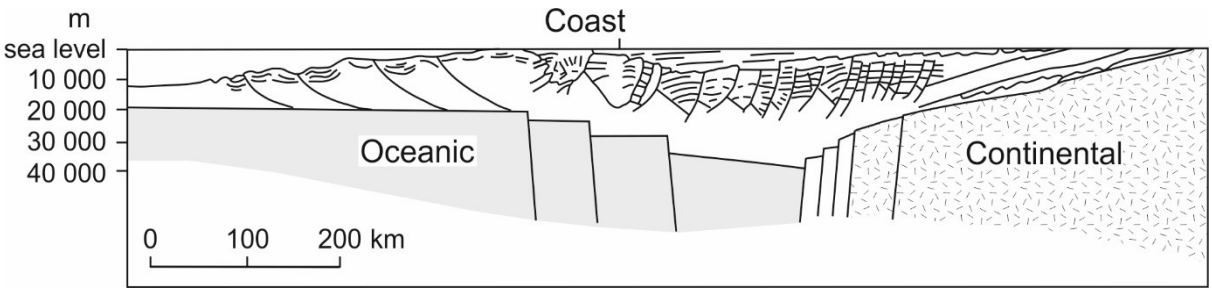

Fig. 2. The Niger Delta, showing many features of an orogen, with normal faulting at the back and thrusts at the front, entirely due to gravity (after Evamy et al. 1979).

It is worth stressing some general aspects of gravity tectonics. Folding of rocks by gravity sliding has nothing to do with compression of colliding plates or shrinking Earth ideas. Such folding, although commonly called 'orogeny', has nothing to do with mountain building, as explained in detail by Ollier and Pain (2000). It is not possible to fold rocks by a lateral push, as suggested by ideas of folded tablecloths or squashed clay in a squeeze-box. The compressive strength of rock is very much lower than the force needed to push a slab of strata a few kilometres thick and hundreds of kilometres wide. If a force capable of moving such a slab were somehow applied, the slab would not move but would simply be crushed where the force was applied. Gravity applies a *body force* that acts on every grain, every molecule in the rock mass and affects the whole mass in a way that an *applied force* cannot do.

Plate tectonics and dykes

In plate tectonics mountains are said to be caused by compression at Active Margins where plates collide. A few quotes from the internet provide simple examples:

"Fold mountains are created where two or more of Earth's tectonic plates are pushed together, often at regions known as convergent plate boundaries and continental collision zones."

"Fold mountains are formed when two plates move together (a compressional plate margin)."

"Fold mountains form when two tectonic plates move towards each other at a convergent plate boundary. When plates and the continents riding on them collide, the accumulated layers of rock may crumple and fold like a tablecloth that is pushed across a table," (Wikipedia).

Similar statements are to be found in many textbooks in explaining mountains at collision sites.

But many mountains are not on collision sites, so how are they formed? One explanation is offered by Owen (2004): "These 'ancient' mountain systems generally have little or no relationship to the present lithospheric plate boundaries and may have begun to have formed many hundreds of millions of years ago." In other words they were formed like the young, active margin mountains but were formed further back in time. Unfortunately, this is not found to be true when we determine the real age of mountain building (Ollier and Pain, 2000; 2020).

If mountains were formed in this way, any dykes present must have been tilted as explained earlier, and this is not found. Colliding plates should be compressing crust regardless of the presence of old dykes. If the Pacific Plate is subducted under South America then one might expect folding of the rocks in the coastal cordillera, but this is not found.

For instance all along the Pacific margin of the Americas there are numerous accounts of dykes, and they are all vertical. Furthermore, there are many other indications of extension in these allegedly compressed areas (Ollier, 2012b).

Conclusion

Vertical dykes indicate that in Earth history folding of the crust does not occur. Folding of sedimentary rocks is found, but is best explained by gravity tectonics.

If this is so then many conventional ideas, including plate tectonics and the geological cycle, need great revision.

References

Amato, J.M., Miller, E.L., Wright, J.E. and McIntosh, W.C., 2003. Dike swarms on Seward Peninsula, Alaska, and their implications for the kinematics of Cretaceous extension in the Bering Strait region. *Canadian Journal of Earth Sciences* 40(6), 865-886 https://doi.org/10.1139/e03-019.

Bilotti, F. and Shaw, J.H., 2005. Deep-water Niger Delta fold and thrust belt modeled as a critical-taper wedge: The influence of elevated basal fluid pressure on structural styles. *AAPG Bulletin*, 89, 1475–1491.

De Jong, K.A. and Scholten, R. (Editors) 1973. *Gravity and Tectonics*. Wiley-Interscience, New York, 502pp.

De Sitter, L.U. 1952. Pliocene uplift of Tertiary mountain chains. *American Journal of Science* 250, 297-307.

Ernst, R.E. and Baragar, W.R.A., 1992. Evidence from magnetic fabric for the flow pattern of magma in the Mackenzie giant radiating dyke swarm. *Nature* 356, 511-513.

Evamy, B.D., Haremboure, J., Kamerling, P., Knaap, W.A., Molloy, F.A. and Rowlands, P.H., 1978. Hydrocarbon habitat of Tertiary Niger delta. *AAPG Bulletin* 62, 1-39.

Grantham, G. H., Armstrong, R. and Moyes, A. B. 2006. The geology of a mafic dyke at Roerkulten, Sverdrupfjella, western Dronning Maud Land, Antarctica. In Hanski, E., Mertanen, S., Ramo, T. and Vuollo, J. (Editors). *Dyke Swarms - Time Markers of Crustal Evolution*. Selected Papers of the Fifth International Dyke Conference in Finland, Rovaniemi, Finland, 31 July- 3 Aug 2005 and Fourth International Dyke Conference, Kwazulu-Natal, South Africa 26-29 June 2001. Routledge, 213- 224.

Hanski, E., Mertanen, S., Rämö, T. and Vuollo, J. (Editors) 2006. Dyke Swarms - Time Markers of Crustal Evolution. Proceedings of the Fifth International Dyke Conference, Rovaniemi, Finland, 31 July-3 Aug 2005, and the Fourth International Dyke Conference, Kwazulu-Natal, South Africa 26-29 June 2001 Taylor and Francis, 272pp.

Korn, H. and Martin, H. 1959. Gravity tectonics in the Naukluft Mountains of South-West Africa. *Bulletin of the Geological Society of America* 70, 1047-1078.

Lopez de Luchi, M. and Rapalini, A.E. 2002. Middle Jurassic dyke swarms in the North Patagonian Massif: the Lonco Trapial Formation in the Sierra de Mamil Choique, Río Negro province, Argentina. *Journal of South American Earth Sciences* 15, 625-641. DOI: 10.1016/S0895-9811(02)00083-4.

Macouin, M., Valet, J.P., Besse, J., Buchan, K., Ernst, R., LeGoff, M. and Scharer, U., 2003. Low paleointensities recorded in 1 to 2.4 Ga Proterozoic dykes, Superior province, Canada. *Earth and Planetary Science Letters* 213, 79-95.

Ollier, C.D. 2011, Dykes, Global Tectonics and Extension. *New Concepts in Global Tectonics* 59, 49-54.

Ollier, C.D. 2012a. Dykes, crustal extension and global tectonics. In Scalera, G., Boschi, E. and Cwojdzinski, S. (Editors). *The Earth Expansion Evidence – a Challenge for Geology, Geophysics and Astronomy*. Selected contributions to the interdisciplinary workshop of the 37th International School of Geophysics EMFCSC, Erice (4-9 October 2011), 207-304.

Ollier, C.D. 2012b. Extension everywhere: rifts, continental margins and island arcs. In Scalera, G., Boschi, E. and Cwojdzinski, S. (Editors). *The Earth Expansion Evidence – a Challenge for Geology, Geophysics and Astronomy*. Selected contributions to the interdisciplinary workshop of the 37th International School of Geophysics EMFCSC, Erice (4-9 October 2011), 61-76.

Ollier, C.D. and Pain, C.F. 2000. *The Origin of Mountains*. Routledge, London, 345 pp.

Ollier, C.D. and Pain, C.F. 2019. Neotectonic mountain uplift and geomorphology. *Russian Journal of Geomorphology* (*Геоморфология*) 4, 3-26. https://doi.org/10.31857/S0435-4281201943-26.

Ollier, C.D. 2020. My memories and ideas about the expanding Earth. In Hurrell, S. (Editor). *The Hidden History of the Expanding Earth*, 105–130.

Owen, L.A. 2004. Cenozoic evolution of global mountain systems. In Owens, P.N. and Slaymaker, O. (Editors). *Mountain Geomorphology*. Edward, Arnold, London, 39-64.

Pallister, J.S., McCausland, W.A., Jónsson, S., Lu, Z., Zahran, H.M., El Hadidy, S., Aburukbah, A., Stewart, I.C., Lundgren, P.R., White, R.A. and Moufti, M.R., 2010. Broad accommodation of rift-related extension recorded by dyke intrusion in Saudi Arabia. *Nature Geoscience* 3, 705-712.

Peel, F.J., Travis, C.J., and Hossack, J.R. 1995. Genetic structural provinces and salt tectonics of the Cenozoic offshore U.S. Gulf of Mexico: A preliminary analysis. In Jackson, M.P.A., Roberts, D.G. and Snelson, S. (Editors). Salt tectonics: A global perspective. *AAPG Memoir* 65, 153–175.

Polyansky, O.P., Prokopiev, A.V., Koroleva, O.V., Tomshin, M.D., Reverdatto, V.V., Selyatitsky, A.Y., Travin, A.V. and Vasiliev, D.A., 2017. Temporal correlation between dyke swarms and crustal extension in the middle Palaeozoic Vilyui rift basin, Siberian platform. *Lithos* 282, 45-64.

Rowan, M.G., Peel, F.J. and Vendeville, B.J. 2004. Gravity-driven fold belts on passive margins. In McClay, K.R. (Editor), Thrust tectonics and hydrocarbon systems. *AAPG Memoir* 82, 157–182.

Rubey, W.W. and King Hubbert, M. 1959. Role of fluid pressure in mechanics of overthrust faulting: II. Overthrust belt in geosynclinal area of western Wyoming in light of fluid-pressure hypothesis. *Geological Society of America Bulletin* 70, 167-206.

Srivastava, R.K., Ernst, R.E. and Peng, P. (Editors) 2020. *Dyke Swarms of the World: A Modern Perspective*. Springer, 492pp.

Steinthórsson, S. and Thorarinsson, S. 1997. Iceland. In: Moores, E.M. and Fairbridge, R.W. (Editors). *Encyclopedia of European and Asian Regional Geology*. Chapman, 341–352.

Valásques, V.F., Riccomini, C., Gomes, C. and Kirk, J. 2011. The Cretaceous alkaline dyke swarm in the central segment of the Asunción Rift, Eastern Paraguay: Its regional distribution, mechanism of emplacement, and tectonic significance. *Journal of Geological Research* 2011, 946701, doi:10.1155/2011/946701.

Van Bemmelen, R.W. 1955. Tectogenese par gravité. Bulletin de la Societe beige de Geologie, de Paleontologie et d'Hydrologie 64, 95-123.

Wingate, M.T. and Giddings, J.W., 2000. Age and palaeomagnetism of the Mundine Well dyke swarm, Western Australia: implications for an Australia–Laurentia connection at 755 Ma. *Precambrian Research* 100, 335-357.

Characteristics of Earthquake Distribution in the Japanese Archipelago —Plate tectonics has not caused earthquakes—

Masahirov Shiba
Museum of Natural and Environmental History, Shizuoka, Japan
shiba@dino.or.jp

Abstract. In this paper, I re-examine the occurrence of earthquakes based on the distribution of hypocenters in the Japanese Archipelago. Analysis of hypocenters at different depths shows different distribution characteristics in some depth ranges. The distribution of earthquakes deeper than 300 km is the lower part of the deep seismic surface, which is quite different from the upper part. Earthquakes with a depth of 50 to 300 km show a distribution of hypocenters that form the upper part of the deep seismic surface that dips from the trench to the island arc side, but this is not seen in the Nankai Trough. Earthquakes of 20-50 km depth are rarely found beneath the spine of the island arc, suggesting that the lower crust in this region may be melting. Earthquakes with depths of 0-20 km are distributed on the spine of the island arc and the surrounding continental slope, with many occurring in the upper crust of the island arc. The upper part of the deep seismic surface dips from the landward side of the trench to the island arc side, and is not subducted from the trench axis. Most earthquakes occur at the boundary between sedimentary basins and their surrounding mountains, not due to subduction of a plate, but due to uplift of island arcs by molten bodies in the lower crust.

Keywords: earthquakes, hypocenters, deep seismic surface, uplift of island arcs, plate subduction.

Introduction

This year marks the tenth anniversary of the massive earthquake that devastated the northeastern part of the Japanese Archipelago, the Tohoku-Pacific Coast Earthquake (The Great East Japan Earthquake). This earthquake occurred at 14:46 on March 11, 2011, with its hypocenter at a depth of about 24 km off Sanriku on the Pacific coast. The magnitude of the earthquake was M 9.0, which is the largest earthquake ever recorded in Japan and the fourth largest earthquake in the world since 1900. This earthquake is considered a typical trench-type earthquake.

The total number of victims of this earthquake and the resulting tsunami was more than 20,000, including the dead and missing. In addition, this earthquake and the resulting tsunami caused a serious accident at the Fukushima Daiichi Nuclear Power Plant, and the radiation released continues to cause enormous damage not only in the Tohoku region but also throughout Japan.

Fig. 1 shows the hypocenter distribution of earthquakes with magnitudes ranging from M 0.1 to M 9.0 that occurred in and around the Japanese Archipelago from October 1, 1997 to August 28, 2011. The hypocenter data was obtained from the Japan Meteorological Agency's hypocenter data, and the distribution map was created using Scat3D software provided by Professor Takayuki Kawabe of Yamagata University. The depth of the hypocenter is indicated by the color of the circle, and the magnitude is indicated by the radius of the circle, but these legends are omitted here because the focus is on the location of the hypocenter.

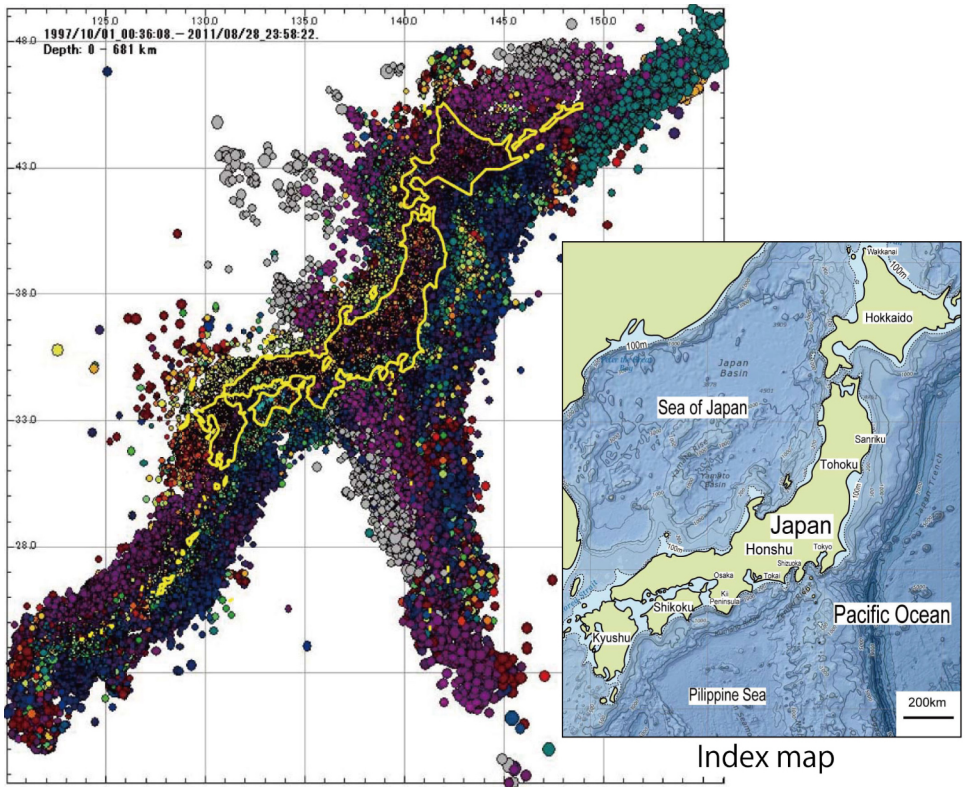

Fig. 1 Left map shows the hypocenter distribution of earthquakes with magnitudes ranging from M 0.1 to M 9.0 that occurred in and around the Japanese Archipelago from October 1, 1997 to August 28, 2011. The Japanese Archipelago appears to be a nest of earthquakes. Right map is the index map.

These data show that many earthquakes occur along the

trenches and island arcs around the Japanese Archipelago, and the Japanese Archipelago appears to be a nest of earthquakes. Seismologists have explained that earthquakes around the Japanese Archipelago are caused by plate subduction. But is it true? Where are the earthquakes actually occurring? In this paper, I will re-examine the occurrence of earthquakes based on the actual hypocenter distribution of earthquakes.

As a result, when the hypocenters of these earthquakes are analyzed by their depths, different distribution characteristics are observed in several depth ranges. And it clearly shows that earthquakes are not caused by the plate tectonics.

Characteristics of earthquake distribution due to differences in hypocenter depth

Depth 300 km to the deepest (681 km)

The earthquakes occurring at this depth range (Fig. 2) are composed of three sets. One is a linear distribution of westward-dipping deep earthquakes from north-northwest to south-east direction that starts south of the Bonin Islands, passes through Ise Bay and Wakasa Bay, and ends near the Yamato Bank in the Sea of Japan. Secondly, there is a north-trending linear distribution in the east-northeast to west-southwest direction extending from the northern part of the Kuril Basin to the vicinity of Wakkanai in Hokkaido. The remainder is distributed in the Japan Basin between these two areas. The entire distribution of earthquakes at this depth appears to be orthogonal as shape of the letter "L" tilted upside down. The hypocenter distribution in this depth range is the lower part of the so-called deep seismic surface, which is discontinuous with the upper part and shows a completely different distribution.

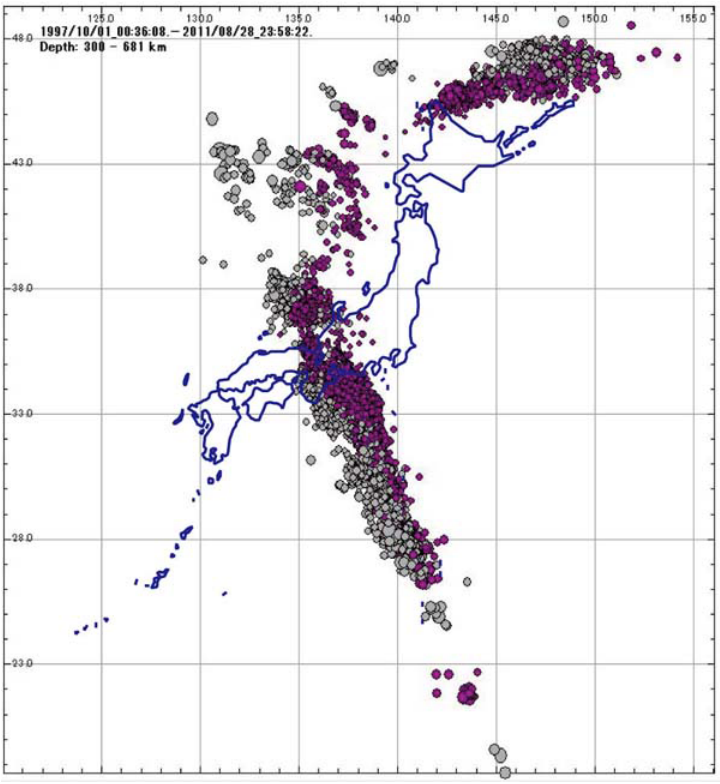

Fig. 2 Distribution of hypocenters in and around the Japanese Archipelago from 300 to 681 km depth. This is the lower part of the so-called deep seismic surface, which is discontinuous with the upper part and shows a completely different distribution.

Earthquakes at depths of 50 to 300 km

The earthquakes at this depth range (Fig. 3) show the distribution of hypocenters that form the upper part of the so-called deep seismic surface, which dips from near the trench to the island arc side. Such deep seismic surfaces are also observed along the Japan Trench, the Kuril Trench, the Izu-Bonin Trench, and the Ryukyu Trench. However, on the Pacific side along the Nankai Trough, there is no equivalent to this deep seismic surface. This may mean that there is no plate boundary in the Nankai Trough that corresponds to a deep seismic surface. In the Nankai Trough area, however, small-scale epicenters are distributed in the Kii Peninsula, the Kumano-nada (the southeast off the Kii Peninsula), and the southeast off the coast of Shikoku.

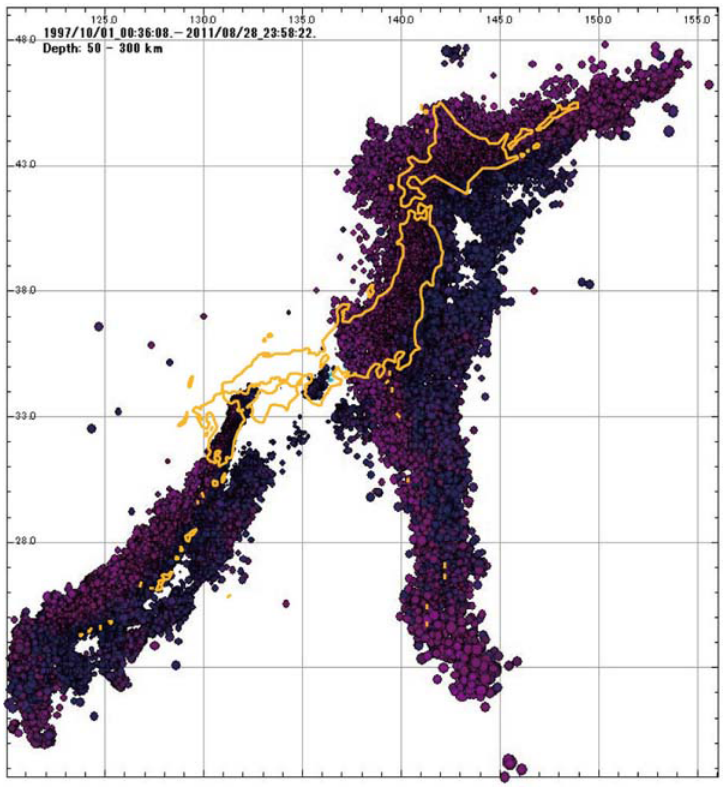

Fig. 3 Distribution of hypocenters in and around the Japanese Archipelago from 50 to 300 km depth. This forms the upper part of the so-called deep seismic surface, which dips from the trench to the island arc side, but is not seen along the Nankai Trough.

Earthquakes at depths of 20 to 50 km

Earthquakes of this depth range (Fig. 4) are distributed on the continental slope on the Pacific side of the island arc, and on the continental slope on the Sea of Japan side in the Tohoku region and near Wakkanai. There are few earthquakes of this depth in

the spine of the island arc, and many are not distributed on the Sea of Japan side in southwest Japan. This depth range corresponds to the lower continental crust below the island arc. In the absence of these earthquakes, there are many very low-frequency earthquakes distributed under the volcanic belts. For those in the lower part of this depth range, it is likely that earthquakes at the top of the deep seismic surface are also included. There are few earthquakes south of the Bonin Islands, and they are concentrated at depths of 25 to 40 km in the Kuril Arc.

Since earthquakes are caused by brittle failure, the absence of earthquakes may indicate that the region is composed of elastic or molten material. The distribution of earthquakes at this depth range also roughly coincides with the distribution of volcanic belts and very low-frequency earthquakes. This suggests the presence of molten magma in the spine of the island arc at depths of 20 to 50 km.

Earthquakes at a depth of 0 to 20 km

Earthquakes of this depth range (Fig. 5) are distributed on the spine of the island arc and the surrounding continental slopes. Those shallower than 10 km are concentrated on land and in some areas, while those 10-20 km deep are distributed on the continental slope. In some areas along the coastline, there are seismic gaps. There are few earthquakes at this depth range in the south of the Bonin Islands, and there is a gap between Hokkaido and the Kuril Arc, where large earthquakes are distributed around 15 km depth. The distribution of earthquakes shallower than 10 km in the land area of the island arc indicates that earthquakes are occurring in the upper continental crust below the island arc.

Trench-type earthquakes

Trench-type earthquakes are generally described as earthquakes that occur beneath the landward slope of an oceanic plate as it subducts in an oceanic trench. This is believed to be caused by the accumulation of strain on the landward plate, which is pushed by the subducting oceanic plate, causing the landward plate to spring up and generate an earthquake fault, which in turn causes an earthquake. Therefore, earthquakes can occur anywhere along the subduction zone of a plate.

In Japan, the area from the Enshu-nada (off the coast of Hamamatsu) to Suruga Bay (off the coast of Shizuoka) along the Nankai Trough has been threatened by the possibility of large earthquakes due to the subduction of the Philippine Sea Plate for the past 50 years (Fig. 6). This is because this area has never had a major earthquake before, i.e., it was a blank area, and therefore, the Tokai Earthquake or the Nankai Trough Earthquake was assumed to occur.

In the case of the Nankai Trough Earthquake, the plate boundary is traced onshore north of Suruga Bay, but no major earthquakes have occurred onshore. If M 7.0 to M 8.0 (and sometimes up to M 9.0) earthquakes can occur anywhere in the plate subduc-

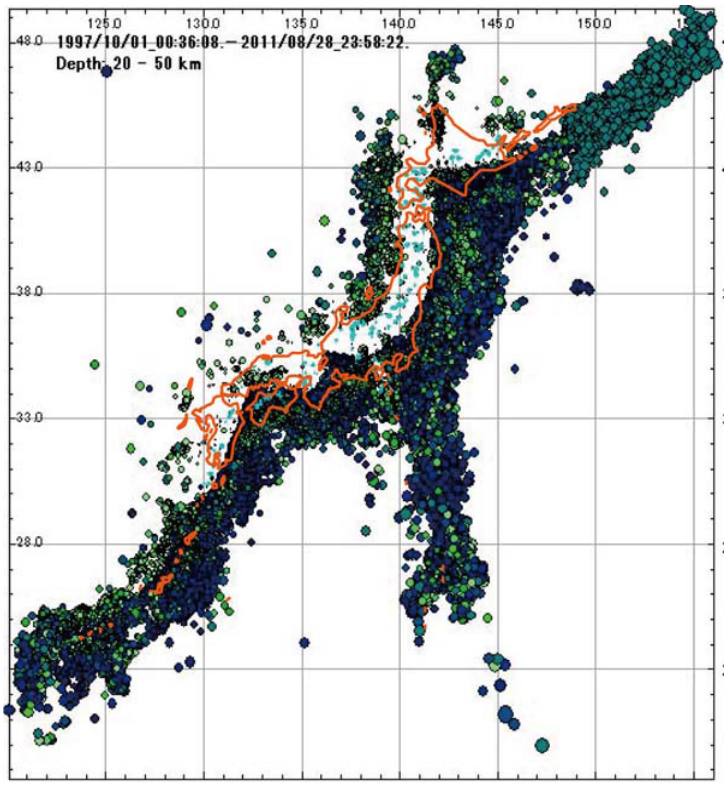

Fig. 4 Distribution of hypocenters in depths of 20 to 50 km in and around the Japanese Archipelago. Light blue circles indicate very low-frequency earthquakes. There are few earthquakes at this depth in the spine of the island arc, and they are accompanied by very low-frequency earthquakes.

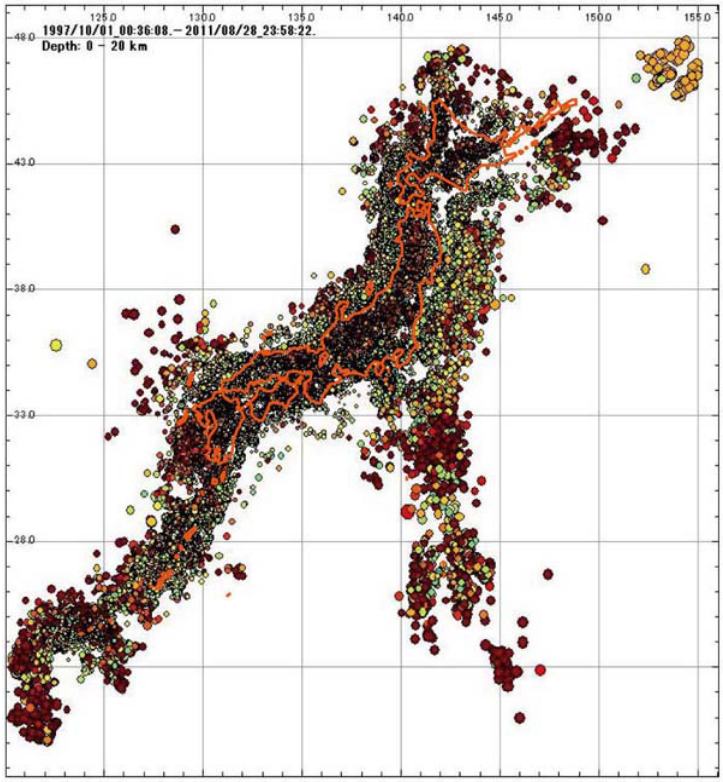

Fig. 5 Distribution of hypocenters from 0 to 20 km depth in and around the Japanese Archipelago. They are distributed on the spine of the island arc and the surrounding continental slopes.

tion zone, why do they occur only in the ocean? The plate boundary is extended on land, but why don't seismologists assume the source region in the landward extension of the Nankai Trough? Also, if earthquakes occur in the subduction zone of a plate, they should occur anywhere in the horizontal direction of the subduction zone, so why is the hypocenter distribution concentrated as the source region?

The Great East Japan Earthquake, which caused extensive damage to the Japanese Archipelago, is considered a typical trench-type earthquake, which is said to occur at plate boundary. In this section, I will take a closer look at this reality. Fig. 7 shows the east-west cross section of the hypocenters of the earthquakes that cut off Sanriku in the Tohoku region. Here, the deep seismic surface has two rows of the upper and the lower seismic surfaces (double deep seismic surface). The top edge of the upper deep seismic surface is not in the trench, but extends to the western margin of the deep-sea terrace. The main shock of the Great East Japan Earthquake is distributed below the trench side than the upward extension of the upper deep seismic surface (24 km depth of a black inverted triangle in Fig. 7).

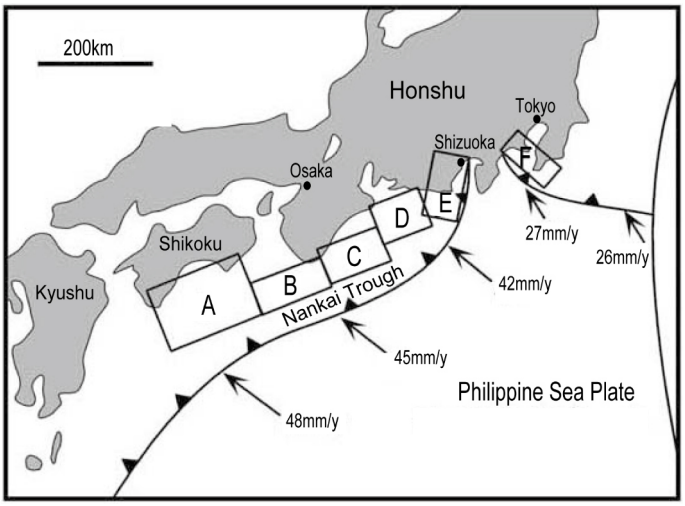

Fig. 6 The source regions of the Nankai Trough Earthquake, which are estimated to occur as a result of the subduction of the Philippine Sea Plate. Squares the A to the C and the D to the E indicate the estimated source regions of the Nankai Earthquake and the Tokai earthquake, respectively. The F indicates the source region of the Kanto Earthquake. Arrows and numbers indicate the direction and speed of the Philippine Sea Plate relative to Honshu (Koyama, 2008).

The top edge of the upper deep seismic surface is not in the trench, but on the landward side, which is a fact not only in the Northeast Japan Arc but also in the Izu-Bonin Arc and the Ryukyu Arc. If the top of the deep seismic surface is not subducting from the trench, is the oceanic plate subducting from the trench? How can the mechanism of the trench-type earthquakes be explained when the subduction zones of oceanic plates do not coincide with deep seismic surfaces?

At the end of the 1960s, a seismologist and a marine geologist showed that the characteristics of the epicenter distribution of the trench-type earthquakes are closely related to the distribution of the deep-sea terrace (forearc basin).

Den (1968) showed the distribution of earthquakes of M 6.0 or greater occurring at depths of 60 km or shallower from 1926 to 1965 and the distribution of the deep-sea terraces, and pointed out that the epicenters are concentrated at the edge of the deep-sea terraces. Den's (1968) figure shows that the Nankai Earthquakes and the East Nankai Earthquake of the 1940s occurred on the margins of the deep-sea terraces in the Kii Channel and off the coast of the Kii Peninsula, respectively, and that no major earthquakes occurred in the Enshu-nada, which has no wide deep-sea terrace.

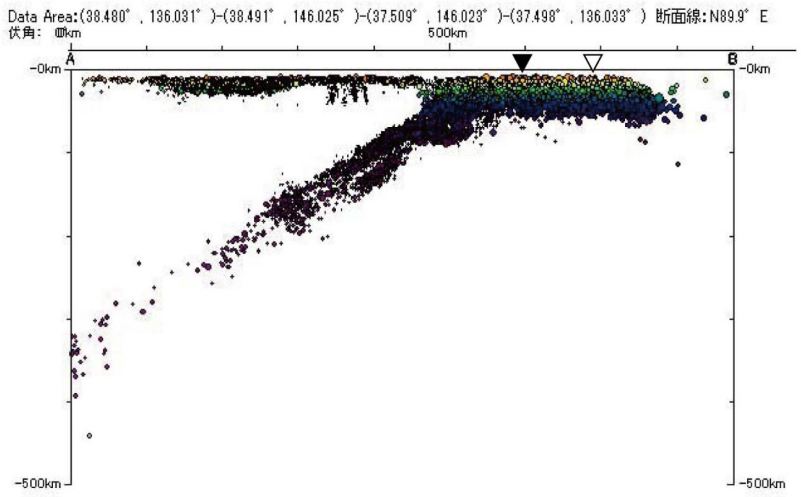

Fig. 7 East-west cross section of the hypocenters of the earthquake that cut off the Sanriku coast in the Tohoku region. The hypocenter of the main shock of the Great East Japan Earthquake was located 24 km beneath at a black inverted triangle, and the Japan Trench at a white inverted triangle. If we assume that the deep seismic surface is a plate subduction zone, then the plate is not subducting in the trench, but is subducting from the landward side by more than 100 km.

Hoshino (1969), based on the relationship between the development of the deep-sea terraces and the distribution of epicenters of extremely shallow earthquakes (shallower than 10 km), found that extremely shallow earthquakes occur frequently where only one level of the deep-sea terrace is developed, and that no extremely shallow earthquakes occur at all where two levels of the deep-sea terrace are distributed, as in Tosa Bay, or where several narrow levels of the deep-sea terrace with different depths are distributed, as in the Enshu-nada. It also states that extremely shallow earthquakes occur where the margins of the Neogene sedimentary basins are isolated and develop into basins with strata thicker than 1,000 meters.

The distribution of the epicenters of the Great East Japan Earthquake and its aftershocks published by the web page of the Japan Meteorological Agency is superimposed on the detailed distribution of deep-sea terraces off the Pacific

coast of Tohoku (Iwabuchi, 1967), and the main shock of the Great East Japan Earthquake occurred at the eastern margin of one deep-sea terrace off Miyagi (Fig. 8).

As mentioned earlier, the Nankai Trough, where the Tokai Earthquake or the Nankai Trough Earthquake are expected, does not have a deep seismic surface (Fig. 3). The trench-type earthquakes are said to occur when oceanic plates subduct, which means that they do not occur in the Nankai Trough. However, all seismologists continue to shout that huge earthquakes in the Nankai Trough will occur in near future.

From the perspective of earthquakes and sedimentary basins, the Tokai Earthquake is examined, although strata of the Neogene and later periods are distributed in the Enshu-nada, they are not distributed in a thick basin-like pattern, and the seafloor topography does not consist of a single level of deep-sea terrace (Fig. 9). This suggests that the seafloor of the Enshu-nada may not be a place where earthquakes occur. In other words, it seems to be that this is one of the reasons why the Tokai Earthquake, which was supposed to occur in the Enshu-nada, did not occur for 50 years.

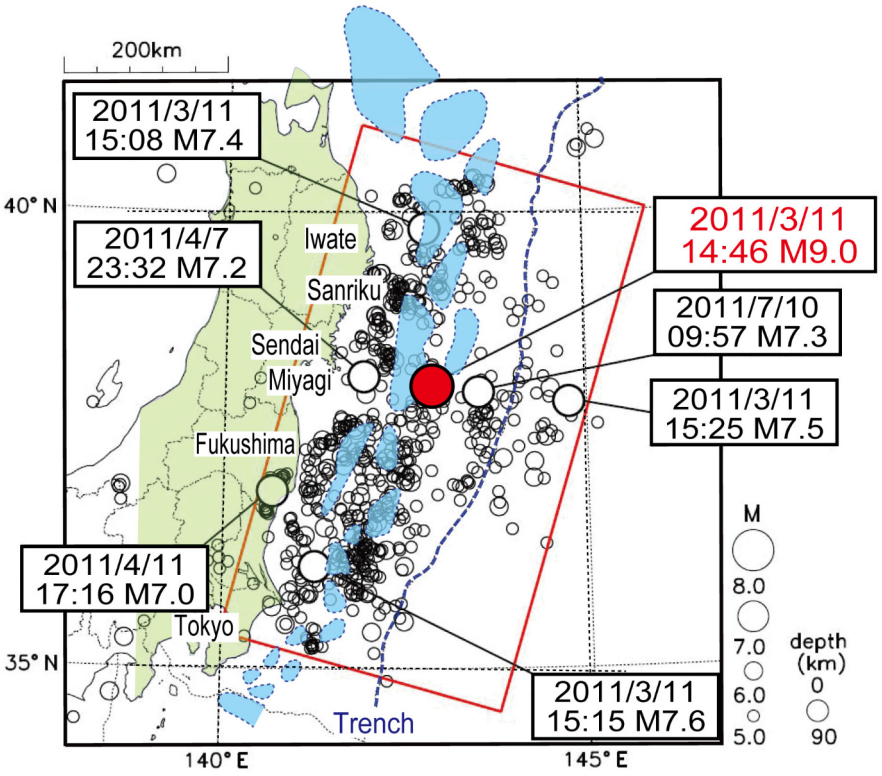

Fig. 8 The distribution of the epicenters of the Great East Japan Earthquake (the web page of the Japan Meteorological Agency) is superimposed on the distribution of the deep-sea terraces of Iwabuchi (1967). Most of the epicenters are not in the deep-sea terraces, but are distributed at the periphery of them.

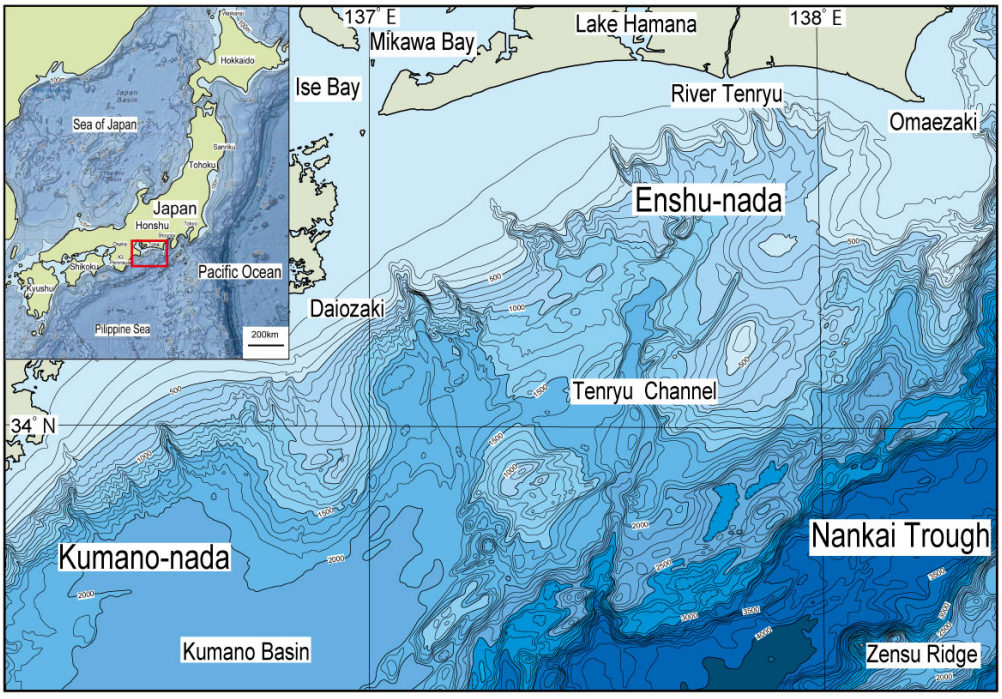

Fig. 9 Sea floor topography from the Enshu-nada to the Kumano-nada (Red box in the index map). In contrast to the Kumano-nada, where a deep-sea terrace (the Kumano Basin) develops, the Enshu-nada has no wide deep-sea terrace.

Sedimentary basins and earthquakes

Fig. 10 shows the distribution of the epicenters of the Southern Hyogo Prefecture Earthquake in 1995, superimposed on a map of the Osaka Plain from Awaji Island. Osaka Bay-Osaka Plain is a sedimentary basin that has accumulated thick sediments left over from the surrounding the Rokko and the Izumi Mountains, which were rapidly uplifted by the Rokko Movement as described by Huzita (1990). This earthquake occurred 16 km beneath the Akashi Strait at the northwestern margin of this basin, and strongly vibrated the northeast-southwest belt from the northern part of Awaji Island to the southeastern boundary of the Rokko Mountains, causing severe damage mainly to the city of Kobe.

Direct inland earthquakes, such as the Southern Hyogo Prefecture Earthquake (M 7.3), occur near the boundary

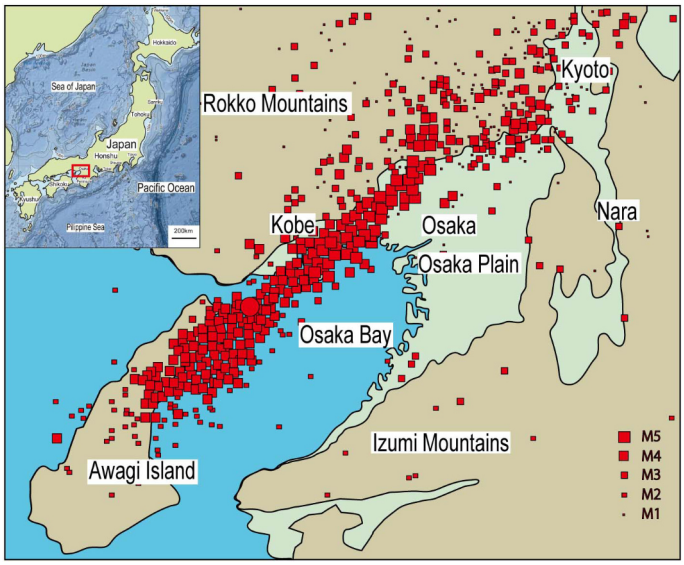

Fig. 10 Distribution of the epicenters of the main and aftershocks of the Hyogo Prefecture Earthquake in the area from Awaji Island to the Osaka Plain, superimposed on a map of the Osaka Bay area (Red box in the index map). A red circle indicates the location of the epicenter of the main shock and a red square indicates the location of the epicenter of the aftershocks. Most of the epicenters are distributed along the boundary between the Rokko Mountains and Osaka Bay-Osaka Plain.

between urbanized plains or basins and around rising mountains. The magnitude of these earthquakes is not as large as the trench-type one, but because the hypocenter is directly under the city, they can cause significant damage. Such earthquakes have often occurred in plains and basins throughout Japan. For example, in the Shizuoka Plain, the Shizuoka Earthquake (M 6.4) occurred in 1935 at the boundary between the southwestern part of the Udo Hills and the Shizuoka Plain, and in the Shimizu Plain, the Shizuoka Earthquake (M 6.1) occurred in 1965 at the boundary with the northern mountains. The 2009 Suruga Bay Earthquake (M 6.5) occurred in the northern margin of the Senoumi Basin in Suruga Bay (Fig. 11).

If the size of the plain or basin is small, the magnitude of the earthquake is small; if it is large, the magnitude of the earthquake is large. Some people believe that such earthquakes occur periodically in the same place in the same basin, but according to Shimamura (2011), earthquakes do not have a periodicity. An earthquake similar to the Southern Hyogo Prefecture Earthquake is known as the Keicho-Fushimi Earthquake, which is said to have occurred in 1596 on the Rokko-Awaji Island fault zone. The interval between the two earthquakes is about 400 years, but the two earthquakes did not occur in the same place.

If a trench-type earthquake occurs on a deep-sea terrace, i.e., at the margin of a forearc basin, the mechanism of occurrence is the same as that of an earthquake occurring at the margin of an inland basin, which is called a direct inland earthquake. What distinguishes them is the size of the basin, which has nothing to do with plate subduction.

The topography reflects the geology and tectonic movements of a place. Since erosion is not as pronounced in marine areas as it is on land, sedimentary landforms such as deep-sea terrace are clear, and landforms reflecting tectonic movements such as earthquakes and faults are easily recognized. The larger the size of the forearc basin or the inland basins, the larger the earthquake is likely to be. Therefore, more research on geomorphology and geology should be incorporated into the future understanding of earthquake generation mechanisms.

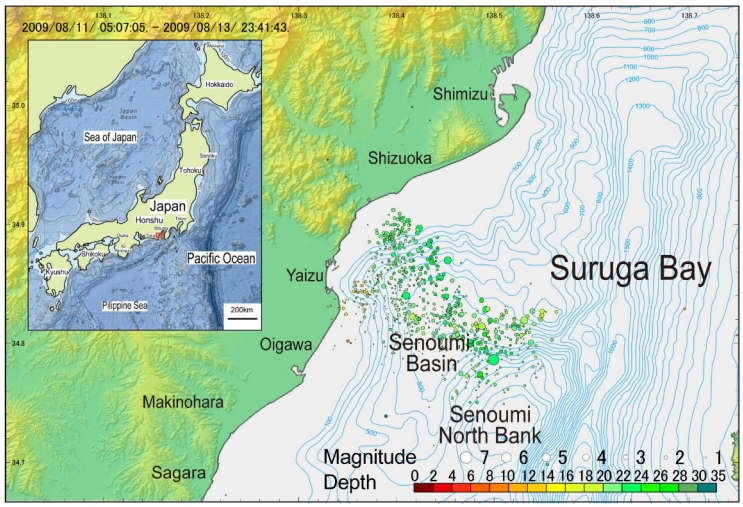

Fig. 11 Distribution of the epicenter of the 2009 Suruga Bay Earthquake (Red box in the index map). The epicenters are limited to the northeastern margin of the Senoumi Basin from Shizuoka to the Senoumi North Bank.

Earthquakes in the Nankai Trough

Fig. 12 shows the distribution of epicenters along the Nankai Trough at depths of 0 to 50 km, and Fig. 13 shows the distribution of hypocenters at depths of 0 to 50 km in four north-south cross sections across the Nankai Trough. Fig. 13 shows that there is no deep seismic surface, and the upper end of the distribution of hypocenters at depths of 20 to 40 km is extended near the coastline and does not coincide with the Nankai Trough axis.

In Fig. 12, there are seismic blank zones in the Akaishi Mountains and the Kii Mountains at a depth of 30 km or less from Shizuoka to the Kii Peninsula, and earthquakes with a depth of 30-50 km are concentrated in the southern part of those mountains. In that sea area, there is a blank zone of earthquakes with a depth of less than 30 km from the Enshu-nada to the Kumano-nada, but the concentration of earthquakes with a depth of 30-50 km is in the southern part of the Kumano-nada (beneath the outer margin of the Kumano Basin) and not in the Enshu-nada. In other words, the concentration of earthquakes with a depth of 30-50 km in this region seems to be distributed along the southern margin of the uplifted massif, including the Akaishi Mountains, the Kii Mountains, and the outer margin of the Kumano Basin (Fig. 12). This suggests that earthquakes in this region are thought to be caused by pushing up the up-

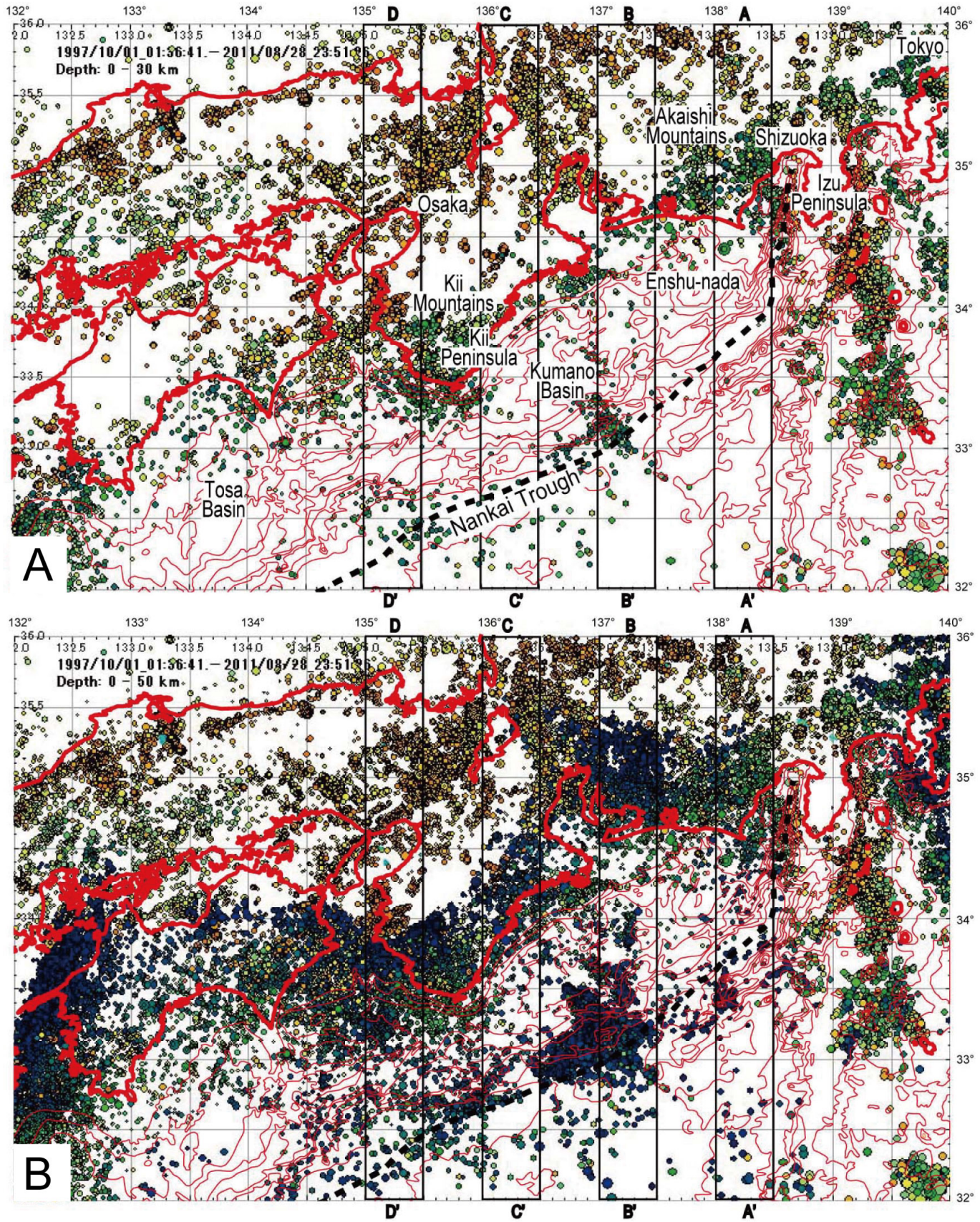

Fig. 12 Distribution of epicenters from 0 to 50 km depth along the Nankai Trough. A: Depth range from 0 to 30 km, B: Depth range from 0 to 50 km.

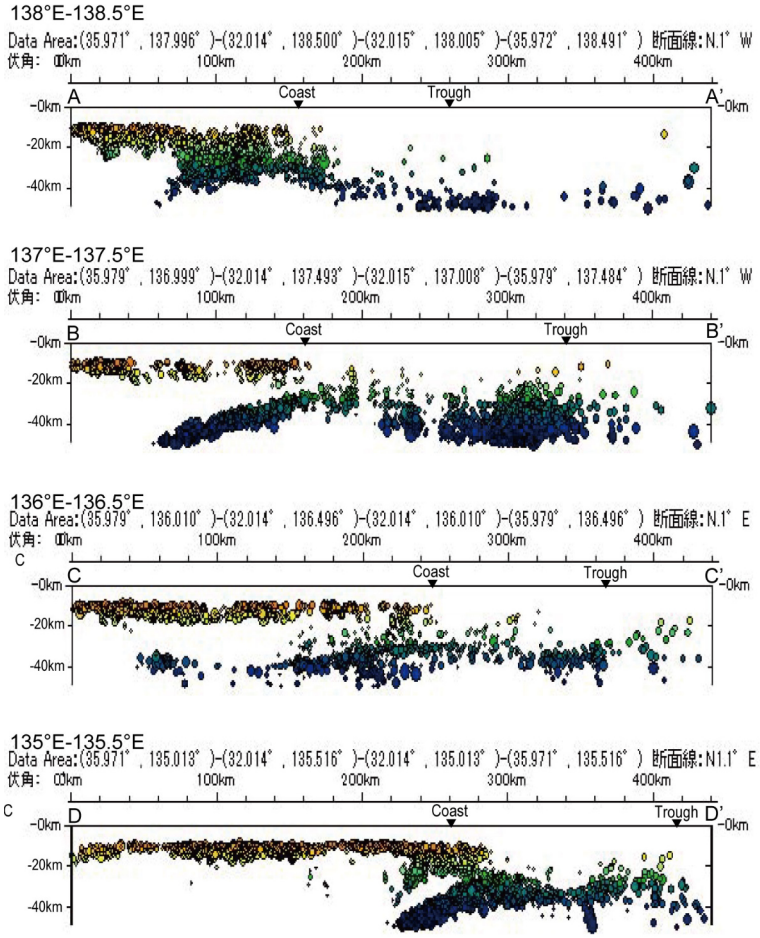

Fig. 13 Distribution of hypocenters from 0 to 50 km depth in four north-south cross sections across the Nankai Trough. Coast is the location of the coastline, and Trough is the location of the deepest axis of the Nankai Trough. No deep seismic surface along the trough is observed in any of the cross sections. In all sections, earthquakes are concentrated below the coast and the landward side. In addition to that, in the B section earthquakes are also concentrated below the landward side of the Nankai Trough (beneath the outer edge of the Kumano Basin).

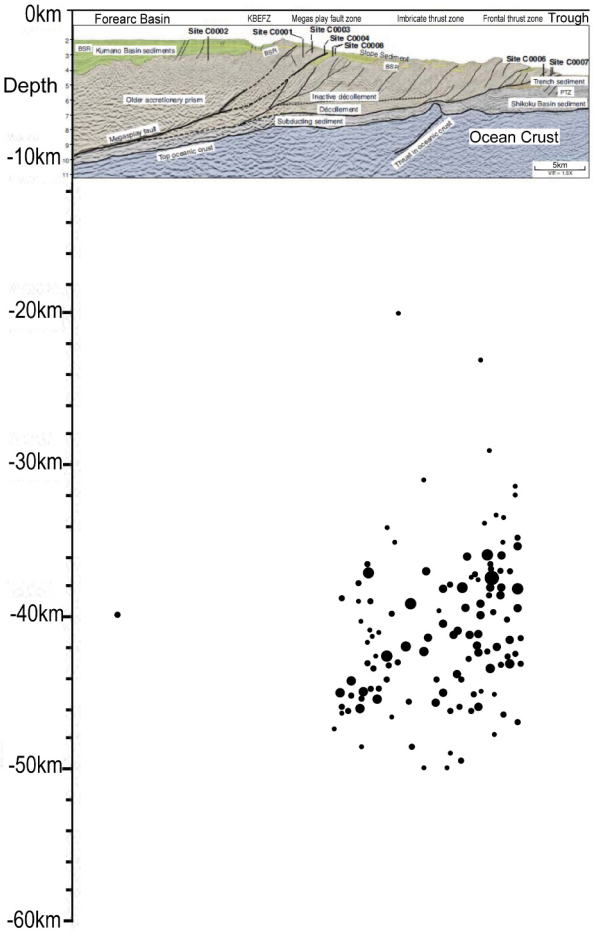

Fig. 14 Distribution of earthquakes beneath the Kumano Basin. Most earthquakes do not occur on the top surface of the ocean crust (the Philippine Sea Plate). Black circles are hypocenters. In fact, the hypocenters are much deeper, at depths of 20 to 50 km, and the earthquakes occur independently of the upper surface of the plate. The top of this figure is the geological cross section of the Nankai Trough from Saffer et al. (2010).

lifted land mass from below.

The hypocenters of earthquakes concentrated in the southern part of the Kumano-nada are located at 30-50 km, and there are almost no earthquakes at depths of 0-10 km, which is the subduction zone of the Philippine Sea Plate (Fig. 14). In other words, there is no relationship between plate subduction zones and the occurrence of earthquakes.

Mountains are uplifted, while basins are relatively subsided. For example, the boundary between Osaka Bay-Osaka Plain region and the rising the Rokko Mountains has been subject to continuous uplift and relative subsidence (sea level rise) caused by the Rokko Movement. Similarly, the Akashi Mountains, the Kii Mountains, the outer ridge of the landward side of the Nankai Trough that formed the deep-sea terrace (forearc basin), and the upper continental slope of the landward side of the trench have been actively uplifted since the Quaternary. The mechanism of uplift movement of mountainous and continental slopes relative to the basin seems to be closely related to the occurrence of earthquakes.

The island arc-trench system is characterized by island arc uplift, volcanic activity, trenches, and earthquakes. The island arc is thought to have been formed by uplift since the late Miocene, especially since about 430 Ka (Shiba, 2017a, 2017b, 2021), and volcanic and seismic activities are thought to be associated with this. Therefore, it is necessary to study earthquakes in relation to the uplift movements and magmatic activities that formed the island arc, rather than considering plate subduction alone as the cause of earthquakes.

Mechanism of earthquake occurrence

In conclusion, I believe that earthquakes are not caused by a simple mechanism of the plate tectonics, as is commonly believed, in which the landward side of a plate is pushed by a subducting oceanic plate, causing the landward

side to spring up due to accumulated strain.

Hosoi (1996) argued that the "destruction" of individual parts of the crust can be considered when it progresses gradually at a very low speed, but it is questionable what kind of "reality" of destruction exists in the crust where there is no surrounding space when instantaneous energy is released, such as in an earthquake. He believes that the fluid (water) itself, which can flow explosively, plays a major role in the occurrence of instantaneous ruptures such as earthquakes.

As for the mechanism of earthquake occurrence, I believe that one of the most likely causes of earthquakes is the shock proposed by Hosoi (1996), which is an explosive flow of high-pressure water from an anomalous high-pressure block to the adjacent layer, breaking through a weak part of the fault wall. Especially in the case of earthquake swarm occurring in hot spring areas, the increase in ground heat or steam pressure and the change in groundwater flow are consider to be closely related to the occurrence of earthquake swarm. Therefore, the interrelationship between regional uplift zones and basins, as well as the stress and heat increase and changes within the crustal interior and the upper mantle that cause the uplift, are important in understanding the cause of earthquakes.

However, I am not able to predict where and when the next earthquake will occur. Even for earthquakes that have occurred in the past, nobody is not possible to clearly explain the specific mechanism that caused them. However, since most earthquakes occur at the boundary between uplift zone and basin, something must be causing the uplift of the crust. The causes of earthquakes are probably closely related to changes in the low-velocity layers at the lower crust, magmatic activity, and resulting changes in vapor pressure, such as heat and hydrothermal fluids in the crust or strata.

Acknowledgments: In compiling this paper, I would like to express my gratitude Dr. Michihei Hoshino and Dr. Takayuki Kawabe. Dr. Hoshino is a professor emeritus of Tokai University, who has conducted pioneering research on the relationship between earthquakes and submarine topography, for guiding the author's research and interest in seismology. Dr. Kawabe is a professor of Yamagata University, who provided us with Scat3D software and gave me suggestions on earthquakes and geological structures.

References

Den, N. (1968) 8. Submarine Topography and Distribution of Epicenters of Shallow Earthquakes. *Geophysical bulletin of the Hokkaido University*, 20, 111-124. (in Japanese with English abstract)

Hoshino, M. (1969) On the relationship between the distribution of epicenter and the submarine topography and geology. *Journal of the School of Marine Science and Technology, Tokai University*, 3, 1-10. (in Japanese with English abstract)

Hosoi, H. (1996) The role of fluids in the mechanism of earthquake generation - The direct cause of earthquakes is underground pore water. In Shibasaki, T., Uemura, T. and Yoshimura, N. (eds) *Great Earthquake What did the geologists do then?* Tokai University Press, 189-206. (in Japanese with English abstract)

Huzita, K. (1990) Manchidani unconformity and Rokko movements -Middle Pleistocene fault-block movement and sea-level rise in Kinki, Japan. *The Quaternary Research*, 29, 337-349. (in Japanese with English abstract)

Iwabuchi, Y. (1968) Topography of trenches east of the Japanese Islands. *The Journal of the Geological Society of Japan*, 74, 37-46. (in Japanese with English abstract)

Koyama, M. (2008) What kind of earthquake is a Tokai earthquake? In Satomura, M. (ed). Earthquake Disaster Prevention, *Academic Book Publishing*, Tokyo, 160p. (in Japanese)

Saffer, D., McNeill, L., Byrne, T., Araki, E., Toczko, S., Eguchi, N., Takahashi, K. and the Expedition 319 Scientists (2010) Expedition 319 summary. *Proc. Integrated Ocean Drilling Program*, 319, 1-46.

Shiba, M. (2017a) Formation of Sauruga Bay – Large-scale uplift and sea level rise -, *Tokai Univ. Press,* Hiratsuka, 406p. (In Japanese)

Shiba, M. (2017b) Geology of the island arcs in the northwestern margin of the Pacific Ocean and their formation by a large scale uplift and sea level rise - the formation of Suruga Bay. *New Concepts in Global Tectonics Journal,* 5, 532-548.

Shiba, M. (2021) Characteristics of crustal uplift since the Pliocene in central Honshu, Japan, and sea level rise. *Earth Science (Chikyu Kagaku),* 75, 37-55. (In Japanese with English abstract).

Shiba, M., Masuda, Y., Shiba, H. and the Research Group of the Damage of Suruga Bay Earthquake (2010) The Characteristic of the Damage Distribution of August 11, 2009 Suruga Bay Earthquake and the Relation to Topography and Geology. *Science Report Museum, Tokai University*, 10, 1-16. (in Japanese with English abstract)

Shimamura, H. (2011) Why huge earthquakes happen - Here's what you need to know. Kadensha, Tokyo, 303p. (in Japanese)

The Japan Meteorological Agency's hypocenter data https://www.data.jma.go.jp/svd/eqev/data/bulletin/hypo.html

The Web page of the Japan Meteorological Agency https://www.jishin.go.jp/main/chousa/11nov_sanriku/f09-1.html.

Hydrocarbon Potential of Sost Aulacogen, Karakoram: an overview

Haleem Zaman Magsi Baloch *

Nazir Zaman Magsi Baloch

Marksistskaya St. 22 Moscow, Russia Federation 109147

* Corresponding author e-mail: zamanhaleemmagsi@gmail.com haleem.m@seismotectonics.com

Abstract:

The Fuel and Energy Complex is an artery of socio-economic sector of one and another country. Pakistan a traditional importer of oil is now importing Natural Liquid Gas to meet demand of Fuel and Energy complex for industry complex and urban development. Therefore, Pakistan is hunting for indigenous hydrocarbon deposits and utilization of sustainable energy resources. The present study is an attempt to evaluate hydrocarbon potential of Sost aulacogen, a tectonic element of Northern Sedimentary Terrain, Karakoram. The paleotectonic conditions of sedimentation of Mesozoic sequence of Alpides of Pakistan, NW Himalayas and Karakoram indicates resemblance. Therefore, authors postulate probability of huge hydrocarbon fuels deposits in Sost aulacogen. However, still detail petroleum system studies and modelling of aulacogen is required for commercial activity.

***Keywords*:** Hydrocarbons, Mesozoic Sequence, Sost Aulacogen, Paleotectonic Conditions, Sources and Reservoirs.

Introduction:

If one follows the socio-economic sector development since stone stage, he will find that it was required to develop invention energy resources considering system of economic relations. The evolutionary and revolutionary dynamics of socio-economic sector development frames target of the Fuel and Energy Complex (FEC). Therefore, viable Fuel and Energy Complex (FEC) is important for one or another country. While viability of FEC depends on availability of hug indigenous hydrocarbon fuels and energy resources.

Pakistan is blessed with an enormous amount of renewable and natural energy resources. It has an excellent solar insolation; an extremely good wind energy potential; massive hydroelectric resource, substantial reserves of natural gas, 1054 KM long coastal line with a resource of tidal energy; large livestock population and agricultural waste to generate bioenergy. In addition, Pakistan has one of the largest coal resources in the world amounting to 185 billion tons of lignite located in Sindh province.

Despite massive renewable energy potential in the country, today only 70% of population has access to grid electricity in Pakistan. In terms of access to natural gas network, about 25% of population has access to natural gas network. This indicates that about two-third of population must rely on inefficient and unhealthy recourses such as fuels wood, dung, and other biomass to meet their basic energy needs for cooking, space heating and water heating etc. Certainly, the demand would continue to grow further as the population increases. According to Arkhipov et al., (2014) gas demand of fuel and energy complex will reach peak in 2040 in Pakistan. Moreover, emerging global megaproject China – Pakistan Economic Corridor (CPEC), a locomotive of socio-economic sector of region will also make relevant correction in targets of Fuel and Energy Complex of Pakistan. The above-mentioned future scenario of FEC target will eventually enhance hefty import bills of Pakistan, a traditional importer of oil and now is importing liquid natural gas (Brohi 2018).

The critical choice for affordable and reliable supply of hydrocarbon fuels and energy depend on exploration of indigenous hydrocarbon fuels deposits and the effective utilization of energy resources. Therefore, Pakistan is hunting for indigenous hydrocarbon fuels deposits and planning to enhance utilization of renewable energy sources to make sustainable FEC in accordance with future target.

The Oil and Gas Companies are targeting Palaeozoic, Mesozoic, and Cenozoic sedimentary sequences in Pakistan because clastic and carbonate rocks of above-mentioned Eras are hydrocarbon sources and reservoirs rocks in onshore and offshore basins of Pakistan (Bender and Raza 1995, Craig et al., 2018, Carmichael et al., 2009, Oakley 2016, Qadri 1995, Voskresenskiy et al., 1971 and Wandrey et al., 2004).

Craig et al., (2018) and Oakley (2016) have studied petroleum system and hydrocarbon potential of NW Himalaya of Pakistan and India and indicated Palaeozoic and Mesozoic sequences as sources and reservoir rocks in NW Himalayas. Wadia (1931) has categorized NW Himalayas as NW Himalaya Syntaxis. While Burtman (2013) and Khain (1979) have linked Trans Indus Range and Salt Range with NW Himalayas Syntaxis and termed as Pamir-Punjab Syntaxis. Whereas Balasundaram and Ray have connected Karakoram Mesozoic geosyncline with Mesozoic Himalaya geosyncline south of Tibet. Despite Karakoram Meganticlinorium (Khain 1979), an internal tectonic element of Pamir-Punjab Syntaxis (Burtman 2013 Khain 2000) and comprises Palaeozoic and Mesozoic clastic and carbonate rocks (Desio 1974, Gaetani 1997, Schneider 1957, 1960, Zanchi and Gaetani 1994, 201) is excluded from petroleum system and hydrocarbon potentials studies of NW Himalayas Syntaxis (Craig et al., 2018, Oakley 2016).

However, Magsi (2018, 2019) has overviewed abiotic and biotic hydrocarbons potential of Northern Sedimentary Terrain, Karakoram.

The object of present study is to examine petroleum system and hydrocarbon potentials of Mesozoic sequence (Donnelly 2004 and Zanchi and Gaetani 1994, 2011) of Sost aulacogen, Northern Sedimentary, Northern Karakoram Terrain (Fig.1) in accordance with correlation of paleotectonic conditions of sedimentation of Mesozoic sequence of sources and reservoir rocks of NW Himalayas.

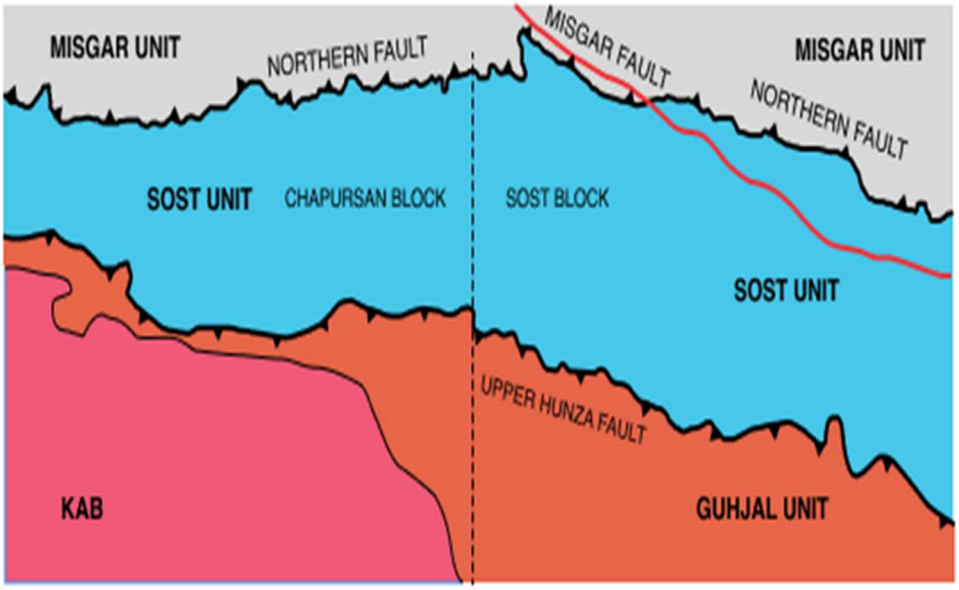

Figure 1 Tectonostratigraphic units of Sost Aulacogen (after Zanchi and Gaetani 1994 with Changes). KAB - Karakoram Axial Batholithic.

Tectonic and Stratigraphic Context of Sost Aulacogen:

Schneider (1957,1960) delineated 5 zones of Karakoram meganticlinorium (Khain 1979, Belyayevskiy 1966) from north (Northern Sedimentary Zone) to south (Gilgit zone). Gattinger (1961) assumed 7 zones of Karakoram meganticlinorium. While Desio (1974) split Karakoram segment into 6 zones: Northern Sedimentary Zone also term as Northern Sedimentary Terrain (Zanchi and Gaetani 2011); Axial Granite (Batholithic) Zone; Central Metamorphic Zone or Southern Sedimentary Zone (Zanchi and Gaetani 2011); Chalt Green Schist Zone; Basic Intrusion Zone and Gilgit Zone. However, Gaetani (1997), Gansser (1964), and Zanchi and Gaetani (2011) suggested three zones from north (Northern Sedimentary Zones to south Southern metamorphic Zone) and defined Chalt Green Schist zone as Karakoram - Kohistan suture, Basic Intrusion Zone and Gilgit Zone as part of Kohistan Arc. According proponent

of plate tectonic (Gaetani 1997, Gansser 1964, Tahirkheli et al., 1990, and Zanchi and Gaetani 2011) Karakoram – Kohistan Suture Zone serves as collision boundary between Kohistan Arc with Karakoram segment. Whereas Balasundaram and Ray (1973) considered Karakoram- Kohistan Suture Zone as eugeosyncline that linked with Mesozoic geosyncline south of Tibit. Belousov et al., (1979), Belyayevskiy (1966), Bolt and Choi (2005), Gattinger (1961), Schneider (1957, 1960), Smoot (2007, 2018) also decline collision of Kohistan Arc and Karakoram Arc. The fold and block model of Garhwal Himalaya dis not support traditional plate tectonic concepts (Rogozhin et al., 2020).

The Northern Sedimentary Terrain, Karakoram stretches between Northern fault also term as Kilik Fault (Zanchi and Gaetani 2011) and Axial Batholithic Zone (Fig.1). Whereas Reshun – Upper Hunza Fault splits Northern Sedimentary Terrain into Northern and Southern Units (Zanchi and Gaetani 2011), where the Sost unit and Guhjal Unit are internal tectonostratigraphic elements of Northern Unit and Southern Units respectively (Fig.1). Zanchi and Gaetani (2011) have elucidated morphological reactivation of Reshun- Upper Hunza Fault where segments of fault change morphology as reverse, normal and strike slip faults. Belousov (1976) categorized morphological changing structure faults as overthrust slashes. Belyayevskiy (1966) and Khain (1991) termed overthrust slashes as abyssal faults which control geoblocks dynamics. The abyssal faults are present in Tien Shan and Caucasus mountains where serve as boundaries between neotectonic uplifts and subsidences (Belousov 1980, Belyayevskiy 1966). Therefore, Reshun – Upper Hunza Fault being abyssal fault influences on the Northern Sedimentary basin dynamics. The Upper Hunza Fault and Northern Fault (Fig.1) are major thrusts plane stacking Guhjal block and Misgar Block on the Sost Block respectively (Donnelly 2004, Zanchi and Gaetani 2011). Authors postulate that Upper Hunza Thrust Fault and Northern Thrust Fault form Sost Aulacogen tectonic element (Fig.2).

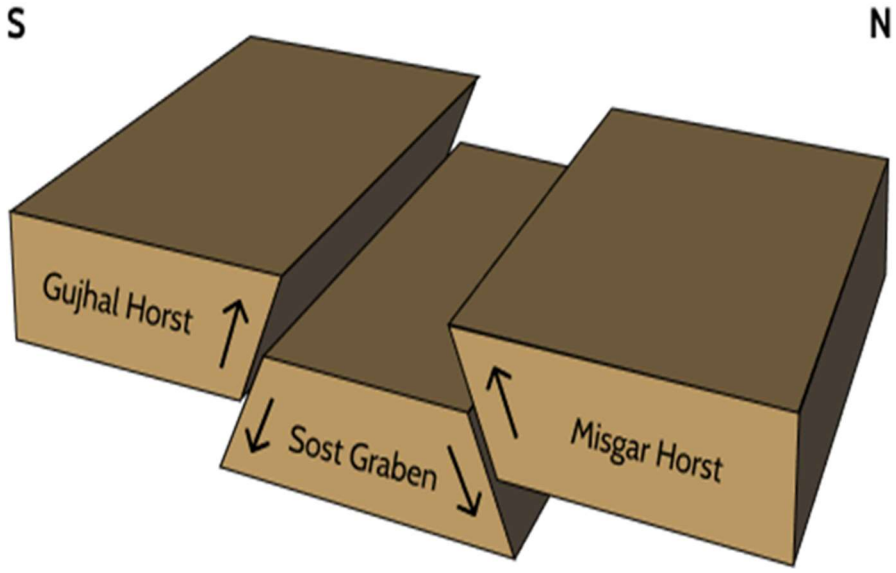

Figure 2. Sost Aulacogen, Northern Karakoram Terrain

The Sost graben structure comprises of a thick pile of folded and thrusted sheets forming antiformal stack, where strike slip faults with E-W strike disturb the structures (Donnelly 2004, Zanchi and Gaetani 2011).

The Northern Sedimentary Terrain, Karakoram is comprised of Paleozoic and Mesozoic clastic and carbonate rocks (Gaetani 1997, Gaetani 1997, Zanchi and Gaetani 1994, 2011) where outcrop rocks ratio is: volcanic 0.5%, Plutonic 4-5%) Sedimentary 67% and Metamorphic 28% (Desio 1974). Whereas Sost graben consists of thick Permian and Mesozoic clastic and carbonate sediment sequences, Gricha formation (Permian) outcrops as core of Sost anticline (Zanchi and Gaetani 1994). The coals seams are present in Ashtigar and Yashkuk formations in Chapursan block of Sost graben (Donnelly 2004). Guhjal horst characterises with anticline and syncline structures controlled with faults (Fig.3). Gricha formation black slates and sandstone (Permian) overlain by massive carbonate (Permian – part of undefined Mesozoic) of Guhjal Formation and well bedded Buattar Limestone, marl, and shaly sandstone (Permian)

interbedded with Gricha and Guhjal formations (Zanchi and Gaetani 2011). Whereas dark slates, arkose sandstone, quartzite, bioclastic limestone and strongly deformed Shaskar granitoid outcrops in Misgar horst.

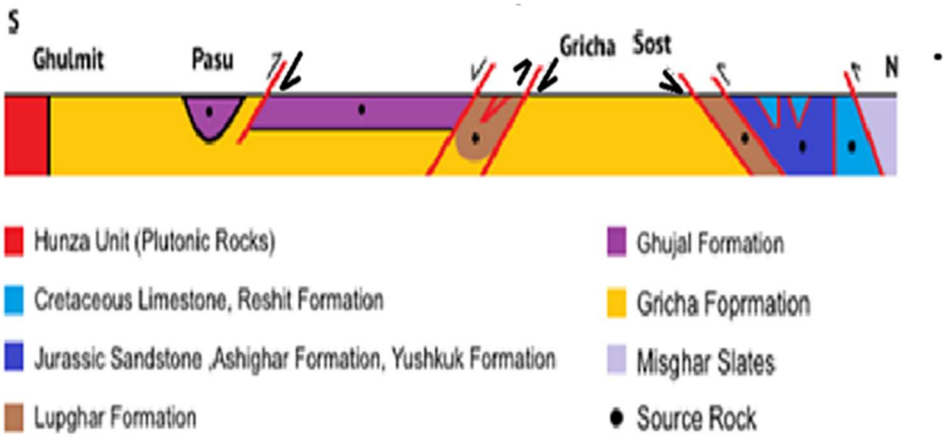

Figure 3. Geological Cross Section Guhjal Unit and Sost Unit.

Discussion and Conclusion:

The sustainable and prolonged subsidence of the earth's crust refers as basin. The basin dynamics frames sedimentation trends and progressive lithogenesis that sedimentary rocks - the composition and the structure, whereas the lithogenesis processes make favourable environment for the formation, accumulation, and preservation of hydrocarbons (Galimov 1989).

Bender and Raza (1995), Carmichael et al., (2009), Craig et al., (2018) Oakley (2016), Qadri (1995), Voskresenskiy et al., (1971) and Wandrey et al., (2004) examined petroleum system and hydrocarbon potentials of Alpides, Pakistan, NW Himalayas and Offshore Indus Basin of Pakistan and delineated Alpides, NW Himalayas into Indus basin, Balochistan Basin, Kohat- Potwar Basin, Peshawar Basin, Lesser Himalaya basin, Trans Indus Range, Salt Ranges, Kashmir Basin, Indus Offshore Basin and Makran offshore Basin as prospective hydrocarbon producing basins. According to Bender and Raza (1995), Carmichael et al., (2009), Craig et al., (2018) Oakley (2016), Qadri (1995), Voskresenskiy et al., (1971) and Wandrey et al., (2004) Mesozoic clastic and carbonate rocks are hydrocarbon source and reservoir rocks in Lesser and Sub Himalayas, Trans Indus, Range, Salt Range and NW Himalayas of Pakistan. The Mianwali formation shale (Early Triassic) and Chichali formation shale (Jurassic – Early Cretaceous) are sources rocks and Kingriali formation dolomite (Upper Triassic) and Datta formation sandstone and Samansuk formation limestone are reservoir rocks in Lesser Himalaya, Sub-Himalaya, Trans Indus Range and Salt Range, respectively (Craig et al., 2018, Oakley 2016 and Wandrey et al., 2004).

The correlation between clastic and carbonate (Triassic – Cretaceous) outcrops of Sost aulacogen (Donnelly, Zanchi and Gaetani 2011) and Mesozoic sequences of NW Himalayas, Lesser and Sub Himalayas basin source and reservoir rocks indicates resemblance of palaeotectonic environments of sedimentation of Mesozoic sequences (Fig.4.). While Khain and Limonov (2004), Gaetani (2015), Gaetani (1997), Desio (1979), Voskresenskiy et al., (1971), and Zanchi and Gaetani (2011) are of opinion that new stage of tectonic development history of Alpides, Alpine-Karakoram (Desio 1979) started on the border of Palaeozoic Era and Mesozoic Era. Khain and Limonov (2004), Gaetani (2015), Gaetani (1997), Desio (1979), Voskresenskiy et al., (1971), and Zanchi and Gaetani (2011) categorized Permian-Triassic complex as Cimmerian Folding system. The gradual transition is sediment deposition is documented from Permian period to Triassic period in Kirthar -Sulaiman of Alpides (Voskresenskiy et al., 1971) and Sost aulacogen, Northern Sedimentary Terrain (Gaetani 1997, and Zanchi and Gaetani 2011). The Early Triassic shale deposition and limestone accumulation in second half of Triassic period occurred in all basin (Donnelly 2004, Voskresenskiy et al., 1971 and Zanchi and Gaetani 2011).

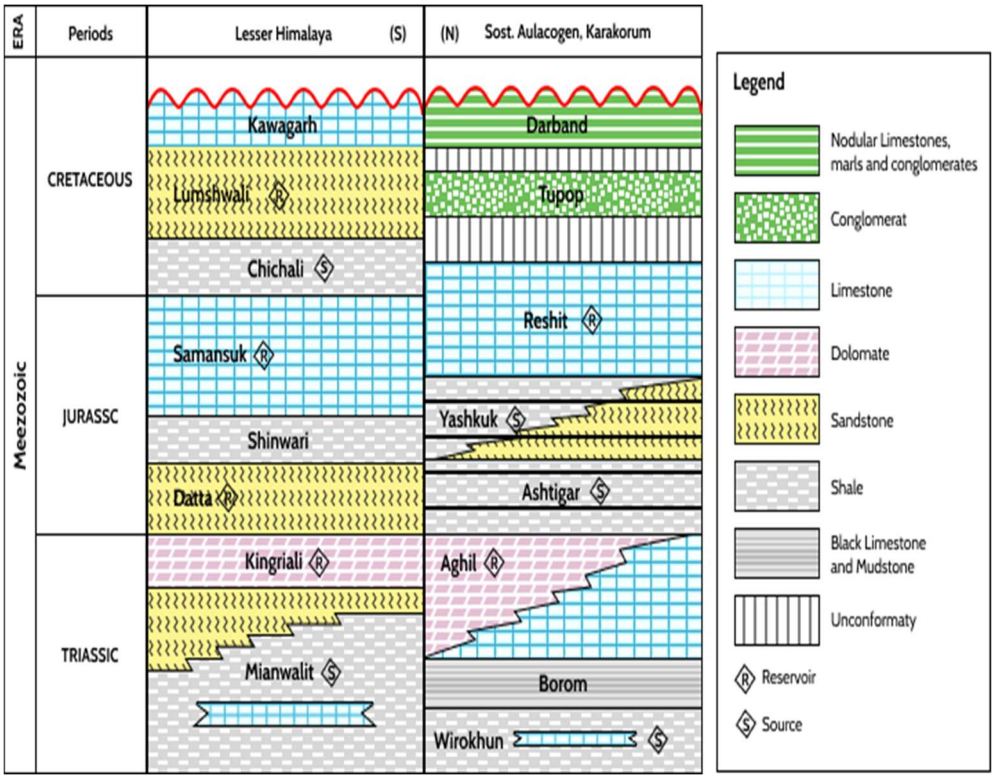

Figure 4 Correlation of Mesozoic sedimentary sequence of Lesser Himalayas and Northern Sedimentary Terrain (after Craig et al., 2018, Donnelly 2004, Zanchi and Gaetani 2011).

The paleotectonic environment of Triassic period indicates that Alpides of Pakistan, Karakoram, and Higher Himalayas were connected with each other (Fig. 5). Balasundaram and Ray (1973) also elucidate link between Mesozoic geosyncline south of Tibit with Karakoram Mesozoic geosyncline. While Khain (1979)) and Voskresensky et al., (1971) have indicated that deposition of shale and carbonate (Lower Triassic) occurred during start of new tectonic development stage base on weak Henrician Orogeny in Karakoram and NW Himalayas which covered Alpides of Pakistan. The present petroleum system and hydrocarbon potentials studies base on the evaluation of paleotectonic conditions sedimentation of Mesozoic sequence in Alpides of Pakistan, NW Himalayas, and Karakoram. It is observed that deposition conditions of Mesozoic sequence in all above-mentioned basins are approximately similar. Since Mesozoic sequence of Sost aulacogen, Norther Sedimentary Terrain, Karakoram and other tectonic elements of Alpine-Himalaya Belt of Pakistan is same, so authors postulate Sost aulacogen can be hydrocarbon rich structure. The Sukkur aulacogen structure of Indus basin is one of main gas producing structure in Pakistan (Voskresenskiy et al., 1971, Wandrey et al., 2004).

In authors opinion Wirokhun formation black shale (Early Triassic) and Jurassic Ashtigar Formation shale and marl interbedded with coal seams and Yashkuk formation sandstone and siltstone along with coal seams (Donnelly 2004, Zanchi and Gaetani 2011) can be prospective hydrocarbon sources rocks. While limestone and dolomite of Aghil formation (Triassic), Guhjal Formation (Permian -? Mesozoic) and Jurassic – Cretaceous limestones can be reservoirs of hydrocarbon in Sost aulacogen. The Jurassic – Cretaceous limestones is may be reservoir in Sost aulacogen. However, further studies of petroleum system and modelling of Sost Aulacogen can clarify hydrocarbon potentials.

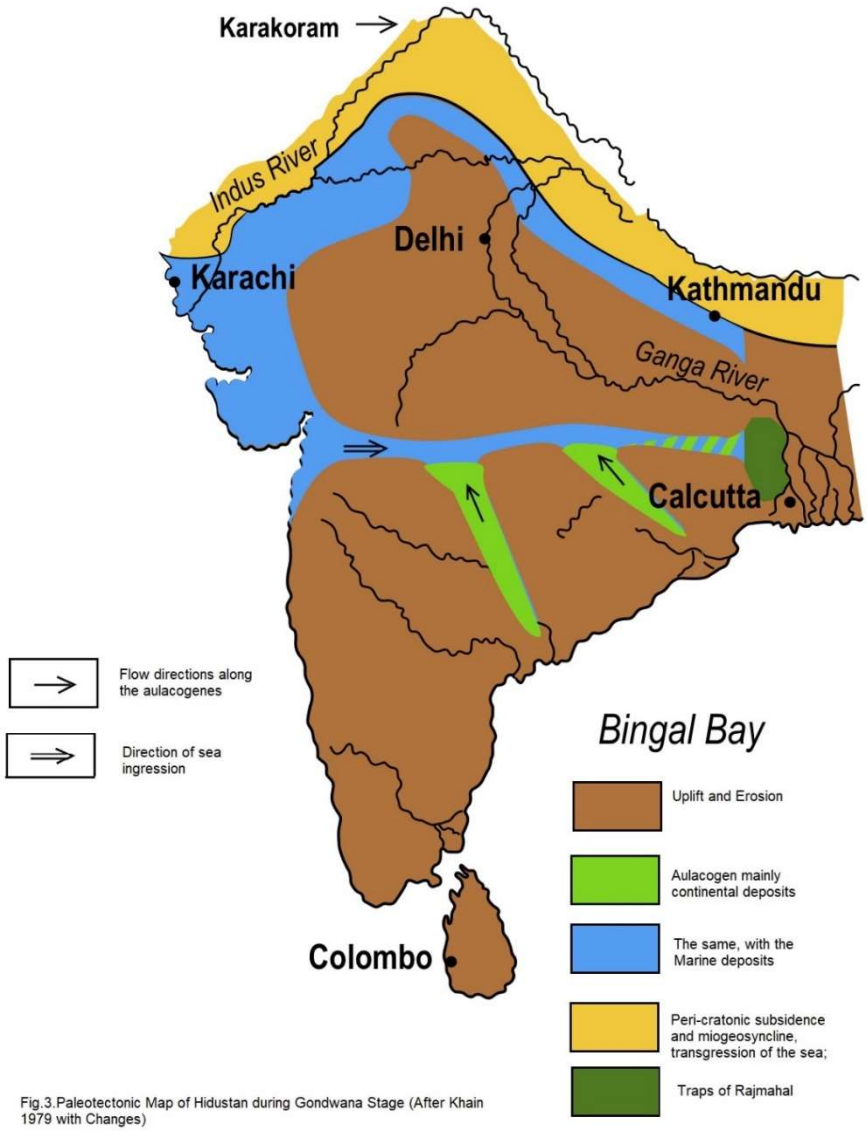

Figure 5: Triassic Palaeotectonic Map of Pak-Indian Platform (Khain 1979 with changes).

Acknowledgement: Authors thank anonymous reviewer for comments and Dr. Louis Hissink for editing of the paper.

References:

Arkhipov N.A., Galkin Yu. V., Galkina A. A., Gimadi V. I., and others 2014. The Forecast For The Development Of Energy Of The World And Russia till 2040. Moscow pp. 170 (In Russian).

Balasundaram M. and Ray D. (1973). Tectonic Framework and Evolution of India. Geol. Soc. Malaysia, Bulletin 6, pp. 17-25.

Bender F. and Raza H. 1995. Hydrocarbons. Geology of Pakistan [ed.] and Raza H., Bender F. Berlin -Stuttgart: Gebruder Borntraeger, pp. 182-202.

Belousov, V., 1976. Geotectonics. M. Nedra, p. 264 (in Russian).

Belousov, V.V., Belyavsky, N.A. and Borisov, A.A., 1979. The structure of the lithosphere the profile of deep seismic sounding of the Tien Shan, Pamir-Karakoram Himalaya. Sovetskaya Geology, no. S, p. 11-28. (In Russian).

Belyayevskiy N.A. (1966) Principal geological features of Karakoram, International Geology Review, 8:2, 127-143, DOI: 10.1080/00206816609474268

Blot, C. and Choi, D., 2005. Forerunners of the catastrophic Kashmir Earthquakes (8 October 2005) and their Geological significances. New Concepts in Global Tectonics Newsletter, no. 37, p. 4-16.

Brohi S. 2018. Oil & Gas Exploration &Production in Pakistan, Issues in Legal Framework on Community Development & Environment. PDI pp. 82 www.pdi.org.pk.

Burtman V. S. (2013) Geodynamics of Pamir-Punjab Syntaxis. Geotectonika № 1, pp. 36–58 (In Russian)

Craig J, Hakhoo, N., Bhat G.M. Hafiz M., Khan M.R., Misra R., Pandita S. K, Raina B. K., Thurow J., Thusu B., Ahmed W., Khullar S. 2018. Petroleum systems and hydrocarbon potential of the North-West Himalaya of India and Pakistan. Earth-Science Reviews 187 pp. 109–185 www.elsevier.com/locate/earscirev

Carmichael S. M., S. Akhter S., J. K. Bennett J. K., M. A. Fatimi M. A., K. Hosein K., R. W. Jones R. W., M. B. Longacre M. B., M. J. Osborne M. J and R. S. J. Tozer R. S. J. 2009. Geology and hydrocarbon potential of the offshore Indus Basin, Pakistan. Petroleum Geoscience, Vol. 15, pp. 107–116

DOI 10.1144/1354-079309-826.

Donnelly L.J. 2004. Geological investigations at a high altitude, remote coal mine on the Northwest Pakistan and Afghanistan frontier, Karakoram Himalaya.

International Journal of Coal Geology 60 pp. 117– 150

Desio, A., 1979. Geological Evolution of the Karakoram. In: Farah, A., and DeJong, K.A. (eds.), Geodynamics of Pakistan. Geol. Surv. Pak., Quetta, p. 111-124.

Desio, A. 1964 Geological Tentative Map of the Western Karakorum 1:500,000. Milan (Instituto di Geologia).

Desio A., 1974 Karakorum mountains Geological Society, London, Special Publications, 4, 255-266, DIO 10.1144/GSL.SP.2005.004.01.14

Gaetani M 1997 The Karakorum Block in Central Asia, from Ordovician to Cretaceous. Sedimentary Geology, Vol. 109, pp. 339-359.

Gaetani M. 2015. Blank on the Geological Map. Rendiconti Lincei. Scienze Fisiche e Naturali. DOI: 10.1007/s 12210-015-0494-2

Galimov E. 1989 Sources and mechanisms of formation of hydrocarbon gases in sedimentary rocks. Geochemistry, Vol. 2, pp. 163-180. (in Russian).

Gansser A., 1964. The Geology of Himalayas. John Wiley & Sons Ltd. pp. 289

Gattinger T., 1961. Geologischer Querschnitt des Karakorum vom Indus zum Shaksgam. Geologische Ergebnisse der Österreichischen Himalaya-Karakorum-Expedition 1956. JB. Geol. B. A. Sonderband 6 S 3—118.

Khain, V.E., 2000. Tectonics of continents and oceans. Moscow. Pp. 585. (in Russian).

Khain, V.E., 1979. Regional Geotectonics of Asia and Australia M. Nedra. (in Russian).

Khain, V.E., (1991) Abyssal Faults, Geoblocks, Terranes and Plate Tectonics, International Geology Review, 33:12, 1155-1163, DOI: 10.1080/00206819109465743

Khain V., Limonov L. 2004. Regional Tectonics. 2004. (In Russian)

Kravchenko, K., 1979. Tectonic Evolution of the Tien Shan, Pamir, and Karakorum. In: Farah, A., and DeJong, K.A., (eds.), Geodynamics. Geol. Sur. Pak. Quetta. pp.25-40.

Le Fort P., Tongiorgi M. & Gaetani M. 1994. Discovery of a crystalline basement and an Early Ordovician marine transgression in the Karakorum mountain range, Pakistan. Geology, Vol. 22, pp. 941-944.

Magsi H.Z. 2018. The question of the oil and gas potential of western and central Karakorum, Pakistan. Proceedings of the International Geological and Geophysical Conference GeoEurasia 2018. Modern technologies of studying and development of Eurasian resources » pp.104-107

Magsi H.Z. 2019 The Potential of Biotic and Abiotic Hydrocarbons in Karakoram, Pakistan. New Concepts in Global Tectonics Journal, V 7 N 1, pp 63-73 March 2019 www.ievpc.org.

Oakley, J., 2016. Pakistan's Kohat Plateau: The Rise of a Formerly Frontier Province. Petroleum Exploration Society of Great Britain (PESGB), pp. 44–47.

Qadri I. 1995 Petroleum Geology of Pakistan. Karachi: Pakistan Petroleum Limited. p. 300.

Rogozhin E.A., Sokolova E. Yu., Somala S.N., Andreeva N.V., and Raghucharan M.C. 2020. Deep Structure and Folded-Block Structure of the Garhwal Himalayas (India): Results of Integrated Geological and Geophysical Study. Geotectonics, Vol. 54, No. 1, pp. 75–82.

Schneider H., 1957, Tektonik und Magmatismus im NW-Karakorum. Geol. Rdsch., 46,426-476.

Schneider H.,1960, Geosynklinale Entwicklung und Magmatismus an der Wende Palaozoikum- Mesozoikum im NWHimalaya und -Karakorum. Geol. Rdsch., 50, 334-352.

Smoot N., 2018. Observations on the Southern and African plates. New Concepts in Global Tectonics Journal, v.6, no. 2, pp. 149-170 ww.ncgtjournal.com.

Smoot N., 2007. Wherefore the Tethys Sea(s)? New Concepts in Global Tectonics Newsletter, no. 45, pp. 21-30.

Tahirkheli R., Dongli S., Yusheng P., Wangming D., Yuquan Z., Baqri S., and Dawood H., 1990. Review of Stratigraphy of the Upper Hunza Valley (UHV), NW Karakoram Pakistan. Geol. Bull. Uni. Peshawar, Vol. 23, pp. 203-214.

Voskresensky, I., Kravchenko, K., Movshovich, E. and Sokolov, B., 1971. Outline of Geology of Pakistan. M. Nedra, p. 166. (in Russian).

Wadia, D.N., 1931. The syntaxis of the northwest Himalaya: its rocks, tectonics, and orogeny. Records of the Geological Survey of India, pp. 189–220.

Wandrey, C.J., Law, B.E., Shah, H.A., (2004). Patala - Nammal composite total petroleum system, Kohat-Potwar geological province, Pakistan. In: Wandrey, C.J. (Ed.), Petroleum Systems and Related Geologic Studies in Region 8, South Asia. United States Geological Survey Bulletin, pp. 1–18.

Zanchi A. & Gaetani M. 1994. Introduction to the Geological map of the Northern Karakoram Terrain, from Chapurson valley to Shimshal Pass. Riv. It. Paleont. Strat., 100(1), 125-136.

Zanchi, A. and Gaetani, M., 2011. The Geology of the Karakoram range, Pakistan: the new 1:100,000 geological map of Central –Western Karakoram. Ital. J. Geo.sci. (Boll. Soc. Geol. It.), v. 130, no. 2, p. 161-262, 91. DOI: 10.3301/ IJG .2011.09.

ABOUT THE NCGT JOURNAL

The NCGT Newsletter, the predecessor of the NCGT Journal, was begun as a result of discussions at the symposium "Alternative Theories to Plate Tectonics" held at the 30th International Geological Congress in Beijing in August 1996. The name is taken from an earlier symposium held in association with the 28th International Geological Congress in Washington, D. C. in 1989. The first issue of the NCGT Newsletter was December 1996. The NCGT Newsletter changed its name in 2013 to the NCGT Journal.

Aims of the NCGT Journal include:

1. Providing an international forum for the open exchange of new ideas and approaches in the fields of geology, geophysics, solar and planetary physics, cosmology, climatology, oceanography, electric universe, and other fields that affect or are closely related to physical processes occurring on Earth from its core to the top of its atmosphere.

2. Forming an organizational focus for creative ideas not fitting readily within the scope of dominant tectonic models.

3. Forming the basis for the reproduction and publication of such work, especially where there has been censorship or discrimination.

Submission of content

Manuscripts, letters, articles and notes should be submitted as Microsoft Word documents, Margins, top 2.54cm, 1 inch, bottom, left and right 1.27 cm, 1/2 inch. Times New Roman font. Drawings and images should be uncompressed png, tiff, format, No Jpegs. No PDF's will be accepted. A minimal number of styles are accepted. Language should be US English. No page or section breaks are permitted. All images are to be presented as individual graphic files and no images are to be embedded in the text. Tables should be submitted as Microsoft Excel work sheets and will be added to the page as images (png) rather than active tables that potentially create problems with column sizes etc.

I uuse Microsoft Word to edit the text and either Microsoft publisher or Affinity Publisher to layout the journal pages when text frames and imagen frames are used. Word is a writing/editing word processor, Publisher and Affinity Publisher are specific desktop publishing applications where layout is paramount.